Natural selection is less efficient at species range edges

Authors: Chloé Schmidt[1,*], Jussi Mäkinen[2], Jean-Philippe Lessard[3], Colin J Garroway[4]

Affiliations:
[1] German Centre for Integrative Biodiversity Research (iDiv) Halle-Jena-Leipzig; Leipzig, 04103, Germany
[2] Research Center for Ecological Change, Faculty of Biological and Environmental Sciences, University of Helsinki; Helsinki, Finland
[3] Department of Biology, Concordia University; Montréal, H4B 1R6, Canada
[4] Department of Biological Sciences, University of Manitoba; Winnipeg, R2T 2N2, Canada

***Correspondence:** chloe.schmidt@idiv.de

Keywords: genetic drift, genetic diversity, macrogenetics, species distributions, central-marginal hypothesis

Abstract

Changing species distributions due to global change underscore a pressing need to better understand range limits. However, our knowledge of general determinants of range limits remains poor despite over a century of work. Theoretical models demonstrate that genetic drift should strengthen across environmental gradients. This can limit natural selection to the point where populations can no longer adapt to new conditions and range edges form. How widely this theory holds in real-world populations is uncertain. With data comprising 37,397 genotypes sampled across the ranges of 59 mammal species, we found support for a central role of genetic drift-imposed limits to selection in setting range limits. While range limits are often considered in terms of environmental tolerances at the species level, the efficiency of selection is limited at the population level. This can explain idiosyncratic patterns of range expansion and collapse due to climate change and human land use.

Introduction

No species occurs everywhere. While the distributional limits of species sometimes align with physical barriers or abrupt changes in environmental conditions, they also commonly taper off gradually. This is puzzling from an evolutionary perspective because, given sufficient time and genetic variation, theory predicts that populations should be capable of adapting and expanding into neighboring environments (Antonovics, 1976; Bradshaw, 1991; Bridle & Vines, 2007; Gaston, 2003; Polechová, 2018). The ubiquity of range edges without clear barriers suggests there are general evolutionary mechanisms that limit adaptation to produce such range edges. Conventional theory suggests that population size should peak in the best environmental conditions for a species and gradually decrease with distance from the peak as the environment becomes less suitable (Brown, 1984) (Fig. 1). This ecological explanation for the emergence of range edges, widely known as the abundant center or central-marginal hypothesis, is hotly debated and empirical support for it remains equivocal (Dallas et al., 2017; Eckert et al., 2008; Fristoe et al., 2022; Hargreaves et al., 2014; Kottler et al., 2021; Lee-Yaw et al., 2016; Pironon et al., 2017; Sagarin & Gaines, 2002; Santini et al., 2019; Singhal et al., 2022). This hypothesis is agnostic about the reasons why species cannot expand their geographical distribution by continuously adapting to environmental changes at range margins.

The population genetics of range edges

From a population genetic perspective, genetic drift–the random fluctuation of allele frequencies from one generation to the next–could set range limits by preventing adaptation and range expansion (Bridle & Vines, 2007; Brussard, 1984; Connallon & Sgrò, 2018; Kirkpatrick & Barton, 1997). Genetic drift erodes genetic diversity, reducing the raw material available for selection to act upon. Natural selection is also less efficient at facilitating the spread of beneficial

alleles when drift is the dominant evolutionary force, as random allele sampling overwhelms the deterministic forces of selection. The strength of genetic drift is inversely proportional to population size, thus central-marginal patterns of abundance predict parallel variation in the intensity of drift and consequently, the efficiency of natural selection across species ranges. Bringing ecological and evolutionary perspectives together, the central-marginal hypothesis predicts that as environments become less suitable, population sizes decline, genetic drift strengthens to a point where natural selection can no longer drive adaptation, and populations are no longer viable and fail to establish (Connallon & Sgrò, 2018) (Fig. 1).

We can test whether edge populations experience stronger genetic drift by quantifying effective population size and genetic diversity at multiple locations across species ranges. The effective population size estimates the strength of genetic drift, which should be reflected in reduced genetic diversity. Spatially isolated populations experiencing stronger drift should become increasingly genetically differentiated (Fig. 1). Empirical tests of the genetic consequences of the central-marginal hypothesis that are generalizable across species have not yet been possible because they require comparable population-level data collected across the ranges of many species from different regions ((Eckert et al., 2008) but see (Singhal et al., 2022)). We leveraged open-source genetic data for terrestrial mammals worldwide to overcome these challenges. Access to raw data allowed us to consistently estimate effective population size, genetic diversity, and differentiation using genotypic data collected from 37,397 individuals, 1,271 sample locations, and 59 species (Fig. 2, S1, Table S1). We modeled the relationship between range position and genetic composition using spatially and phylogenetically explicit Bayesian generalized linear mixed models (see Methods).

Methods

Data

Genetic data. We systematically harvested publicly archived genetic data for mammal species sampled across the globe to test our questions. We expanded a database of raw microsatellite genotypes for mammal species from Canada and the USA, initially compiled between 2017-2021 (Schmidt et al., 2020; Schmidt & Garroway, 2022), to cover archived data for mammals globally. For detailed methods on dataset assembly methods see Schmidt et al. (Schmidt et al., 2020). Briefly, we obtained a list of 5216 names of species with ranges occurring outside of the United States and Canada from the IUCN database to use as keywords in addition to a 'microsat*' search term (e.g., *Alces alces microsat**). We then performed a systematic search of the Dryad Digital Repository (https://datadryad.org/stash) by accessing the Dryad API using a custom R (R Core Team, 2021) script. This produced 269 results which we then manually checked for suitability ensuring genotype data were available for the correct species, samples were collected from natural wildlife populations, the study used neutral microsatellite markers, sample design was appropriate for estimating normal levels of genetic diversity and differentiation (e.g., samples were not taken after a disturbance or recent bottleneck, if parentage analysis, offspring were excluded), and with sampling locality and population grouping information (Data S1).

For each sample location, we recorded latitude and longitude in decimal degrees, year of sampling if applicable, and sequence of sampling (for populations sampled over time at the same location. We recorded the number of loci and individuals sampled from the data directly in R. We retained sites with at least 5 individuals sampled, and species with at least 5 sample sites. We retained only the most recent time point for the few species with temporal sampling.

We estimated four metrics of genetic composition for each sample site. First, we estimated gene diversity, a measure of evenness which gives the probability of randomly sampling two different alleles from a group of individuals ('Hs' function in the *adegenet* package; (Jombart et al., 2017). Because gene diversity is computed from allele frequencies and not counts of alleles, it is not strongly affected by sample size (Charlesworth & Charlesworth, 2010). Allelic richness was our second measure of genetic diversity. We estimated rarefied allelic richness using the ('allelic.richness' in *hierfstat;* (Goudet & Jombart, 2015) using 10 alleles as the minimum sample size to ensure estimates were comparable across the entire dataset. We used population-specific F_{ST} as a measure of genetic differentiation ('betas' in *hierfstat*). This metric is described in more detail in the *Mapping population structure* section below. Finally, we estimated the contemporary effective population size of the parental generation for each sample site using the linkage disequilibrium method implemented in the NeEstimator software (version 2.1; (Do et al., 2014) accessed from R with the rLDNe package (https://github.com/zakrobinson/RLDNe). The linkage disequilibrium method implemented in NeEstimator is among the more accurate for estimating contemporary effective population size (Gilbert & Whitlock, 2015), and it performs especially well for small populations. However, an estimate of infinity is returned when effective population sizes are extremely large, or when small sample size makes signals of genetic drift difficult to detect. We treated these estimates as NA values and excluded them from analysis.

Range data. We downloaded range maps from the IUCN (https://www.iucnredlist.org/resources/spatial-data-download). We filtered species range data based on presence, origin, and seasonality, retaining portions of the range where species populations were identified as extant, native, and resident. Many species ranges were fragmented, represented by multiple disjunct polygons. Measuring the distance of a genetic sample site to the nearest edge of a polygon thus did not necessarily represent a site's position

with respect to the center and margin across an entire range. Instead, we measured the distance from each site to: 1) the nearest edge of a convex hull encompassing the species range, and 2) the geographic range centroid. We drew convex hulls and calculated centroids in the *terra* package, ensuring centroids were located within range polygons. We note that this restriction on range centroids to be inside polygon boundaries means they are not necessarily true centroids. Two species, brown bears *Ursus arctos* and moose *Alces alces*, had ranges across North America and Eurasia. In these cases, we treated range polygons across continents separately and drew convex hulls and centroids for the range on each continent. We measured the geodesic distance, or the shortest distance between two points along a curved surface, using the *geosphere* package in R (Hijmans, 2019).

Although we excluded introduced populations in our genetic data where identifiable and removed portions of species ranges classified by the IUCN as *introduced*, *re-introduced*, *vagrant*, *uncertain*, or *assisted colonization*, 4 species had sites (22 sites in total) located outside the species' convex hull. We chose to retain these sites, as they may represent expansion not yet recorded in IUCN range data and we predicted they should nevertheless adhere to interior-marginal patterns. We made these distances negative to maintain the directionality and interpretation of our distance measure (higher values of distance indicate moving toward the range interior).

Bayesian hierarchical models

We modeled the genetic composition at sample sites as a function of range position using a series of four Bayesian generalized linear mixed models (GLMMs; 1 per genetic response variable). All variables were scaled and centered so that models were comparable. We expected substantial

variation in mean values of genetic composition variables across species, and variation in the effect of distance to range edge across species (Eckert et al., 2008). We captured this structure in our models using random effects that allowed intercepts and slopes to vary across species. This method has considerable advantages over modeling each species separately because it reduces Type I error rates, and partial pooling in hierarchical models allows less well sampled species to borrow statistical strength from better sampled species, resulting in better estimates of effect sizes. We fit models in R version 4.1.2 using the integrated nested Laplace approximation with the INLA package (Lindgren & Rue, 2015).

We accounted for spatial autocorrelation in effective population size, gene diversity, allelic richness, and population-specific F_{ST} model residuals by modeling a spatial random effect using a Besag-York-Mollié-type random effect (Besag et al., 1991). We defined the connectivity structure of the sample sites with a k-nearest neighbor method by fixing the number of neighbors per a site to 1 for effective population size, 6 for population-specific F_{ST}, and 8 for gene diversity and allelic richness. We chose these connectivity structures by running model candidates with numbers of connections per a site varying from 1 to 8 and chose the model with the best fit to the data according to the Deviance Information Criteria (DIC) (Spiegelhalter et al., 2002) and WAIC (Gelman et al., 2014). Both criteria supported the selection of the same model candidates for further analysis (Table S3). All candidate connectivity structures captured the neighborhood structures on each continent and avoided between-continent connections. The motivation for using a spatial random effect in the model was only to explain the spatially correlated residual variation without a more in-depth analysis of the posterior of the spatial random effect. Finally, we accounted for potential phylogenetic dependence in our species sample with a phylogenetic random effect. We defined the random effect as a generic random effect, for which the inverse of

the phylogenetic distance matrix capturing cross-species dependencies was computed with the function inverseA from R-package *MCMCglmm* (Hadfield, 2018).

Mapping population structure

We explored spatial patterns of genetic differentiation for species using an approach from Kitada et al. (Kitada et al., 2021) that combines estimates of population-specific F_{ST} and pairwise F_{ST} to characterize spatial population structure in an evolutionary context. Population-specific F_{ST} (Weir & Goudet, 2017) is a measure of population divergence estimated for individual samples—not pairs of samples—that uses proportions of matching alleles for pairs of alleles drawn from within and between populations to estimate differentiation. Population-specific F_{ST} can be interpreted evolutionarily as how far individual sites have diverged from a common ancestor of all the sites in the sample. We note that a simplifying assumption underlying this interpretation of population-specific F_{ST} is that populations with the highest genetic diversity are identified as most ancestral. This assumption does not always apply, for example in cases of extensive admixture or when ancestral populations have undergone a bottleneck (Kitada et al., 2021). However, because we use microsatellite markers, we interpret population-specific F_{ST} in terms of contemporary population structure. Because it is an estimate of differentiation relative to a single, common ancestral population, population-specific F_{ST} does not provide information about how differentiated sample sites are relative to each other. For this, we use pairwise F_{ST}. Combining population-specific F_{ST}, pairwise F_{ST}, and spatial metadata can provide a general idea about regions connected by gene flow and directions of population differentiation. We estimated both F_{ST} metrics in the hierfstat package, using the 'pairwise.neifst' function to estimate Nei and Chesser's pairwise G_{ST} (Nei & Chesser, 1983), and 'betas' to estimate population-specific F_{ST}.

To visualize patterns of differentiation, we generated 2 plots per species to represent population structure in complementary ways (Fig. 4, Fig. S4); for detailed description of these methods see (Kitada et al., 2021). We focused on 12 species that had good coverage of their range. The first plot showed population-specific F_{ST} values across species' ranges. To visualize the major axes of genetic differentiation, we performed a principal coordinates analysis (PCoA) on the pairwise genetic differentiation matrix and plotted sites positions on the first two PCoA axes.

Results and Discussion

We found repeated, consistent gradients in genetic composition across mammal species and regions of the world that align with the view that genetic drift intensifies and natural selection becomes less efficient closer to range edges. For nearly all species, populations sampled nearer the edge of their distribution had smaller effective population sizes, indicating that drift is stronger near the range edge (Table 1, Fig. 3). This result was corroborated by lower genetic diversity closer to the range edge, in terms of both the abundance and evenness of alleles (allelic richness and gene diversity, respectively) in local populations (Table 1, Fig. 3, Fig. S3). Finally, edge populations also tended to be more genetically differentiated from populations in the range interior, suggesting that reduced effective population size at the edge is due in part to reduced gene flow (Table 1, Fig. 3, Fig. S3). Phylogenetic correlations were low across all genetic metrics (Fig. S2), suggesting that these patterns are more related to contemporary ecological factors and microevolutionary change than conserved traits or shared demographic histories. These patterns held for models that did not explicitly account for species relatedness (Table S2). We also found similar relationships when quantifying range position as the distance to the geographic range centroid (Fig. S3). Together, these results support the idea that populations

nearer range edges tend to be smaller and more spatially isolated than interior populations, increasing the strength of genetic drift and removing genetic diversity from populations more rapidly. Strong drift, ineffective selection, low gene flow, and low genetic diversity are not conducive to adaptive evolution in changing environments. Genetic drift could therefore play a central role in the formation of range limits regardless of the identity of species or geographic location of range edges.

Genetic drift and range change dynamics

The patterns of effective population size, genetic diversity, and genetic differentiation in relation to range edges we find (Fig. 3) have direct implications for our understanding of range edge dynamics under climate change. Our empirical results align with theoretical models suggesting the interaction between environmental gradients and the evolutionary process of genetic drift combine to produce expansion thresholds at the population level that determine distributional limits for species (Connallon & Sgrò, 2018; Polechová, 2018) (Fig. 1). These expansion thresholds can also help explain and predict range expansion and collapse amid global changes (Kirkpatrick & Barton, 1997; Polechová, 2018; Polechová & Barton, 2015). In these theoretical models, when rates of environmental change are constant across a species range and populations are large and genetically diverse, populations are above expansion thresholds and ranges can expand across environmental gradients indefinitely due to continuous local adaptation. With constant rates of environmental change and low genetic diversity, populations can fall below expansion thresholds, causing fragmentation into a network of locally adapted populations or eventual whole range collapse (Polechová, 2018). Finally, when rates of environmental change accelerate, the population size and genetic diversity required for ongoing local adaptation to new

environments can increase until local adaptation is no longer possible, and a range edge forms at the expansion threshold.

The concept of expansion thresholds caused by genetic drift provides a mechanism for understanding how the effects of human-caused global change on populations can drive wholesale changes in species distributions. Local changes to habitat connectivity or population size might increase or decrease expansion thresholds (Bridle et al., 2019) with range-wide effects. For example, populations in the range interior will likely be more capable of adapting to climate change than populations at the edge. This is because interior populations will tend to be large and have high genetic variation relative to edge populations, placing these populations above their expansion threshold. According to this idea, the evolutionary fates of edge populations will be unpredictable on both trailing and leading edges of the range. The varied regional effects of climate change, which can include changes in temperature, precipitation, seasonality, and species interactions among others, can flatten or steepen environmental gradients at range edges. Because expansion thresholds apply to populations rather than species, range dynamics in response to climate change should be highly variable due to intraspecific variation in population structure and the environmental gradients limiting adaptation across the range. Indeed, although poleward range shifts were typically predicted to occur as species track their environmental niche, empirically, there is substantial variation in range change dynamics. Poleward shifts account for less than half of documented range movements (Platts et al., 2019; Rubenstein et al., 2023).

Predicting the consequences of habitat loss and fragmentation due to human land use may be more straightforward than predicting range changes due to climate change. Rapid reduction of population size and population fragmentation can cause populations to drop below the size

needed for ongoing adaptation at any position in a range, not only near edges (Fig. 1). Urbanization gradients, for example, are consistently associated with stronger genetic drift, reduced genetic diversity, and higher genetic differentiation in mammal populations (Schmidt et al., 2020; Schmidt & Garroway, 2022). Although locally adapted and fragmented metapopulations can persist for long periods (Polechová, 2018), they are vulnerable to continued environmental change. Interior populations that have been fragmented due to human land use may be less capable of adapting to climate change, meaning it would be unreliable to base management decisions on the assumption that more centrally located populations will tend to be more resilient. Thus, monitoring and maintaining genetic diversity and connectivity throughout species ranges is important for understanding range stability and change.

The current most widely used tool to understand and predict range dynamics is species distribution modeling (SDMs) (Guisan & Thuiller, 2005), which associates species occurrences with environments to infer suitable habitats for species as a whole. Using future climate scenarios, they are used to make predictions about how ranges will shift, expand, or contract in response to changes in the availability of suitable habitat. Species distribution models thus typically predict range dynamics as a direct outcome of species-habitat associations, and ignore local evolutionary processes (see (A. Lee-Yaw et al., 2022; Zurell et al., 2009) for static SDMs, but (Benito Garzón et al., 2011; Hällfors et al., 2016) for non-stationary SDMs). Microevolutionary processes have been shown to be important for predicting changes in species distributions, as locally adapted populations are differentially affected by environmental change (Bay et al., 2018; Fitzpatrick et al., 2021; Jay et al., 2012). Not considering microevolutionary responses to environmental change presents a source of bias in the predictions of future ranges (D'Amen & Azzurro, 2020; Hanspach et al., 2011).

Resolving inconsistencies

Tests of the abundant center hypothesis are data intensive, and syntheses of this topic have had to contend with methodological heterogeneity across studies that add statistical noise to formal meta-analyses (Eckert et al., 2008; Fristoe et al., 2022; Sagarin et al., 2006; Sagarin & Gaines, 2002; Santini et al., 2019; Soberón et al., 2018). We were able to overcome these drawbacks by harvesting publicly available genetic data, enabling us to consistently estimate metrics of genetic composition and range position across disparate studies. A prominent reason why the central-marginal hypothesis has been so debated stems from differences in how range position is defined. Several continuous and categorical metrics have been used to describe range position, including distance from the range edge, the geographic range center, or the environmental niche center (Eckert et al., 2008; Fristoe et al., 2022). We have focused on distance from the range edge, a measure of peripherality that makes no assumption about where in the range the core population lies. We note however, that we find similar results when estimating patterns using distance from the geographic range center. Genetic diversity is higher, and differentiation is lower nearer range centroids, although we detected no effect of centroid distance on effective population size (Fig. S3).

Central-marginal patterns are likely better thought of in terms of core-marginal patterns, of which the abundant center is a special case (Fristoe et al., 2022). Cores, wherever they occur in a range, should be well-connected and have high gene flow and genetic diversity, with populations extending toward a range edge becoming increasingly differentiated and less diverse (Fig. 1). The spatial genetic predictions we test here do not make any assumption about the location of the range center, and depend only on population-level evolutionary dynamics through space in relation to range edges. To visualize the position of range cores, we mapped spatial genetic

structure using pairwise F_{ST} (Nei, 1987) and population-specific F_{ST} (Weir & Goudet, 2017) for a subset of species with the best geographic sampling across ranges (Fig. 4, S4, See SI Methods). These maps suggest that although core populations tend to be in the range interior, they often cover very large proportions of the range. Large core populations and the assumption that cores occur in the geographical center of ranges likely contribute to different strengths of effect sizes we find across species (Fig. 3) and mixed support for core-marginal patterns in the literature. Core-marginal patterns may be weak and difficult to detect in most places, leading the pattern to be masked by limited sampling.

Range limits and the arrangement of biodiversity

Recent work showing that genetic diversity also decreases as populations approach transitional zones between biogeographic regions suggest that drift-associated limits to adaptation within species ranges scale to shape broader biodiversity patterns (Schmidt et al., 2022). Given species ranges are the unit of organization for higher level biodiversity patterns, this is to be expected. Wallace (Wallace, 1876) first delineated regionally distinct biota in 1876, and biogeographic regions have since become a cornerstone of modern biogeography, macroevolution and conservation biology. Boundaries of biogeographic regions coincide with a relatively high number of range edges, and drift-mediated limits to range expansion also appear to prevent widespread homogenization of regional biota (Schmidt et al., 2022). If drift-mediated limits to range expansion stand scrutiny, they could be fundamental to the stability and maintenance of many important facets of biodiversity, all of which are the focus of global conservation efforts (Pollock et al., 2017).

The search for explanations for the striking global patterns of biodiversity we see in nature has long occupied the interest of naturalists and evolutionary ecologists (Holt et al., 2013; Sclater, 1858; Udvardy, 1975; von Humboldt, 1807; Wallace, 1876). Nevertheless, establishing how microevolutionary processes contribute to macro-scale patterns in biodiversity has remained a longstanding challenge (reviewed in (Charlesworth et al., 1982; Hancock et al., 2021)). The global configuration of biodiversity is typically understood in light of contemporary and historical climate (Ficetola et al., 2021; Holt et al., 2013), the movement of tectonic plates (Mazel et al., 2017), the historical spread of lineages between continents (Jønsson et al., 2011), and speciation-extinction dynamics occurring through deep time (Hagen et al., 2021; Holt et al., 2013; Lomolino et al., 2016). Our results highlight a mechanism by which contemporary, micro-scale, population-level demographic and evolutionary processes can contribute to macroecological patterns in species distributions. The maintenance of these patterns, and how they will change in the future under global warming and widespread land conversion, depends on contemporary, population-level demographic processes that regulate range dynamics and expansion.

Acknowledgments: We thank the Population Ecology and Evolutionary Genetics group and the Evolutionary Biology BIOL 3300 students at the University of Manitoba for their comments and feedback on manuscript drafts. C.S. gratefully acknowledges the support of iDiv funded by the German Research Foundation (DFG– FZT 118, 202548816). CJG was supported by a Natural Sciences and Engineering Research Council of Canada Discovery Grant.

Data availability: All data underlying this work are publicly available (Table S1). Code and analyzed datasets will be made available upon acceptance.

References and Notes:

A. Lee-Yaw, J., L. McCune, J., Pironon, S., & N. Sheth, S. (2022). Species distribution models rarely predict the biology of real populations. *Ecography*, *2022*(6), 1–16. https://doi.org/10.1111/ecog.05877

Antonovics, J. (1976). The Input from Population Genetics: "The New Ecological Genetics." *Systematic Botany*, *1*(3), 233–245. https://doi.org/10.1007/bf02811127

Bay, R. A., Harrigan, R. J., Underwood, V. L., Gibbs, H. L., Smith, T. B., & Ruegg, K. (2018). Genomic signals of selection predict climate-driven population declines in a migratory bird. *Science*, *359*(6371), 83–86. https://doi.org/10.1126/science.aan4380

Benito Garzón, M., Alía, R., Robson, T. M., & Zavala, M. A. (2011). Intra-specific variability and plasticity influence potential tree species distributions under climate change. *Global Ecology and Biogeography*, *20*(5), 766–778. https://doi.org/10.1111/j.1466-8238.2010.00646.x

Besag, J., York, J., & Mollié, A. (1991). Bayesian image restoration, with two applications in spatial statistics. *Annals of the Institute of Statistical Mathematics*, *43*(1), 1–20. https://doi.org/10.1007/BF00116466

Bradshaw, A. D. (1991). Genostasis and the Limits to Evolution. *Philosophical Transactions: Biological Sciences*, *333*(1267), 289–305.

Bridle, J. R., Kawata, M., & Butlin, R. K. (2019). Local adaptation stops where ecological gradients steepen or are interrupted. *Evolutionary Applications*, 1–14. https://doi.org/10.1111/eva.12789

Bridle, J. R., & Vines, T. H. (2007). Limits to evolution at range margins: When and why does adaptation fail? *Trends in Ecology and Evolution*, *22*(3), 140–147. https://doi.org/10.1016/j.tree.2006.11.002

Brown, J. H. (1984). On the Relationship between Abundance and Distribution of Species. *The American Naturalist*, *124*(2), 255–279.

Brussard, P. F. (1984). Geographic patterns and environmental gradients: The central-marginal model in Drosophila revisited. *Annual Review of Ecology and Systematics*, *128*. http://www.jstor.org/stable/2096942

Charlesworth, B., & Charlesworth, D. (2010). *Elements of evolutionary genetics*. Roberts & Company Publishers.

Charlesworth, B., Lande, R., & Slatkin, M. (1982). A Neo-Darwinian Commentary on Macroevolution. *Evolution*, *36*(3), 474. https://doi.org/10.2307/2408095

Connallon, T., & Sgrò, C. M. (2018). In search of a general theory of species' range evolution. *PLoS Biology*, *16*(6), 1–6. https://doi.org/10.1371/journal.pbio.2006735

Dallas, T., Decker, R. R., & Hastings, A. (2017). Species are not most abundant in the centre of their geographic range or climatic niche. *Ecology Letters*, *20*(12), 1526–1533. https://doi.org/10.1111/ele.12860

D'Amen, M., & Azzurro, E. (2020). Integrating univariate niche dynamics in species distribution models: A step forward for marine research on biological invasions. *Journal of Biogeography*, *47*(3), 686–697. https://doi.org/10.1111/jbi.13761

Do, C., Waples, R. S., Peel, D., Macbeth, G. M., Tillett, B. J., & Ovenden, J. R. (2014). NeEstimator v2: Re-implementation of software for the estimation of contemporary effective population size (Ne) from genetic data. *Molecular Ecology Resources*, *14*(1), 209–214. https://doi.org/10.1111/1755-0998.12157

Eckert, C. G., Samis, K. E., & Lougheed, S. C. (2008). Genetic variation across species' geographical ranges: The central-marginal hypothesis and beyond. *Molecular Ecology*, *17*(5), 1170–1188. https://doi.org/10.1111/j.1365-294X.2007.03659.x

Ficetola, G. F., Mazel, F., Falaschi, M., Marta, S., & Thuiller, W. (2021). Determinants of zoogeographical boundaries differ between vertebrate groups. *Global Ecology and Biogeography*, *30*(9), 1796–1809. https://doi.org/10.1111/geb.13345

Fitzpatrick, M. C., Chhatre, V. E., Soolanayakanahally, R. Y., & Keller, S. R. (2021). Experimental support for genomic prediction of climate maladaptation using the machine learning approach Gradient Forests. *Molecular Ecology Resources*, *21*(8), 2749–2765. https://doi.org/10.1111/1755-0998.13374

Fristoe, T. S., Vilela, B., Brown, J. H., & Botero, C. A. (2022). Abundant-core thinking clarifies exceptions to the abundant-center distribution pattern. *Ecography*, 1–15. https://doi.org/10.1111/ecog.06365

Gaston, K. J. (2003). *The structure and dynamics of geographic ranges*. Oxford University Press.

Gelman, A., Hwang, J., & Vehtari, A. (2014). Understanding predictive information criteria for Bayesian models. *Statistics and Computing*, *24*(6), 997–1016. https://doi.org/10.1007/s11222-013-9416-2

Gilbert, K. J., & Whitlock, M. C. (2015). Evaluating methods for estimating local effective population size with and without migration. *Evolution*, *69*(8), 2154–2166. https://doi.org/10.1111/evo.12713

Goudet, J., & Jombart, T. (2015). *hierfstat: Estimation and Tests of Hierarchical F-Statistics*. https://cran.r-project.org/package=hierfstat

Guisan, A., & Thuiller, W. (2005). Predicting species distribution: Offering more than simple habitat models. *Ecology Letters*, *8*(9), 993–1009. https://doi.org/10.1111/j.1461-0248.2005.00792.x

Hadfield, J. (2018). *MCMC GLMM*.

Hagen, O., Skeels, A., Onstein, R. E., Jetz, W., & Pellissier, L. (2021). Earth history events shaped the evolution of uneven biodiversity across tropical moist forests. *Proceedings of the National Academy of Sciences*, *118*(40), e2026347118. https://doi.org/10.1073/pnas.2026347118

Hällfors, M. H., Liao, J., Dzurisin, J., Grundel, R., Hyvärinen, M., Towle, K., Wu, G. C., & Hellmann, J. J. (2016). Addressing potential local adaptation in species distribution models: Implications for conservation under climate change. *Ecological Applications*, *26*(4), 1154–1169. https://doi.org/10.1890/15-0926

Hancock, Z. B., Lehmberg, E. S., & Bradburd, G. S. (2021). Neo-darwinism still haunts evolutionary theory: A modern perspective on Charlesworth, Lande, and Slatkin (1982). *Evolution*, *75*(6), 1244–1255. https://doi.org/10.1111/evo.14268

Hanspach, J., Kühn, I., Schweiger, O., Pompe, S., & Klotz, S. (2011). Geographical patterns in prediction errors of species distribution models: Patterns in prediction error. *Global Ecology and Biogeography*, *20*(5), 779–788. https://doi.org/10.1111/j.1466-8238.2011.00649.x

Hargreaves, A. L., Samis, K. E., & Eckert, C. G. (2014). Are species' range limits simply niche limits writ large? A review of transplant experiments beyond the range. *American Naturalist*, *183*(2), 157–173. https://doi.org/10.1086/674525

Hijmans, R. J. (2019). *geosphere: Spherical Trigonometry*. https://cran.r-project.org/package=geosphere

Holt, B. G., Lessard, J.-P., Borregaard, M. K., Fritz, S. A., Araújo, M. B., Dimitrov, D., Fabre, P.-H., Graham, C. H., Graves, G. R., Jønsson, K. A., Nogués-Bravo, D., Wang, Z., Whittaker, R. J., Fjeldså, J., & Rahbek, C. (2013). An Update of Wallace's Zoogeographic Regions of the World. *Science*, *339*(6115), 74–78. https://doi.org/10.1126/science.1228282

Jay, F., Manel, S., Alvarez, N., Durand, E. Y., Thuiller, W., Holderegger, R., Taberlet, P., & François, O. (2012). Forecasting changes in population genetic structure of alpine plants in response to global warming. *Molecular Ecology*, *21*(10), 2354–2368. https://doi.org/10.1111/j.1365-294X.2012.05541.x

Jombart, T., Kamvar, Z. N., Collins, C., Lustrik, R., Beugin, M.-P., Knaus, B. J., Solymos, P., Mikryukov, V., Schliep, K., Maié, T., Morkovsky, L., Ahmed, I., Cori, A., Calboli, F., & Ewing, R. J. (2017). *adegenet: Exploratory Analysis of Genetic and Genomic Data*. https://cran.r-project.org/package=adegenet

Jønsson, K. A., Fabre, P.-H., Ricklefs, R. E., & Fjeldså, J. (2011). Major global radiation of corvoid birds originated in the proto-Papuan archipelago. *Proceedings of the National Academy of Sciences*, *108*(6), 2328–2333. https://doi.org/10.1073/pnas.1018956108

Kirkpatrick, M., & Barton, N. (1997). Evolution of a species' range. *The American Naturalist*, *150*(1), 1–23.

Kitada, S., Nakamichi, R., & Kishino, H. (2021). Understanding population structure in an evolutionary context: Population-specific FST and pairwise FST. *G3: Genes, Genomes, Genetics*, *11*(11). https://doi.org/10.1093/g3journal/jkab316

Kottler, E. J., Dickman, E. E., Sexton, J. P., Emery, N. C., & Franks, S. J. (2021). Draining the Swamping Hypothesis: Little Evidence that Gene Flow Reduces Fitness at Range Edges.

Trends in Ecology and Evolution, *36*(6), 533–544. https://doi.org/10.1016/j.tree.2021.02.004

Lee-Yaw, J. A., Kharouba, H. M., Bontrager, M., Mahony, C., Csergo, A. M., Noreen, A. M. E., Li, Q., Schuster, R., & Angert, A. L. (2016). A synthesis of transplant experiments and ecological niche models suggests that range limits are often niche limits. *Ecology Letters*, *19*(6), 710–722. https://doi.org/10.1111/ele.12604

Lindgren, F., & Rue, H. (2015). Bayesian spatial modelling with R-INLA. *Journal of Statistical Software*, *63*(19), 1–25. https://doi.org/10.18637/jss.v063.i19

Lomolino, M., Riddle, B., & Whittaker, R. (2016). *Biogeography: Biological diversity across space and time*. Sinauer Associates.

Mazel, F., Wüest, R. O., Gueguen, M., Renaud, J., Ficetola, G. F., Lavergne, S., & Thuiller, W. (2017). The Geography of Ecological Niche Evolution in Mammals. *Current Biology*, *27*(9), 1369–1374. https://doi.org/10.1016/j.cub.2017.03.046

Nei, M. (1987). *Molecular Evolutionary Genetics*. Columbia University Press.

Nei, M., & Chesser, R. K. (1983). Estimation of fixation indices and gene diversities. *Annals of Human Genetics*, *47*(3), 253–259. https://doi.org/10.1111/j.1469-1809.1983.tb00993.x

Pironon, S., Papuga, G., Villellas, J., Angert, A. L., García, M. B., & Thompson, J. D. (2017). Geographic variation in genetic and demographic performance: New insights from an old biogeographical paradigm. *Biological Reviews*, *92*(4), 1877–1909. https://doi.org/10.1111/brv.12313

Platts, P. J., Mason, S. C., Palmer, G., Hill, J. K., Oliver, T. H., Powney, G. D., Fox, R., & Thomas, C. D. (2019). Habitat availability explains variation in climate-driven range shifts across multiple taxonomic groups. *Scientific Reports*, *9*(1), 1–10. https://doi.org/10.1038/s41598-019-51582-2

494 Polechová, J. (2018). Is the sky the limit? On the expansion threshold of a species' range. *PLOS*
495 *Biology*, *16*(6), e2005372. https://doi.org/10.1371/journal.pbio.2005372
496 Polechová, J., & Barton, N. H. (2015). Limits to adaptation along environmental gradients.
497 *Proceedings of the National Academy of Sciences of the United States of America*,
498 *112*(20), 6401–6406. https://doi.org/10.1073/pnas.1421515112
499 Pollock, L. J., Thuiller, W., & Jetz, W. (2017). Large conservation gains possible for global
500 biodiversity facets. *Nature*, *546*(7656), 141–144. https://doi.org/10.1038/nature22368
501 R Core Team. (2021). *R: A Language and Environment for Statistical Computing*. R Foundation
502 for Statistical Computing. https://www.r-project.org/
503 Rubenstein, M. A., Weiskopf, S. R., Bertrand, R., Carter, S. L., Comte, L., Eaton, M. J., Johnson,
504 C. G., Lenoir, J., Lynch, A. J., Miller, B. W., Morelli, T. L., Rodriguez, M. A., Terando,
505 A., & Thompson, L. M. (2023). Climate change and the global redistribution of
506 biodiversity: Substantial variation in empirical support for expected range shifts.
507 *Environmental Evidence*, 1–21. https://doi.org/10.1186/s13750-023-00296-0
508 Sagarin, R. D., & Gaines, S. D. (2002). The "abundant centre" distribution: To what extent is it a
509 biogeographical rule? *Ecology Letters*, *5*(1), 137–147. https://doi.org/10.1046/j.1461-
510 0248.2002.00297.x
511 Sagarin, R. D., Gaines, S. D., & Gaylord, B. (2006). Moving beyond assumptions to understand
512 abundance distributions across the ranges of species. *Trends in Ecology and Evolution*,
513 *21*(9), 524–530. https://doi.org/10.1016/j.tree.2006.06.008
514 Santini, L., Pironon, S., Maiorano, L., & Thuiller, W. (2019). Addressing common pitfalls does
515 not provide more support to geographical and ecological abundant-centre hypotheses.
516 *Ecography*, *42*(4), 696–705. https://doi.org/10.1111/ecog.04027

Schmidt, C., Domaratzki, M., Kinnunen, R. P., Bowman, J., & Garroway, C. J. (2020). Continent-wide effects of urbanization on bird and mammal genetic diversity. *Proceedings of the Royal Society B: Biological Sciences*, *287*(1920), 20192497. https://doi.org/10.1098/rspb.2019.2497

Schmidt, C., & Garroway, C. J. (2022). Systemic racism alters wildlife genetic diversity. *Proceedings of the National Academy of Sciences*, *119*(43), 0–3. https://doi.org/10.1073/pnas.2102860119

Schmidt, C., Muñoz, G., Lancaster, L. T., Lessard, J., Marske, K. A., Marshall, K. E., & Garroway, C. J. (2022). Population demography maintains biogeographic boundaries. *Ecology Letters*, *25*(8), 1905–1913. https://doi.org/10.1111/ele.14058

Sclater, P. L. (1858). On the general Geographical Distribution of the Members of the Class Aves. *Journal of the Proceedings of the Linnean Society: Zoology*, *2*, 130–145.

Singhal, S., Wrath, J., & Rabosky, D. L. (2022). Genetic variability and the ecology of geographic range: A test of the central-marginal hypothesis in Australian scincid lizards. *Molecular Ecology*, *31*(16), 4242–4253. https://doi.org/10.1111/mec.16589

Soberón, J., Peterson, A. T., & Osorio-Olvera, L. (2018). A comment on "Species are not most abundant in the centre of their geographic range or climatic niche." *Rethinking Ecology*, *3*, 13–18. https://doi.org/10.3897/rethinkingecology.3.24827

Spiegelhalter, D. J., Best, N. G., Carlin, B. P., & Van Der Linde, A. (2002). Bayesian measures of model complexity and fit. *Journal of the Royal Statistical Society: Series B (Statistical Methodology)*, *64*(4), 583–639. https://doi.org/10.1111/1467-9868.00353

Udvardy, M. D. F. (1975). A classification of the biogeographical provinces of the world. In *IUCN Occasional Paper no. 18, International Union for Conservation of Nature* (Issue 8).

von Humboldt, F. H. A. (1807). *Essai sur la geographie des plantes*. von Humboldt.

Wallace, A. R. (1876). *The Geographical Distribution of Animals: With a Study of the Relations of Living and Extinct Faunas as Elucidating the Past Changes of the Earth's Surface* (Vol. 1). Cambridge University Press. https://doi.org/10.1017/CBO9781139097109

Weir, B. S., & Goudet, J. (2017). A Unified Characterization of Population Structure and Relatedness. *Genetics*, *206*(4), 2085–2103. https://doi.org/10.1534/genetics.116.198424

Zurell, D., Jeltsch, F., Dormann, C. F., & Schröder, B. (2009). Static species distribution models in dynamically changing systems: How good can predictions really be? *Ecography*, *32*(5), 733–744. https://doi.org/10.1111/j.1600-0587.2009.05810.x

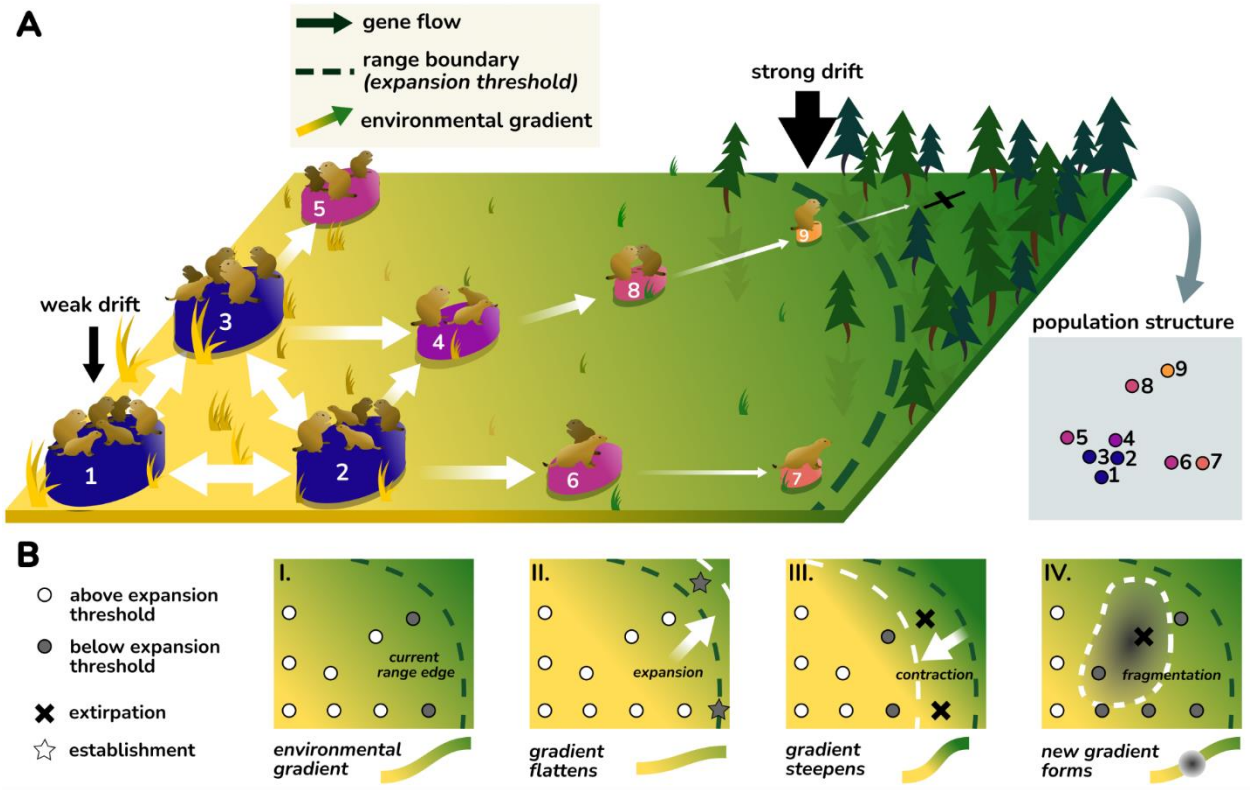

551 **Fig. 1. Conceptual model of drift-limited range expansion.** (**A**) Population sizes are larger and
552 more well-connected toward the range interior where environments are more suitable
553 (populations 1-3). As the environment changes, populations become smaller, more isolated, and
554 more genetically differentiated (populations 4-9). Expansion thresholds form when populations
555 are so small that genetic drift overwhelms natural selection and adaptation is no longer possible
556 (populations 7 and 9). (**B**) Expansion thresholds shift with underlying environmental gradients.
557 Ranges can expand or contract if environmental gradients flatten (II) or steepen (III). Expansion
558 thresholds can also form within species ranges (IV) if new environmental gradients arise (e.g.,
559 urbanization, agricultural gradients), leading to range fragmentation.
560

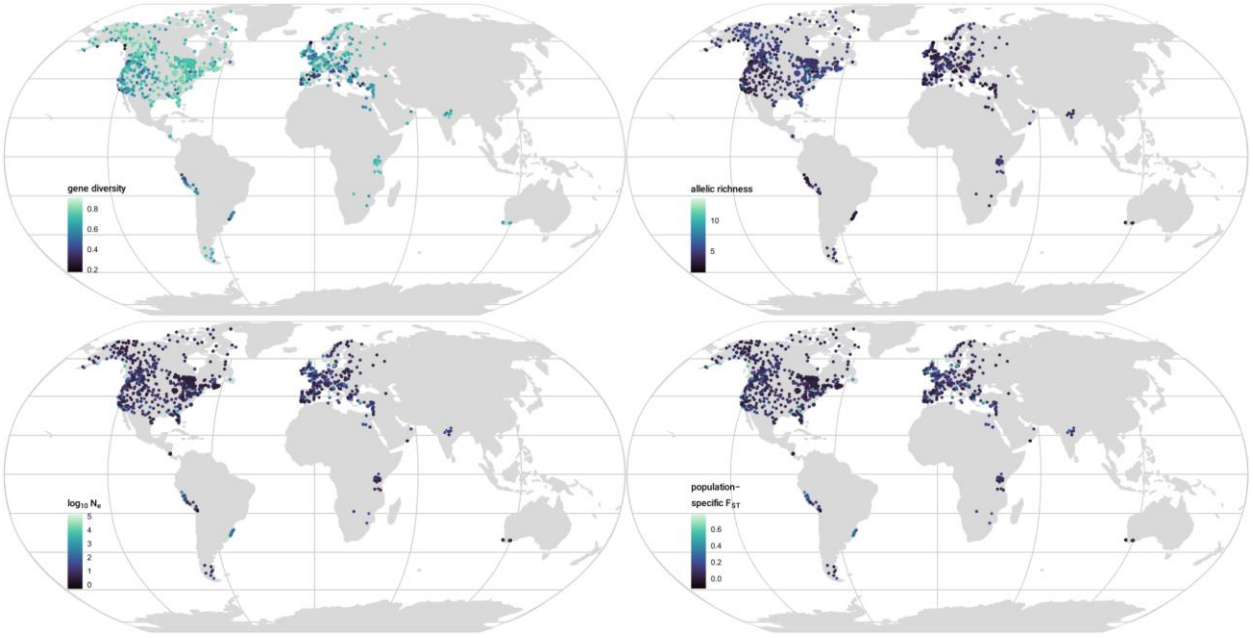

Fig. 2. Genetic data from 1271 locations of 59 mammal species. The spatial distribution of genetic data from 1271 sample locations is shown for each of the four summary statistics measured. Gene diversity and allelic richness are metrics of diversity, effective population size (N_e) measures the strength of genetic drift, and population-specific F_{ST} (fixation index) is a measure of genetic differentiation.

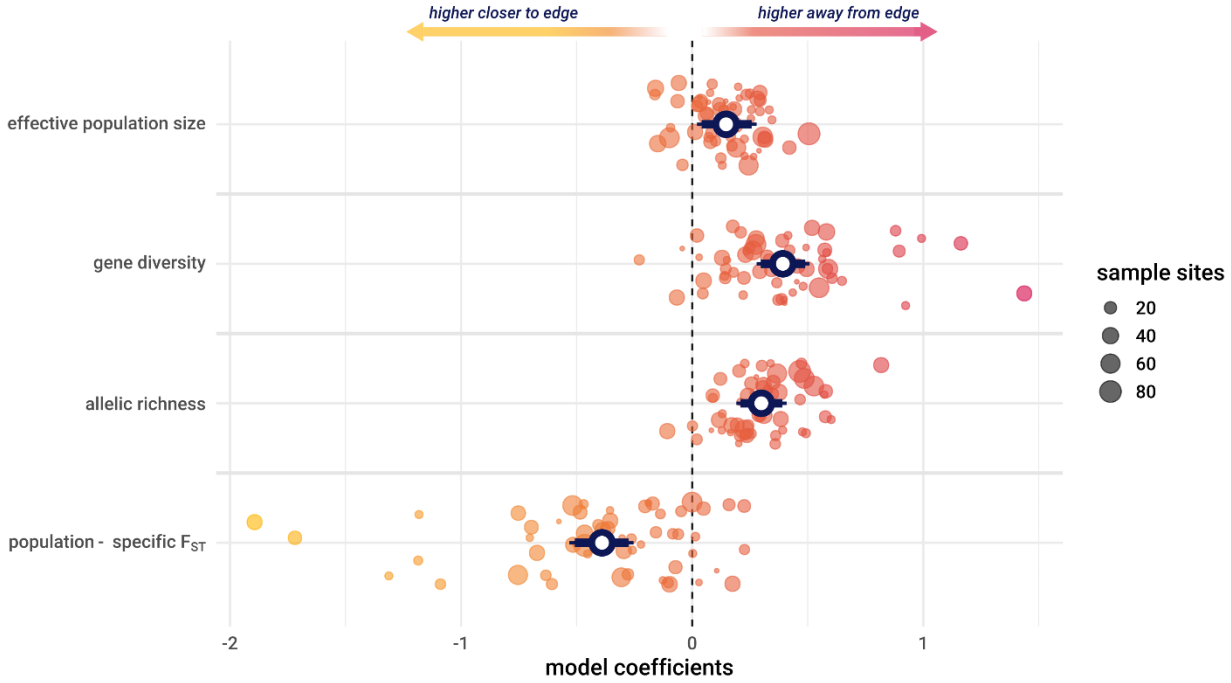

Fig. 3. Variation in genetic diversity and differentiation across species ranges. Model coefficients of the relationship between range position (distance to the edge of range convex hull) and each genetic metric (y axis) from Bayesian generalized mixed models controlling for the spatial distribution of sites and species relatedness. Effective population size is a contemporary effective size estimated using the linkage disequilibrium method for single-samples (SI Methods). Gene diversity and allelic richness (rarefied) are two metrics of genetic diversity. Population-specific F_{ST} is a measure of genetic differentiation that estimates how far single populations have diverged from a common ancestor of all sites in the sample. Open circles represent the relationship between range position and genetic metrics across all species with 90% (thin lines) and 95% (thick lines) credible intervals. Filled circles are estimated species-specific relationships between range position and the genetic metrics. The dashed vertical line indicates an effect size of 0. Positive effect sizes indicate genetic diversity and connectivity increase with increasing distance from the range edge, while negative effect sizes mean genetic diversity is reduced and populations are more differentiated closer to the range edge.

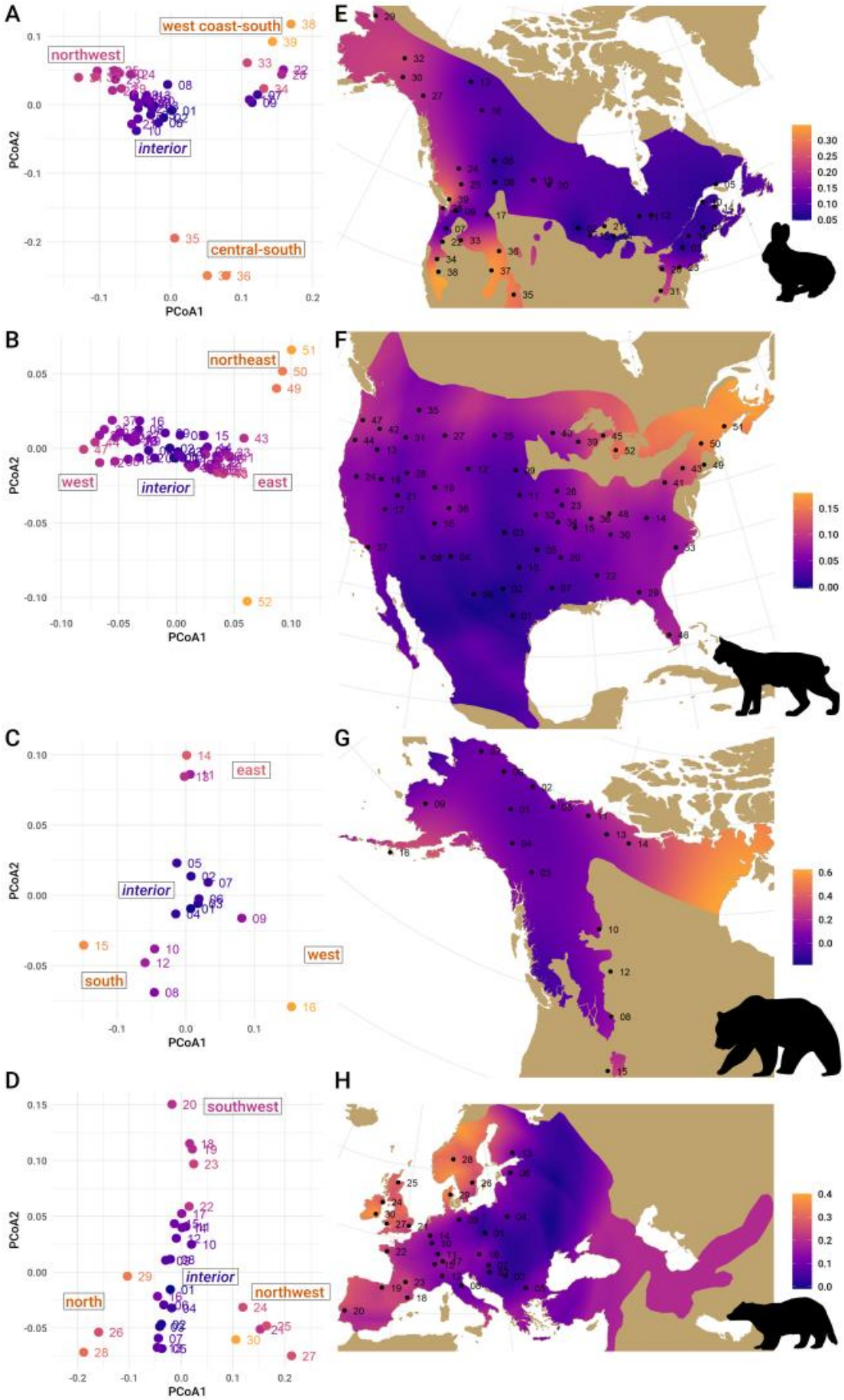
A
west coast-south
northwest
interior
central-south
PCoA1
PCoA2
E
0.30
0.25
0.20
0.15
0.10
0.05
B
northeast
west
interior
east
F
0.15
0.10
0.05
0.00
C
east
interior
west
south
G
0.6
0.4
0.2
0.0
D
southwest
interior
north
northwest
H
0.4
0.3
0.2
0.1
0.0

Fig. 4. Patterns of range-wide population differentiation. Spatial population structure is mapped for species with whole range coverage: snowshoe hare (*Lepus americanus*), bobcat (*Lynx rufus*), grizzly bear (*Ursus arctos*), and Eurasian badger (*Meles meles*); see Fig S4 for additional species. Colors represent population-specific F_{ST} values, with darker blue colors depicting sample sites that are less genetically differentiated from the common ancestor of all sites in the sample relative to orange colored sites, which are the most strongly differentiated. Plots (**A-D**) show major axes of population differentiation from a principal coordinates analyses (PCoA) of Nei's pairwise-F_{ST}, which measures the magnitude of genetic differentiation between pairs of sites. Sites that are least differentiated from the common ancestor are the most well-connected by gene flow (centrally located in PCoA plots). Labels indicate spatial direction of differentiation that correspond to maps in (**E-H**). Large dark blue areas across maps suggests that larger, well-connected core populations can cover large proportions of the species range and are not limited to the geographic range center.

Table 1. Summaries of Bayesian hierarchical models relating genetic metrics to range position. The effect size of range position is given with 95% credible intervals. Range position is described by the distance to the edge of the range convex hull. Models controlled for spatial and phylogenetic correlation. $\sigma_{intercept}$ is the standard deviation of species-specific intercepts, and summarizes variation in mean genetic diversity, effective population size, or F_{ST} across species. σ_{slope} is the standard deviation of species-specific estimates of the effect of distance, and shows variation in species responses to range position. Marginal log-likelihood and DIC (Deviance Information Criterion) are two model fit metrics.

Variable	Range position	$\sigma_{intercept}$	σ_{slope}	Marginal log likelihood	DIC
gene diversity	0.39 (0.28 – 0.51)	0.83 (0.72 – 0.98)	0.41 (0.34 – 0.47)	-985.80	928.06
allelic richness	0.30 (0.19 – 0.41)	0.56 (0.37 – 0.85)	0.32 (0.29 – 0.35)	-1346.52	805.97
effective population size	0.15 (0.02 – 0.23)	0.43 (0.40 – 0.46)	0.32 (0.25 – 0.39)	-950.99	2312.83
population-specific F_{ST}	-0.39 (-0.53 – -0.25)	0.51 (0.37 – 0.69)	0.58 (0.40 – 0.80)	-1616.84	637.75

Supplementary Materials

Figures S1 - S4

Tables S1 - S3

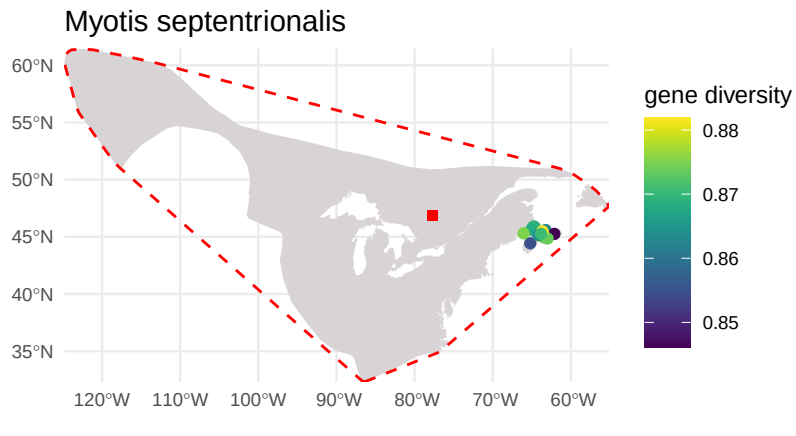
Myotis septentrionalis
60°N
55°N
50°N
45°N
40°N
35°N
120°W
110°W
100°W
90°W
80°W
70°W
60°W
gene diversity
0.88
0.87
0.86
0.85

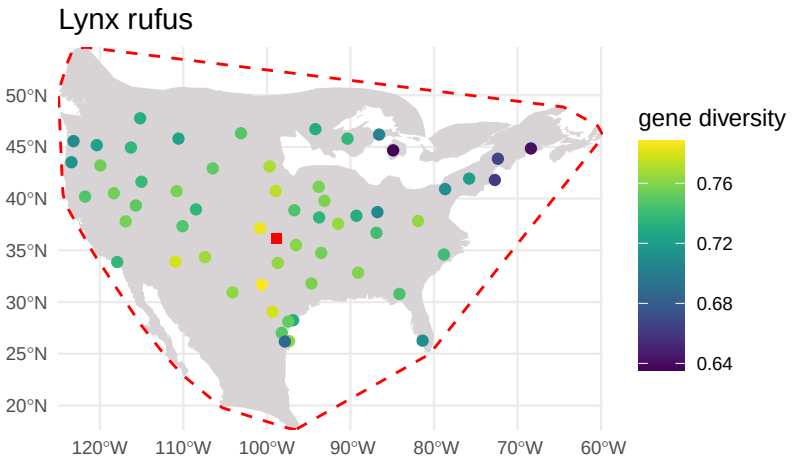
Lynx rufus
50°N
45°N
40°N
35°N
30°N
25°N
20°N
120°W
110°W
100°W
90°W
80°W
70°W
60°W
gene diversity
0.76
0.72
0.68
0.64

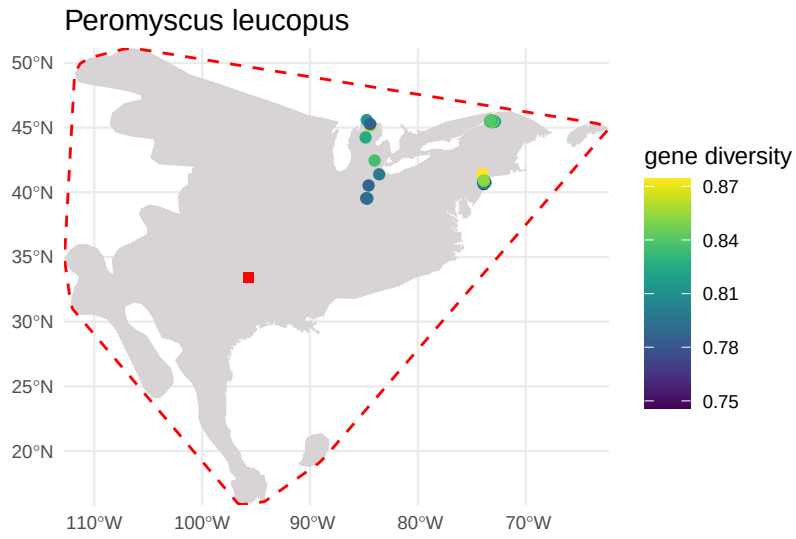
Peromyscus leucopus
50°N
45°N
40°N
35°N
30°N
25°N
20°N
110°W
100°W
90°W
80°W
70°W
gene diversity
0.87
0.84
0.81
0.78
0.75

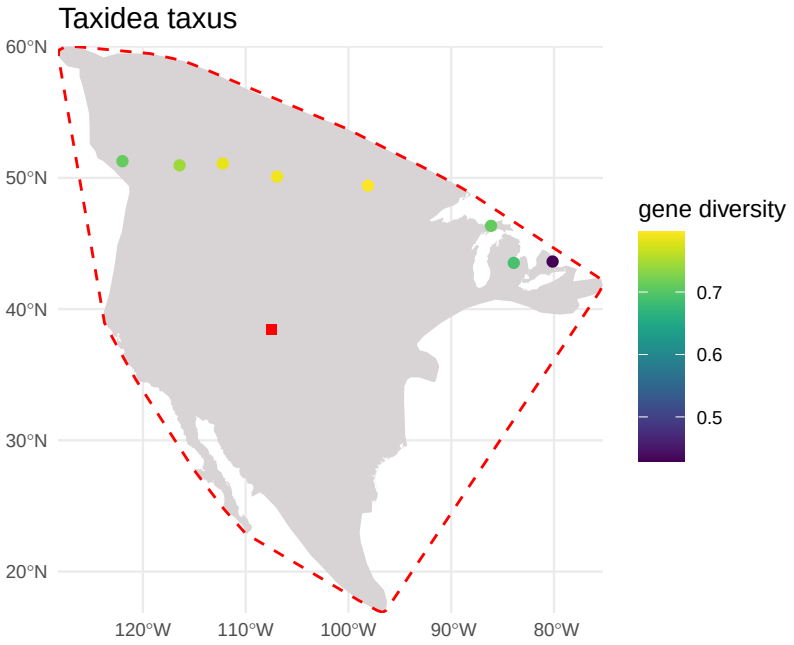
Taxidea taxus
60°N
50°N
40°N
30°N
20°N
120°W
110°W
100°W
90°W
80°W
gene diversity
0.7
0.6
0.5

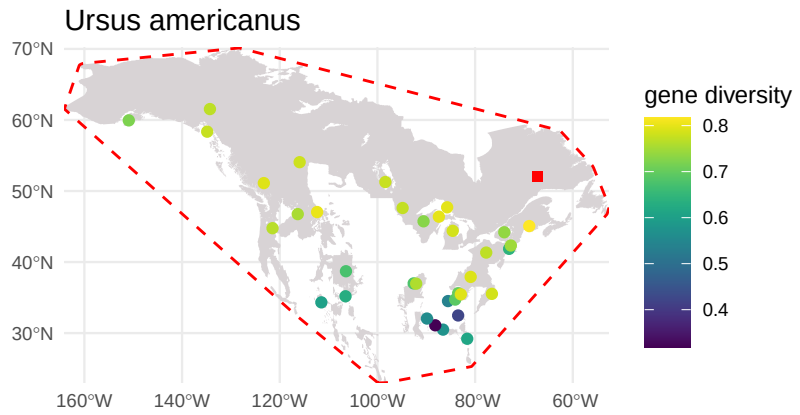
Ursus americanus
70°N
60°N
50°N
40°N
30°N
160°W
140°W
120°W
100°W
80°W
60°W
gene diversity
0.8
0.7
0.6
0.5
0.4

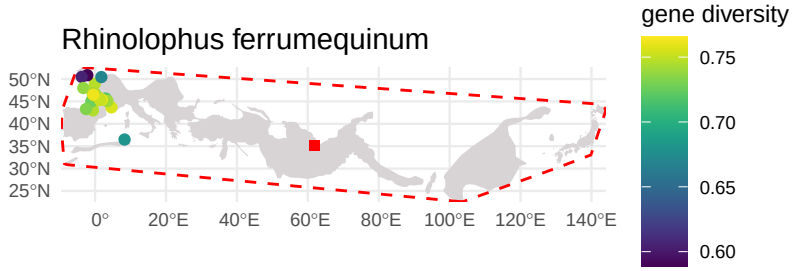
Rhinolophus ferrumequinum
50°N
45°N
40°N
35°N
30°N
25°N
0°
20°E
40°E
60°E
80°E
100°E
120°E
140°E
gene diversity
0.75
0.70
0.65
0.60

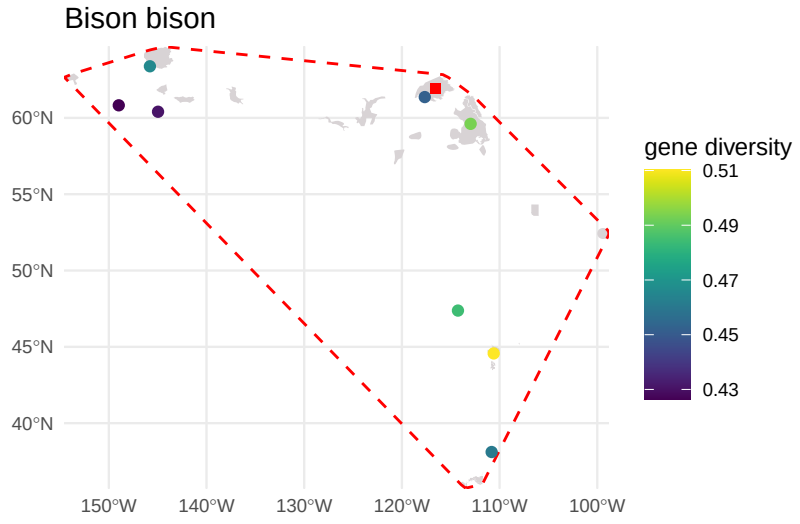
Bison bison
60°N
55°N
50°N
45°N
40°N
150°W
140°W
130°W
120°W
110°W
100°W
gene diversity
0.51
0.49
0.47
0.45
0.43

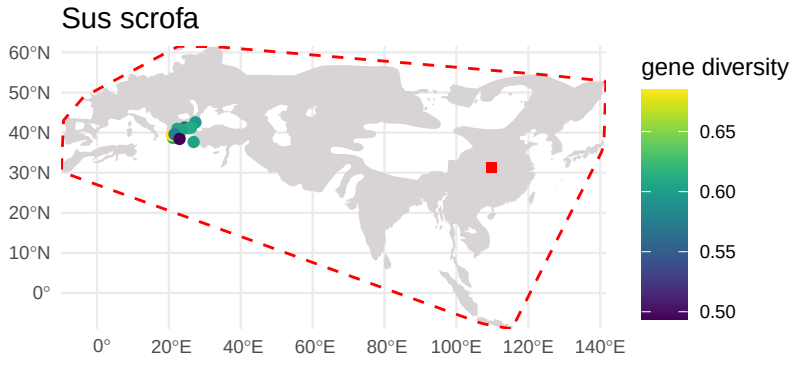
Sus scrofa
60°N
50°N
40°N
30°N
20°N
10°N
0°
0°
20°E
40°E
60°E
80°E
100°E
120°E
140°E
gene diversity
0.65
0.60
0.55
0.50

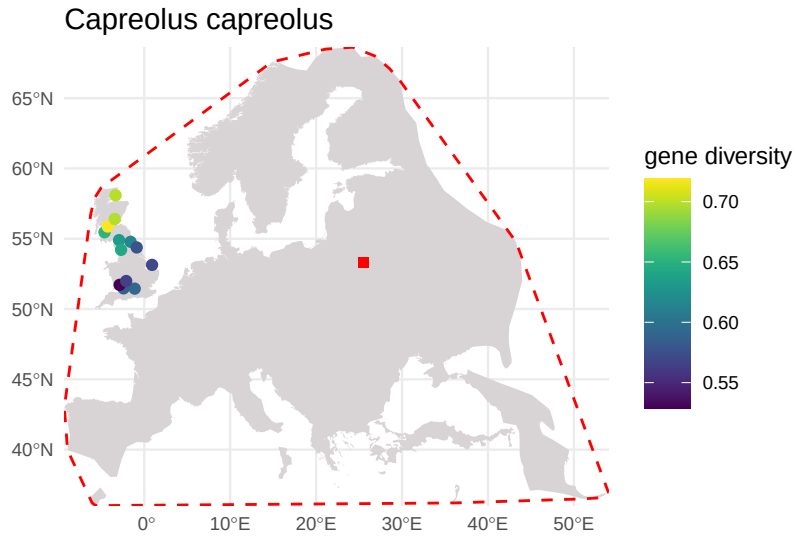
Capreolus capreolus
65°N
60°N
55°N
50°N
45°N
40°N
0°
10°E
20°E
30°E
40°E
50°E
gene diversity
0.70
0.65
0.60
0.55

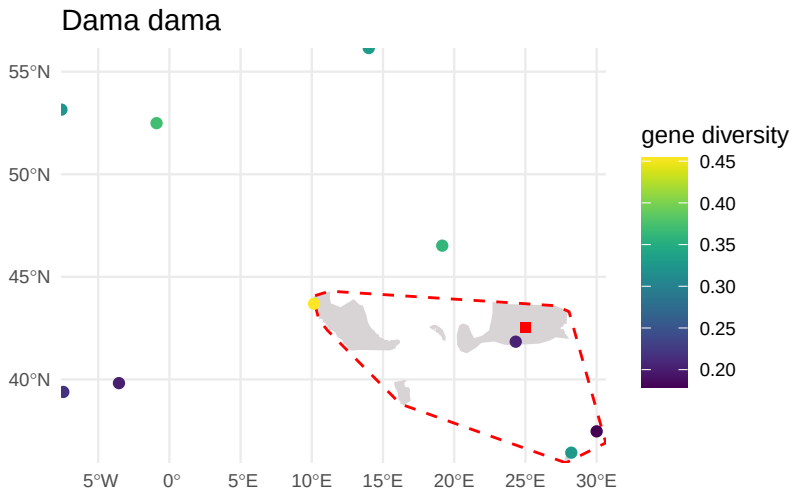
Dama dama
55°N
50°N
45°N
40°N
5°W
0°
5°E
10°E
15°E
20°E
25°E
30°E
gene diversity
0.45
0.40
0.35
0.30
0.25
0.20

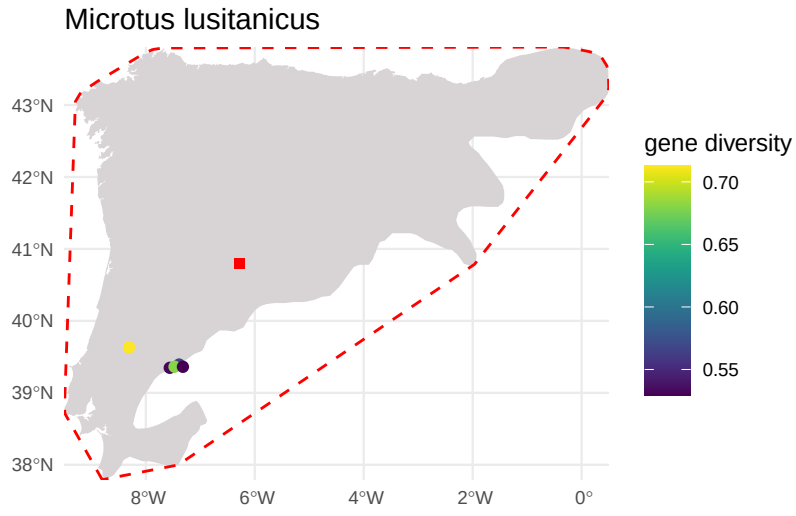
Microtus lusitanicus
43°N
42°N
41°N
40°N
39°N
38°N
8°W
6°W
4°W
2°W
0°
gene diversity
0.70
0.65
0.60
0.55

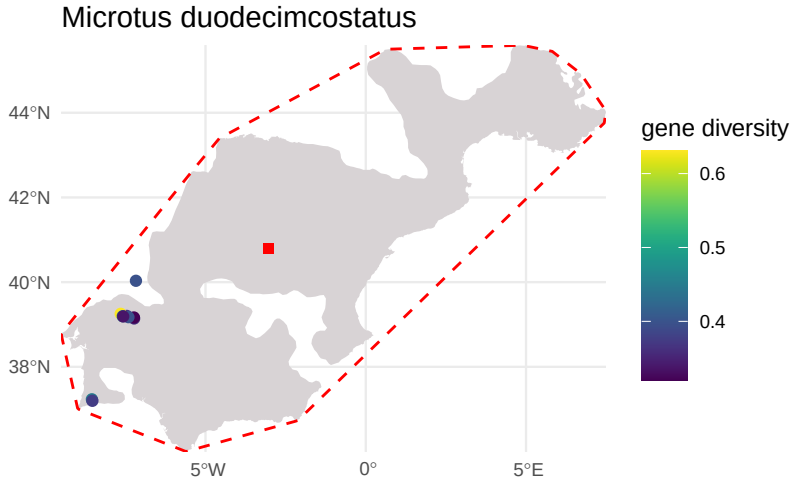
Microtus duodecimcostatus
44°N
42°N
40°N
38°N
5°W
0°
5°E
gene diversity
0.6
0.5
0.4

Myotis lucifugus

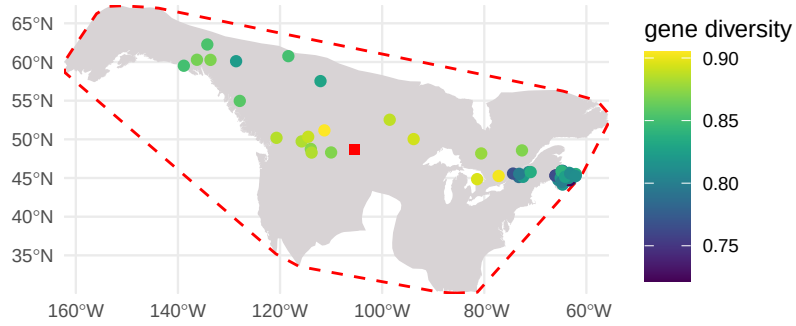

Pekania pennanti

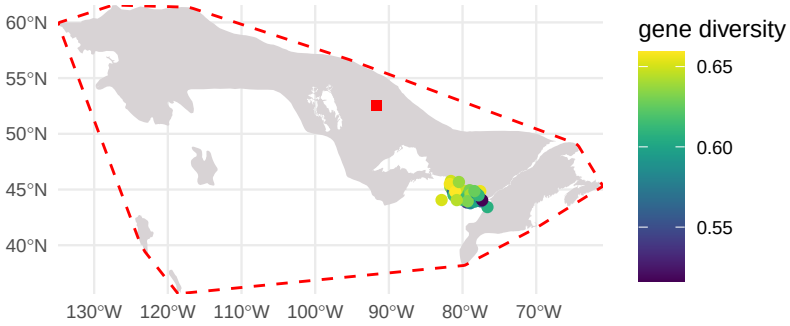

Nyctalus leisleri

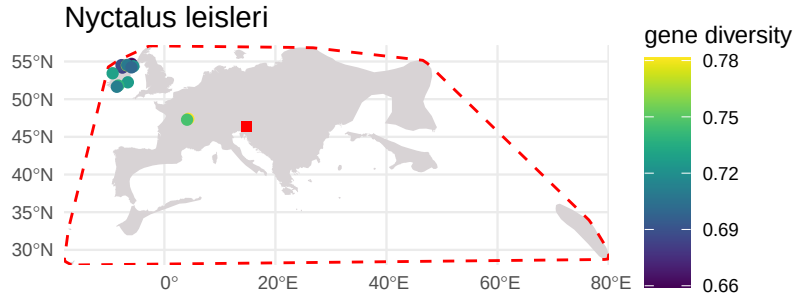

Artibeus jamaicensis

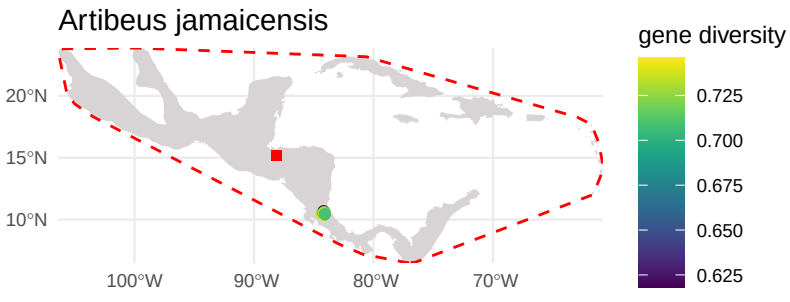

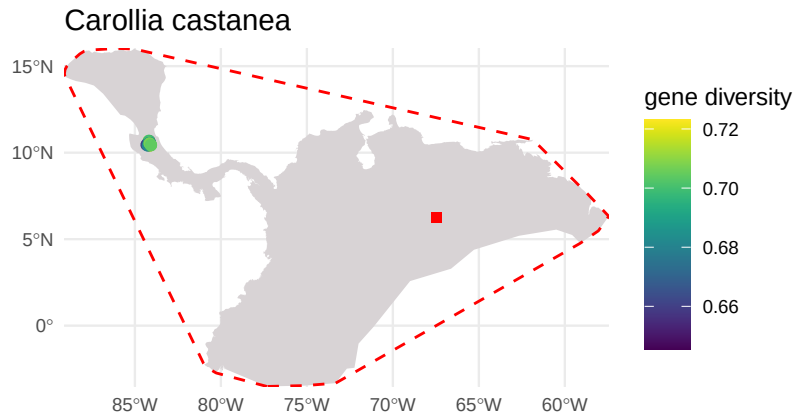
Carollia castanea
15°N
10°N
5°N
0°
85°W
80°W
75°W
70°W
65°W
60°W
gene diversity
0.72
0.70
0.68
0.66

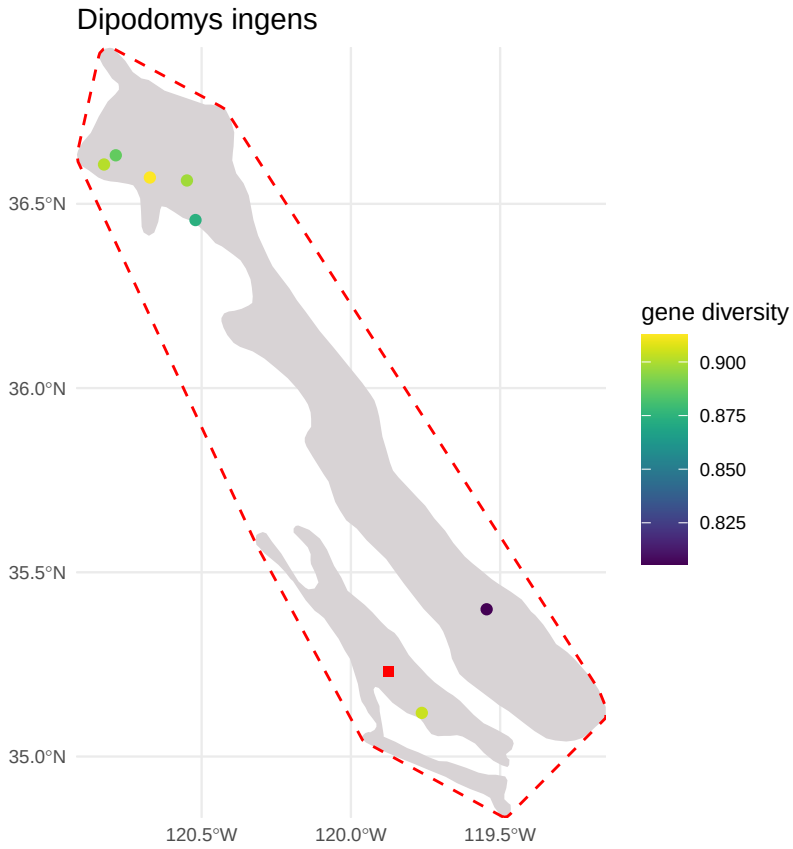
Dipodomys ingens
36.5°N
36.0°N
35.5°N
35.0°N
120.5°W
120.0°W
119.5°W
gene diversity
0.900
0.875
0.850
0.825

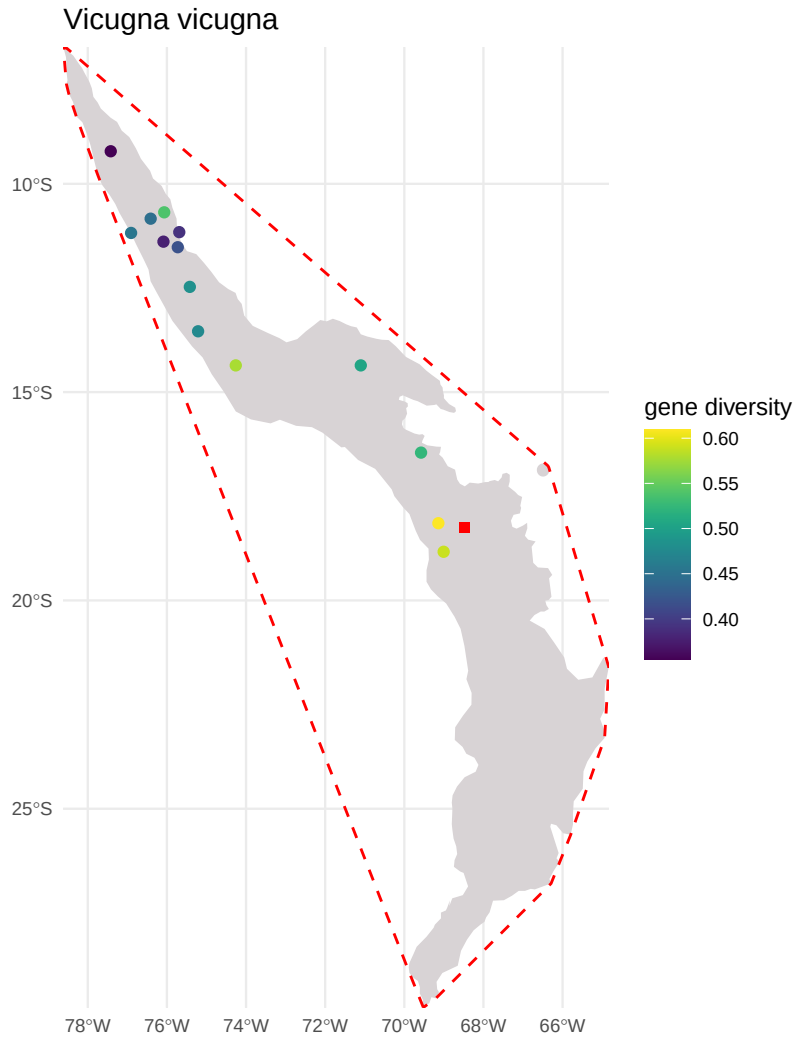
Vicugna vicugna
10°S
15°S
20°S
25°S
78°W
76°W
74°W
72°W
70°W
68°W
66°W
gene diversity
0.60
0.55
0.50
0.45
0.40

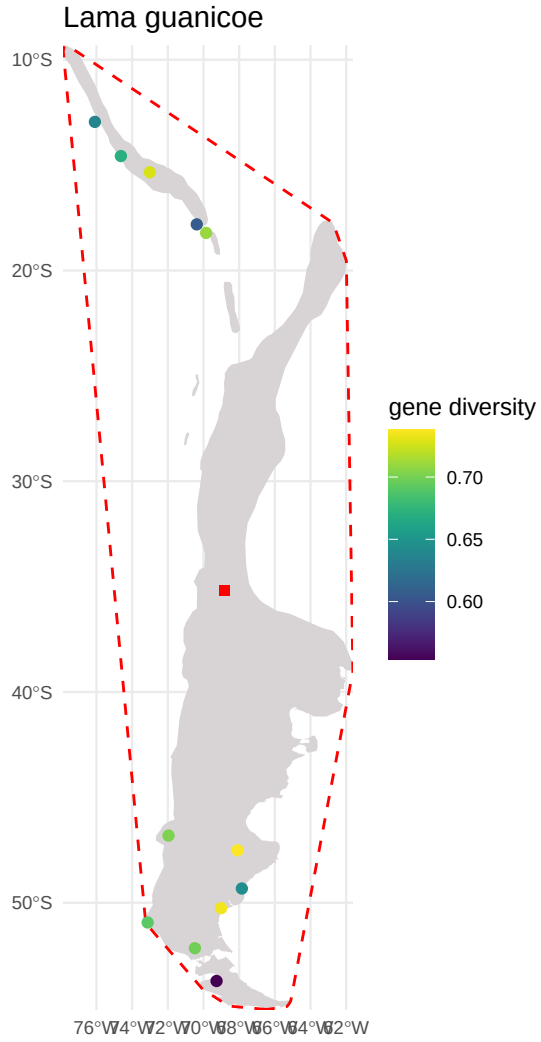
Lama guanicoe
10°S
20°S
30°S
40°S
50°S
76°W
74°W
72°W
70°W
68°W
66°W
64°W
62°W
gene diversity
0.70
0.65
0.60

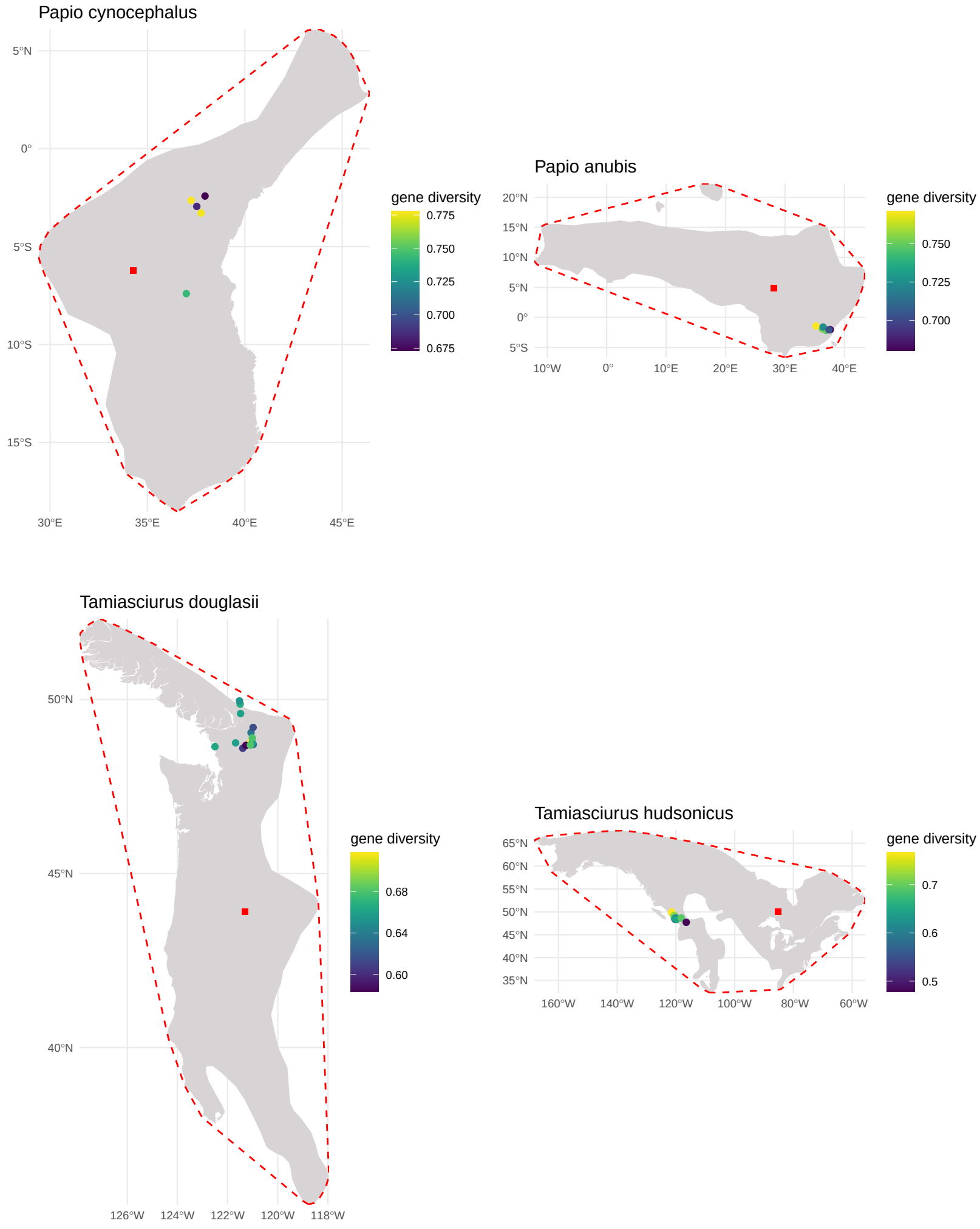
Papio cynocephalus
5°N
0°
5°S
10°S
15°S
30°E
35°E
40°E
45°E
gene diversity
0.775
0.750
0.725
0.700
0.675
Papio anubis
20°N
15°N
10°N
5°N
0°
5°S
10°W
0°
10°E
20°E
30°E
40°E
gene diversity
0.750
0.725
0.700
Tamiasciurus douglasii
50°N
45°N
40°N
126°W
124°W
122°W
120°W
118°W
gene diversity
0.68
0.64
0.60
Tamiasciurus hudsonicus
65°N
60°N
55°N
50°N
45°N
40°N
35°N
160°W
140°W
120°W
100°W
80°W
60°W
gene diversity
0.7
0.6
0.5

Lepus americanus

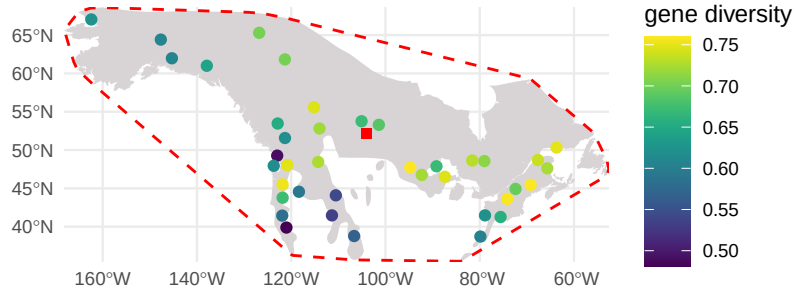

Ovis canadensis

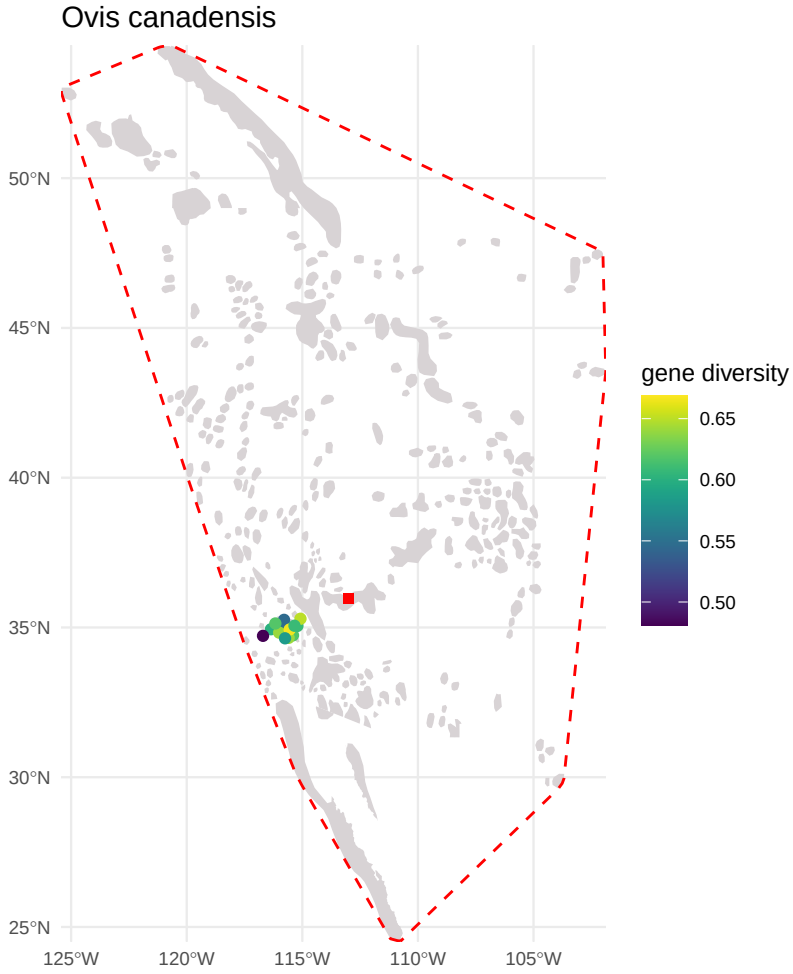

Rangifer tarandus

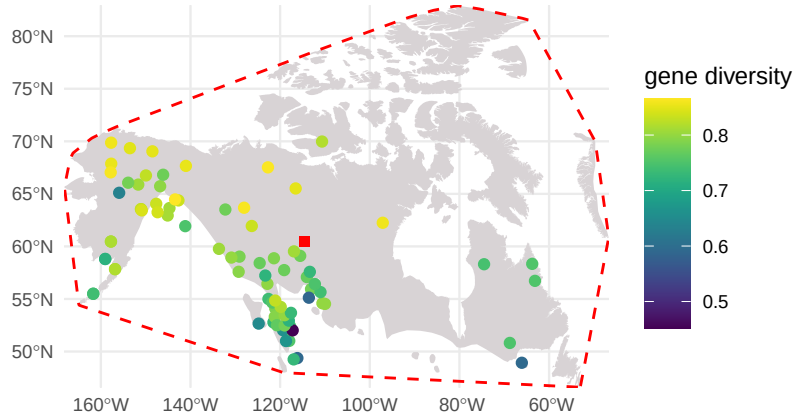

Ursus arctos

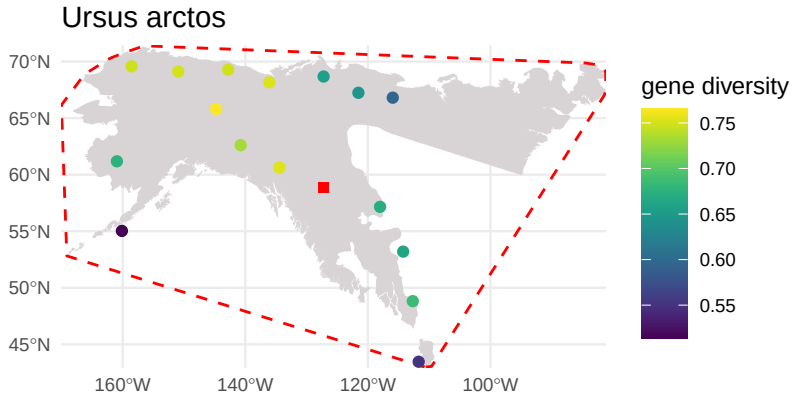

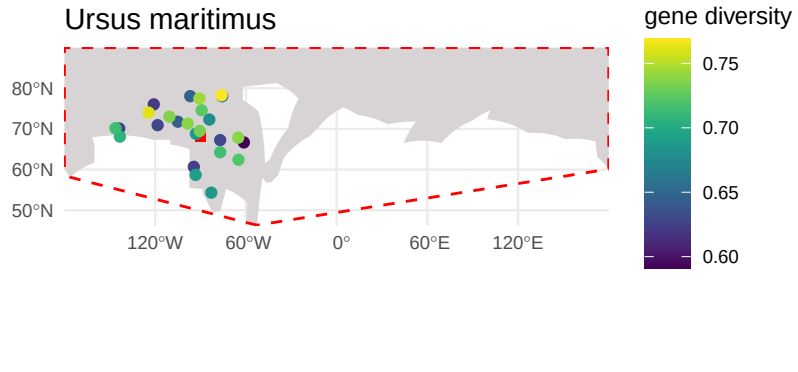
Ursus maritimus
gene diversity
0.75
0.70
0.65
0.60
80°N
70°N
60°N
50°N
120°W
60°W
0°
60°E
120°E

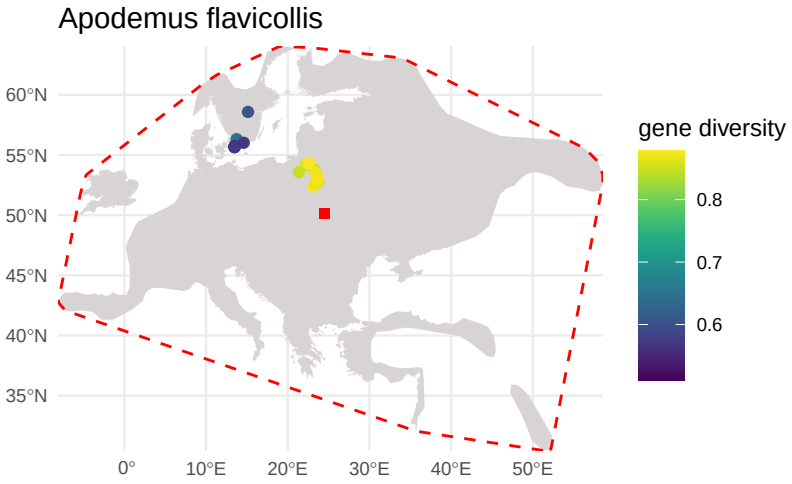
Apodemus flavicollis
gene diversity
0.8
0.7
0.6
60°N
55°N
50°N
45°N
40°N
35°N
0°
10°E
20°E
30°E
40°E
50°E

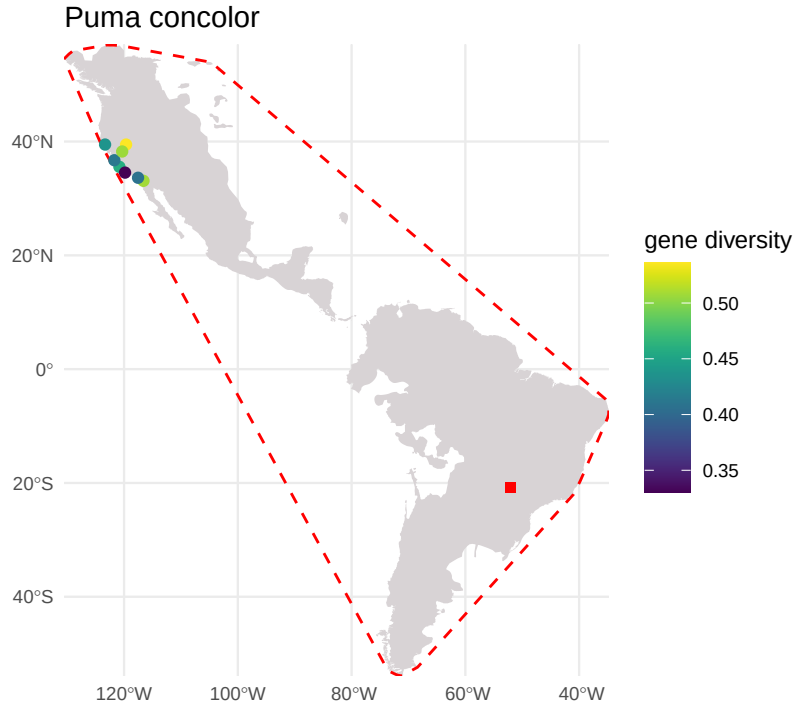
Puma concolor
gene diversity
0.50
0.45
0.40
0.35
40°N
20°N
0°
20°S
40°S
120°W
100°W
80°W
60°W
40°W

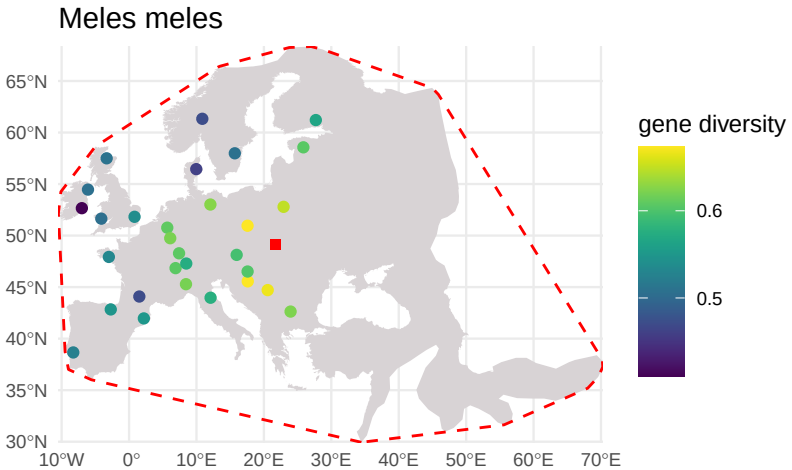
Meles meles
gene diversity
0.6
0.5
65°N
60°N
55°N
50°N
45°N
40°N
35°N
30°N
10°W
0°
10°E
20°E
30°E
40°E
50°E
60°E
70°E

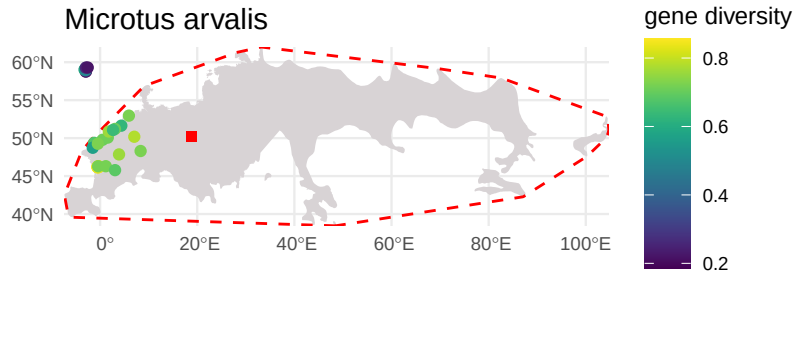
Microtus arvalis
60°N
55°N
50°N
45°N
40°N
0°
20°E
40°E
60°E
80°E
100°E
gene diversity
0.8
0.6
0.4
0.2

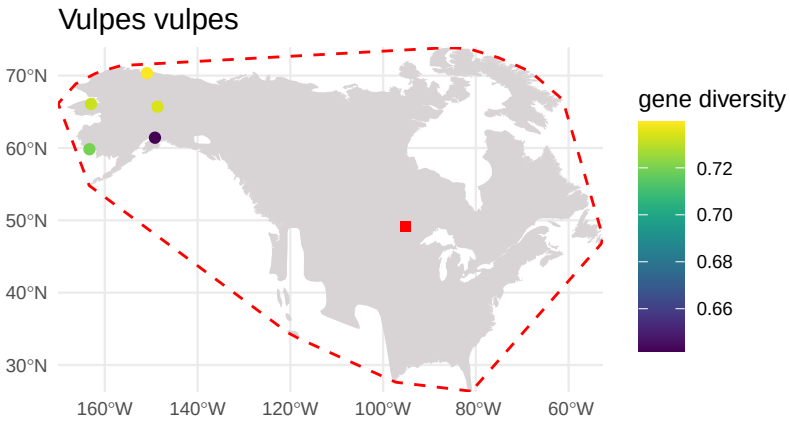
Vulpes vulpes
70°N
60°N
50°N
40°N
30°N
160°W
140°W
120°W
100°W
80°W
60°W
gene diversity
0.72
0.70
0.68
0.66

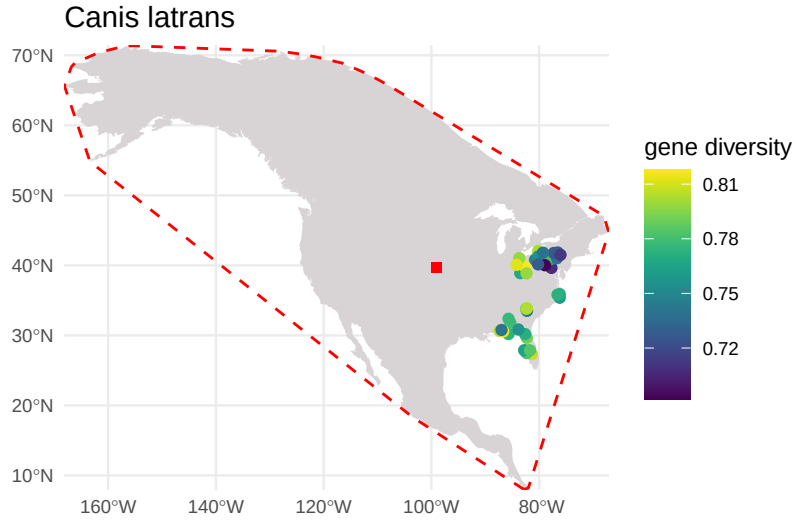
Canis latrans
70°N
60°N
50°N
40°N
30°N
20°N
10°N
160°W
140°W
120°W
100°W
80°W
gene diversity
0.81
0.78
0.75
0.72

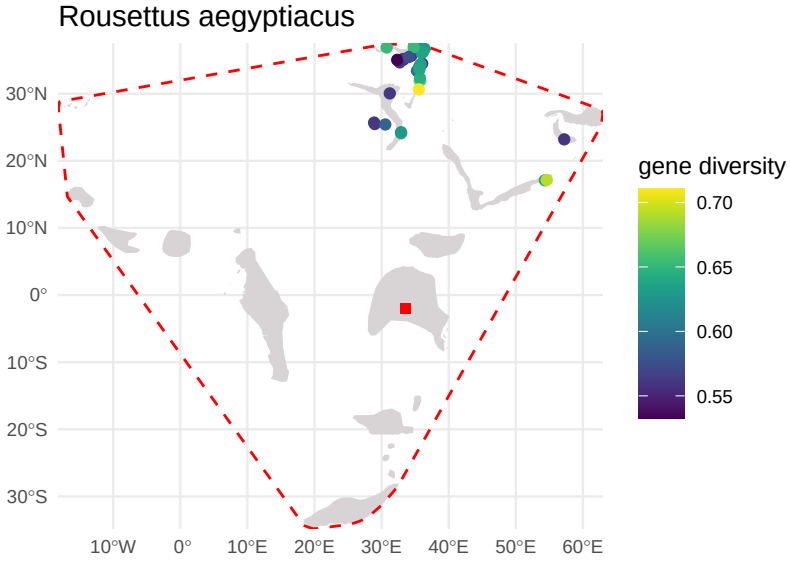
Rousettus aegyptiacus
30°N
20°N
10°N
0°
10°S
20°S
30°S
10°W
0°
10°E
20°E
30°E
40°E
50°E
60°E
gene diversity
0.70
0.65
0.60
0.55

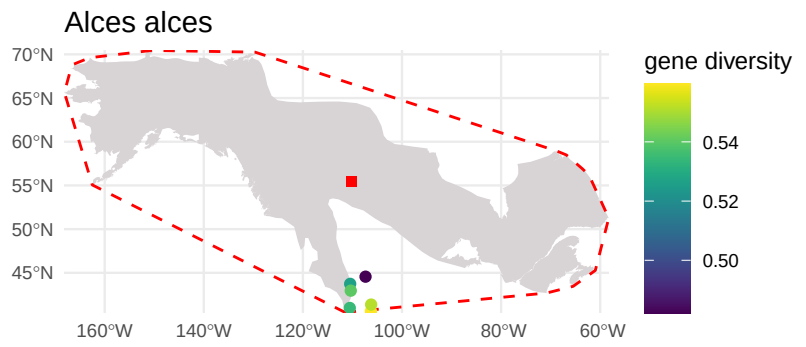
Alces alces
70°N
65°N
60°N
55°N
50°N
45°N
160°W
140°W
120°W
100°W
80°W
60°W
gene diversity
0.54
0.52
0.50

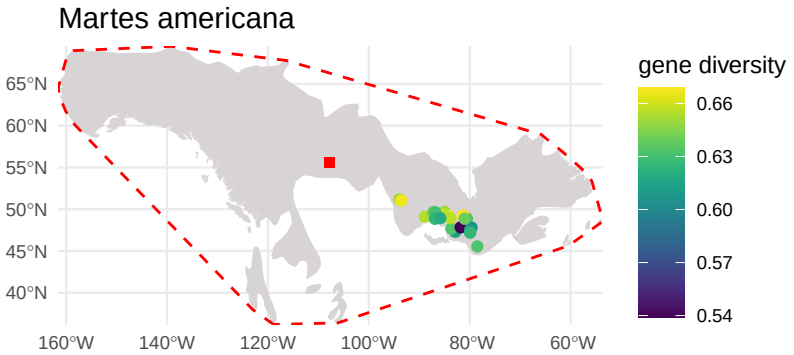
Martes americana
65°N
60°N
55°N
50°N
45°N
40°N
160°W
140°W
120°W
100°W
80°W
60°W
gene diversity
0.66
0.63
0.60
0.57
0.54

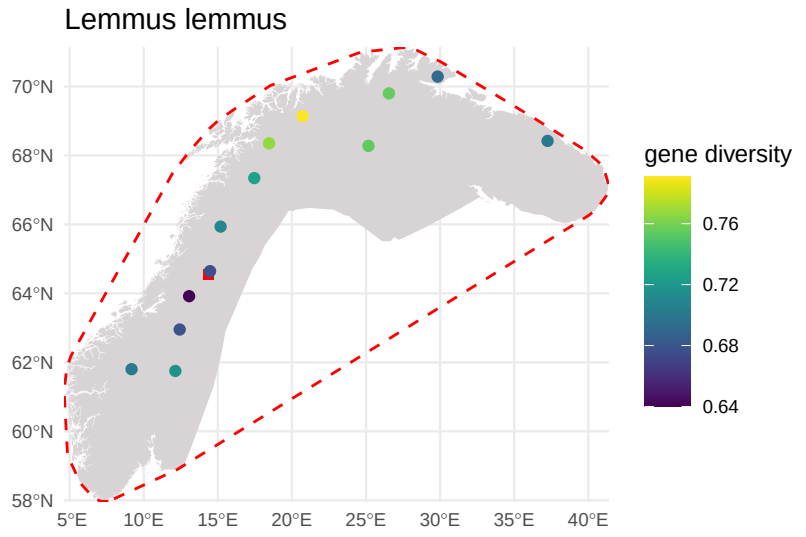
Lemmus lemmus
70°N
68°N
66°N
64°N
62°N
60°N
58°N
5°E
10°E
15°E
20°E
25°E
30°E
35°E
40°E
gene diversity
0.76
0.72
0.68
0.64

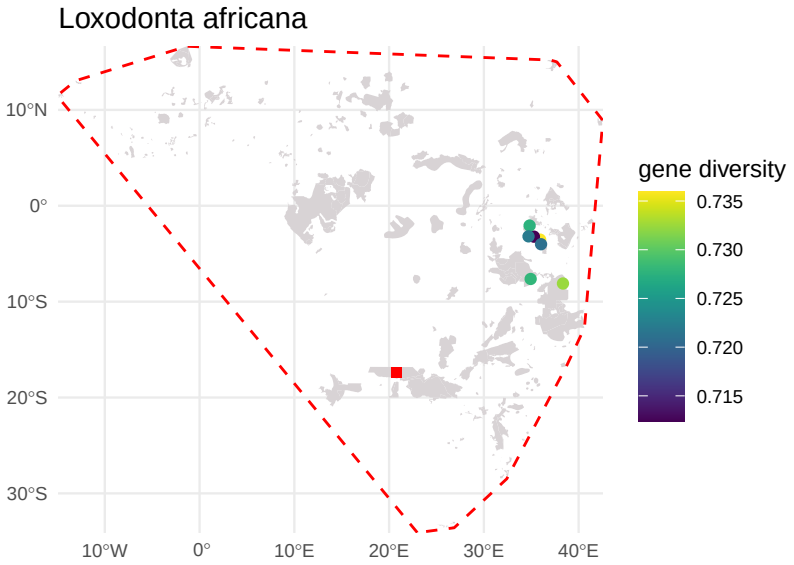
Loxodonta africana
10°N
0°
10°S
20°S
30°S
10°W
0°
10°E
20°E
30°E
40°E
gene diversity
0.735
0.730
0.725
0.720
0.715

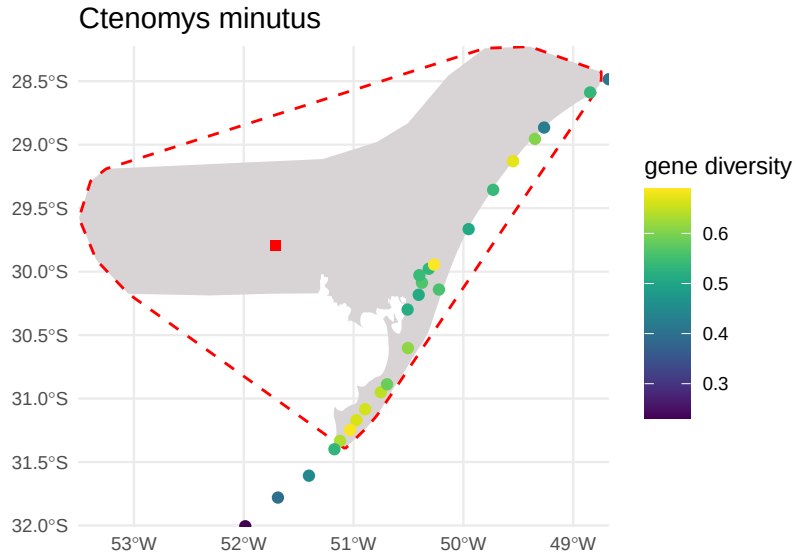
Ctenomys minutus
28.5°S
29.0°S
29.5°S
30.0°S
30.5°S
31.0°S
31.5°S
32.0°S
53°W
52°W
51°W
50°W
49°W
gene diversity
0.6
0.5
0.4
0.3

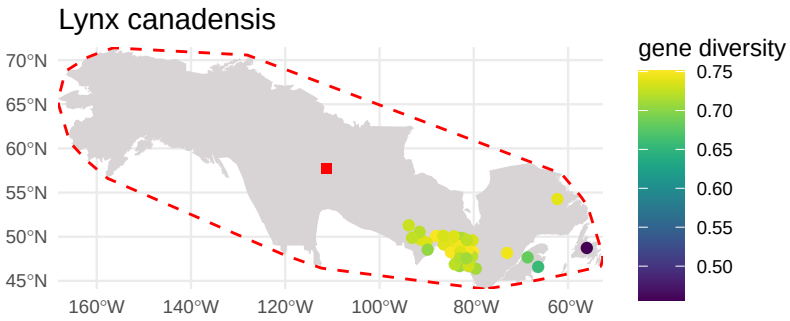
Lynx canadensis
70°N
65°N
60°N
55°N
50°N
45°N
160°W
140°W
120°W
100°W
80°W
60°W
gene diversity
0.75
0.70
0.65
0.60
0.55
0.50

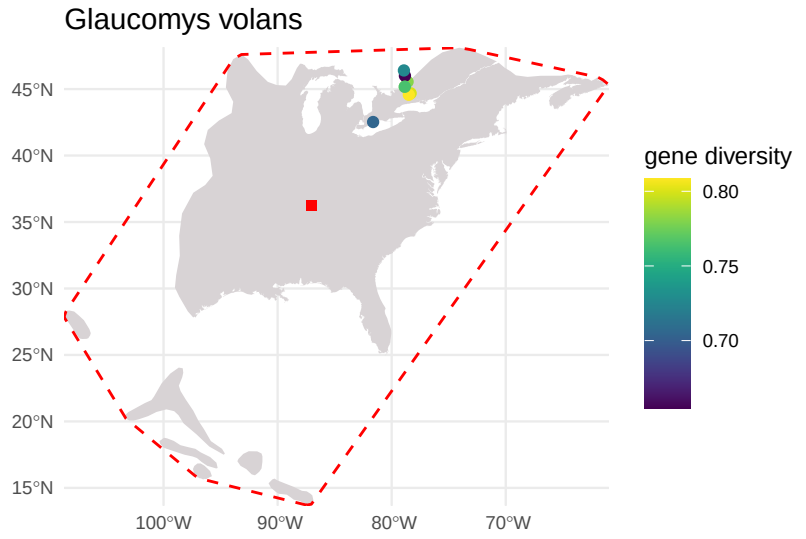
Glaucomys volans
45°N
40°N
35°N
30°N
25°N
20°N
15°N
100°W
90°W
80°W
70°W
gene diversity
0.80
0.75
0.70

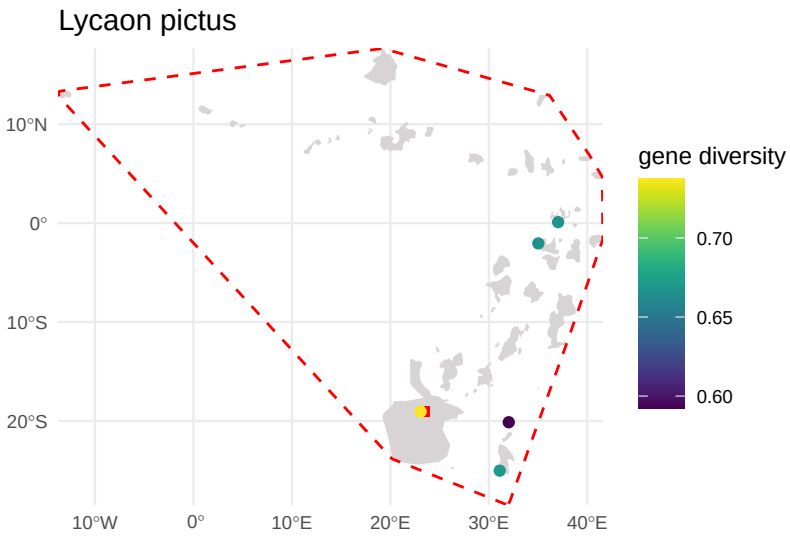
Lycaon pictus
10°N
0°
10°S
20°S
10°W
0°
10°E
20°E
30°E
40°E
gene diversity
0.70
0.65
0.60

Felis silvestris

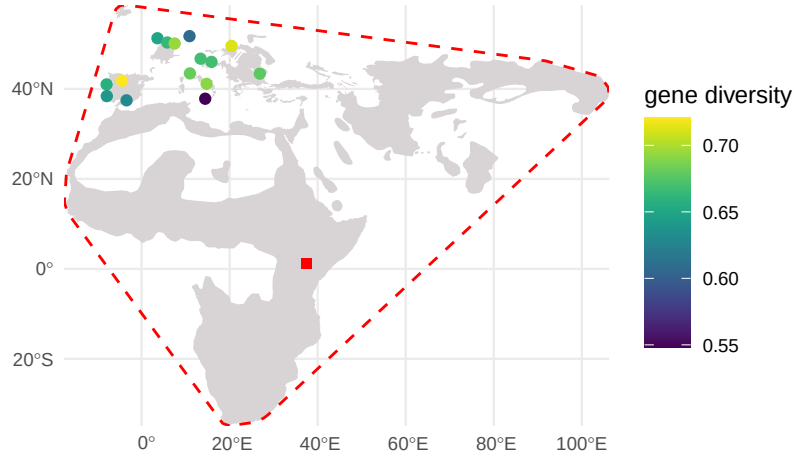

Lepus granatensis

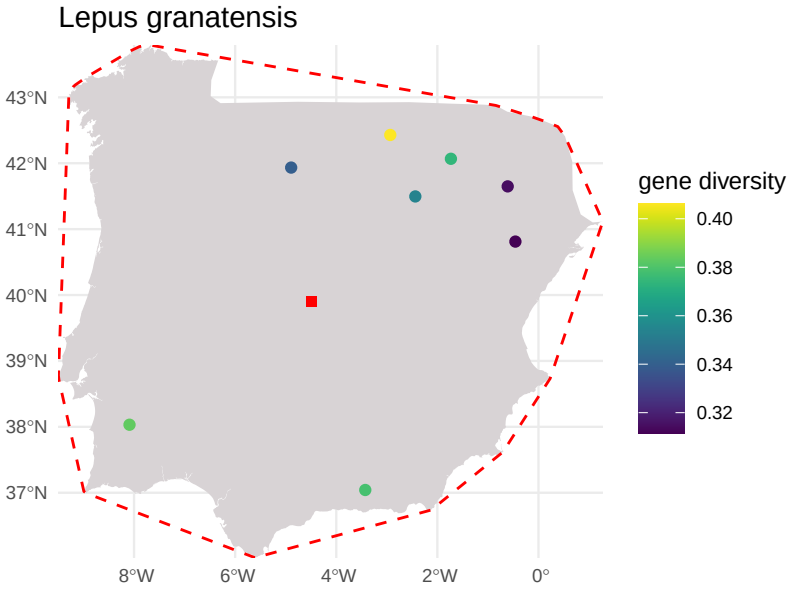

Lepus europaeus

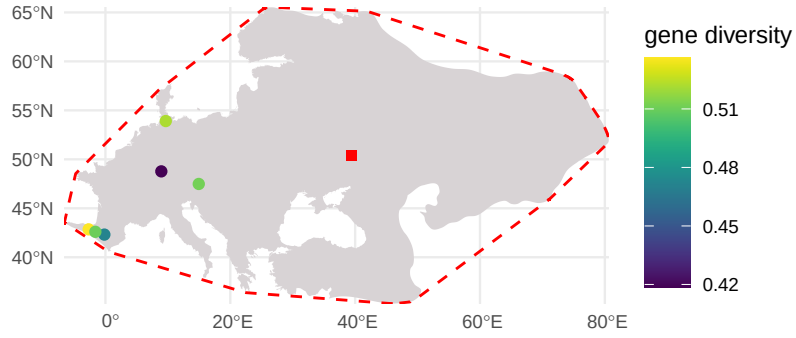

Eptesicus serotinus

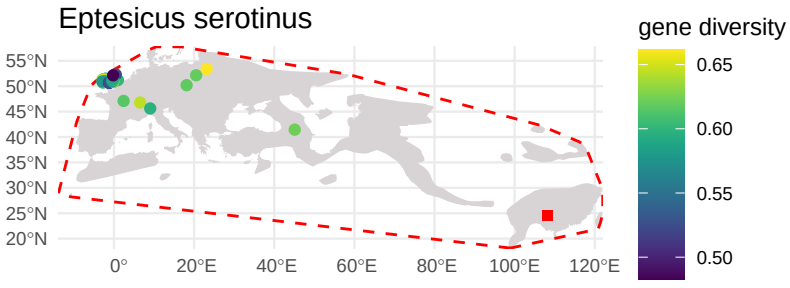

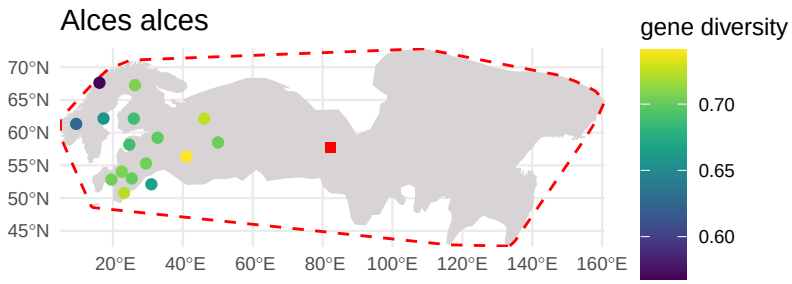
Alces alces
70°N
65°N
60°N
55°N
50°N
45°N
20°E
40°E
60°E
80°E
100°E
120°E
140°E
160°E
gene diversity
0.70
0.65
0.60

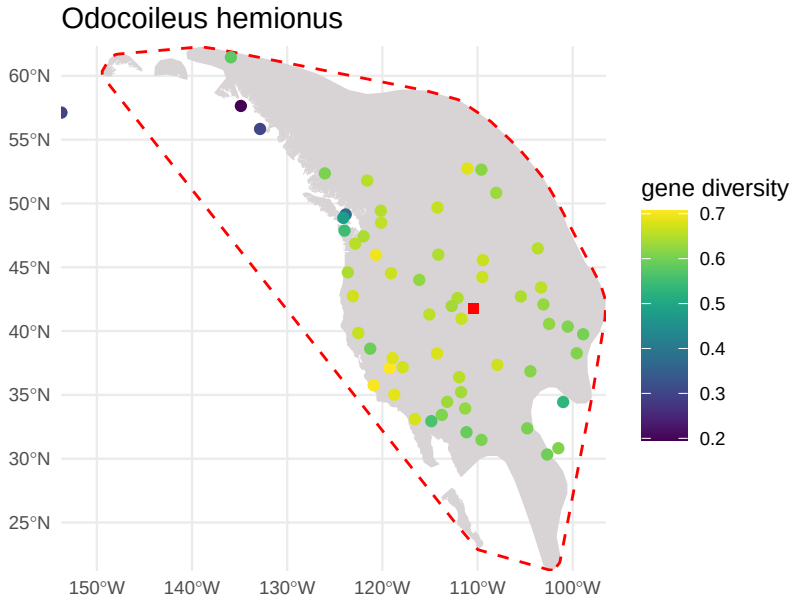
Odocoileus hemionus
60°N
55°N
50°N
45°N
40°N
35°N
30°N
25°N
150°W
140°W
130°W
120°W
110°W
100°W
gene diversity
0.7
0.6
0.5
0.4
0.3
0.2

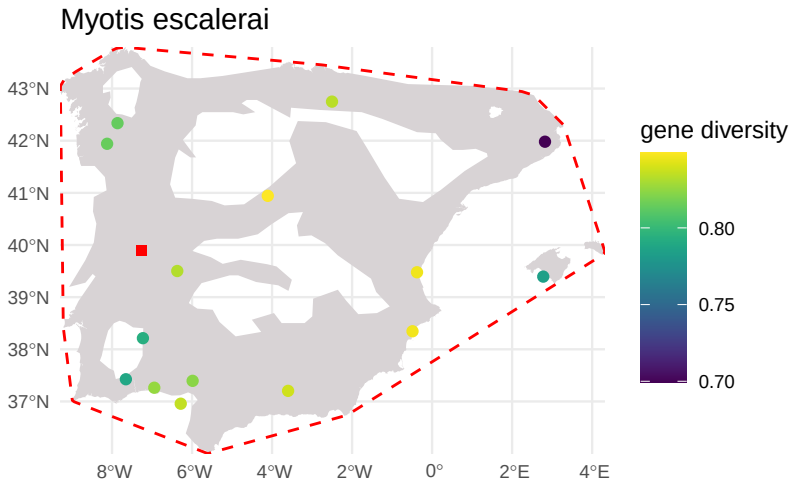
Myotis escalerai
43°N
42°N
41°N
40°N
39°N
38°N
37°N
8°W
6°W
4°W
2°W
0°
2°E
4°E
gene diversity
0.80
0.75
0.70

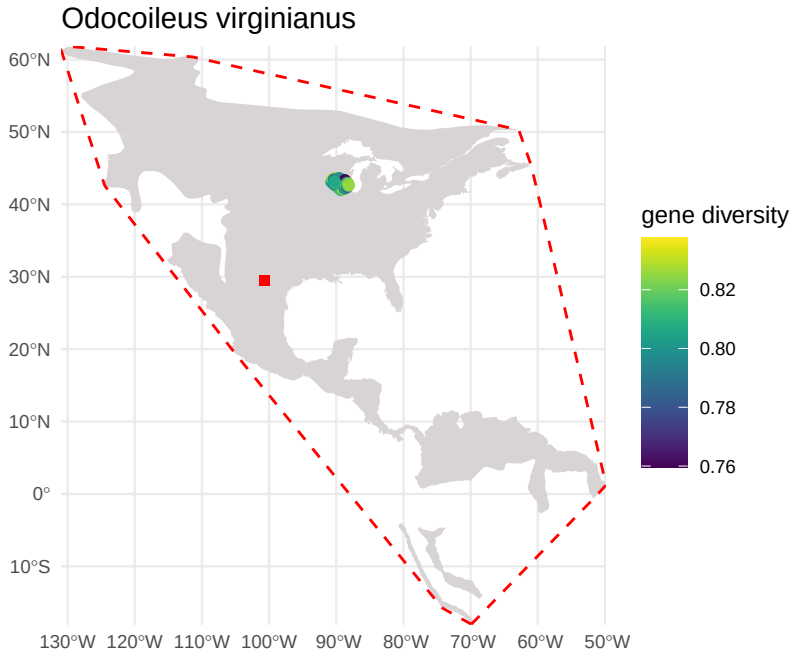
Odocoileus virginianus
60°N
50°N
40°N
30°N
20°N
10°N
0°
10°S
130°W
120°W
110°W
100°W
90°W
80°W
70°W
60°W
50°W
gene diversity
0.82
0.80
0.78
0.76

Peromyscus maniculatus

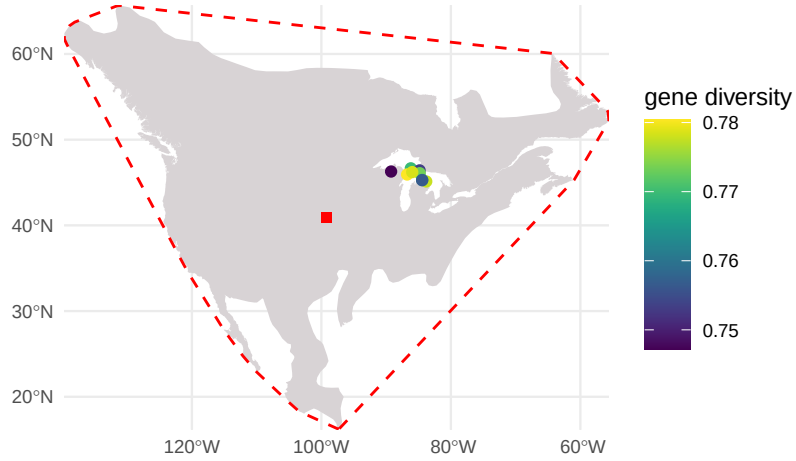

Parantechinus apicalis

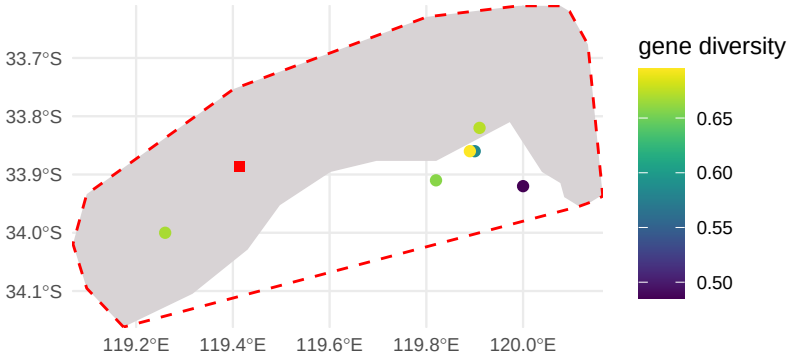

Myodes glareolus

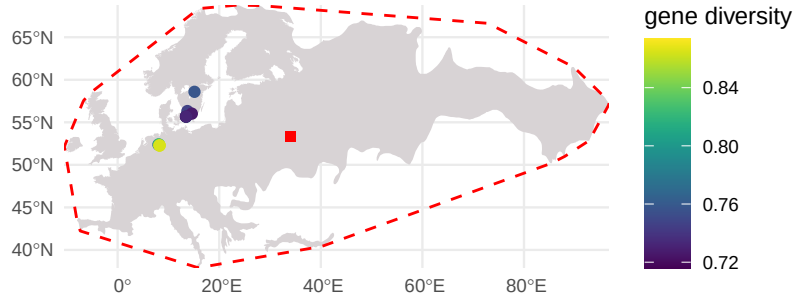

Miniopterus schreibersii

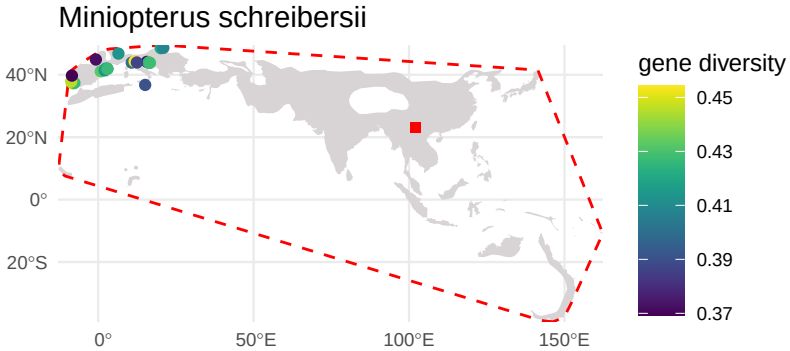

Sorex antinorii

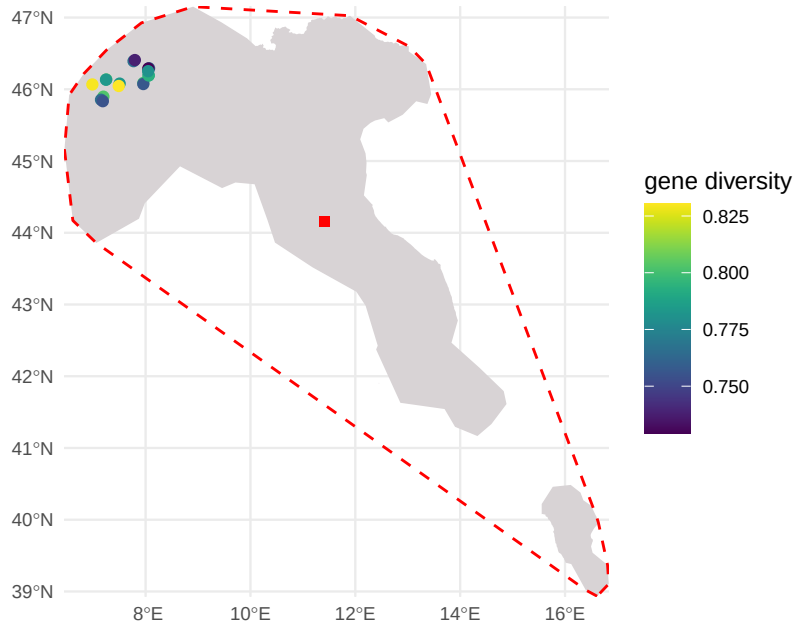

Pseudocheirus occidentalis

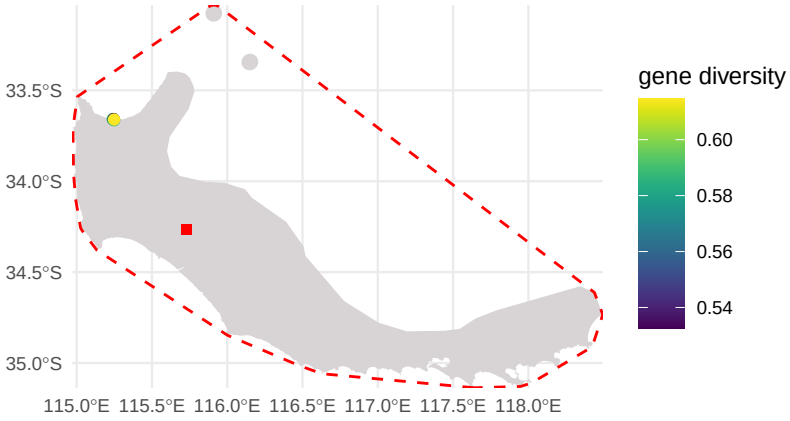

Panthera tigris

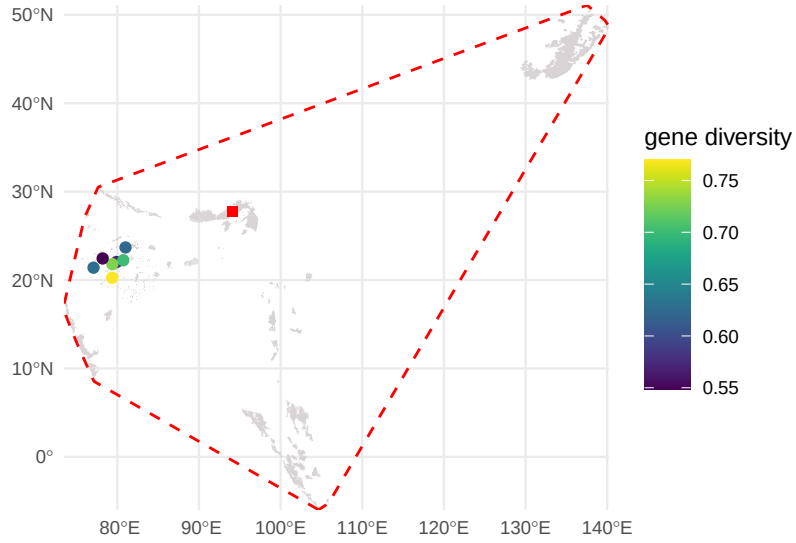

Cervus elaphus

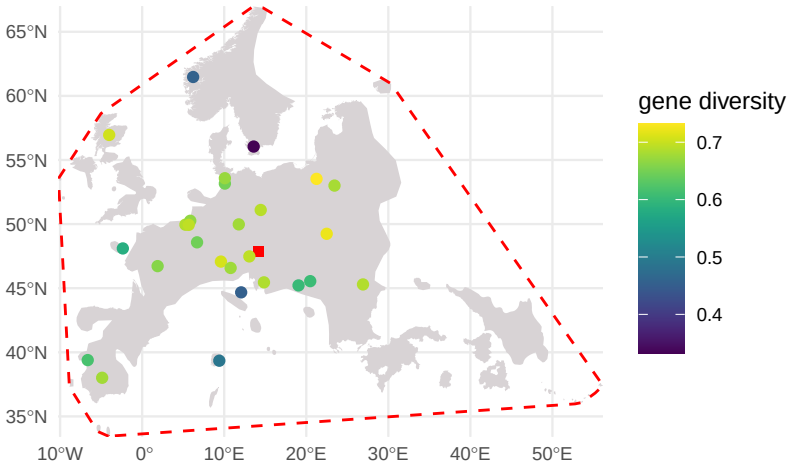

Fig. S1. Species sample sites. Locations of genetic sample sites (points) for each species mapped on their geographic range (grey shaded areas) with minimum convex hulls denoted by red dashed lines, and the range centroid indicated by red squares. Note that the restriction of keeping centroids inside species ranges means that they are not necessarily true polygon centroids. Genetic sample sites are colored according to their genetic diversity as measured by gene diversity.

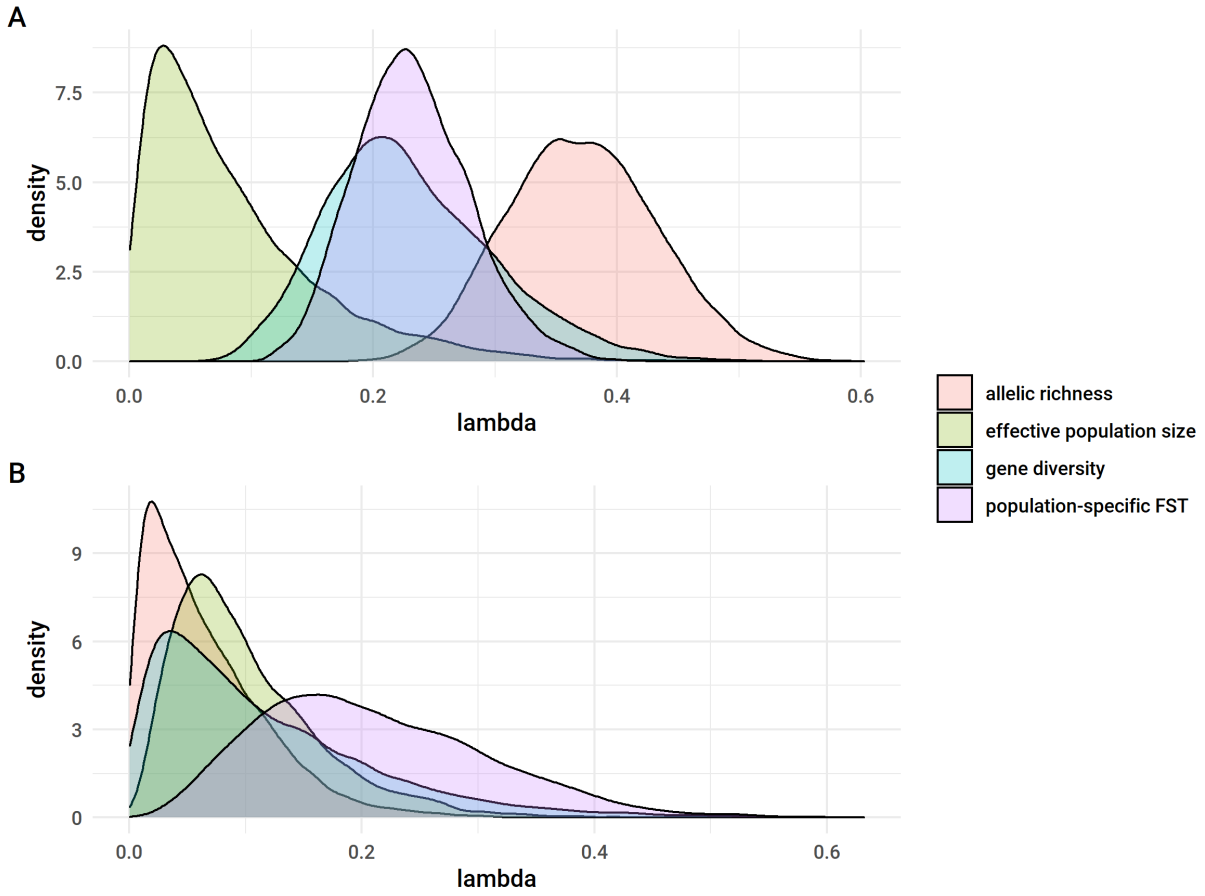

Fig. S2. Phylogenetic signal. Phylogenetic signal (lambda) is the ratio of variation explained by the phylogenic random effect to all variation explained by the model. We took 6000 draws from the posterior distribution to estimate lambda for each model set: (A) convex hull models, (B) centroid models. Density plots show the distribution of lambda values for each genetic response variable. Phylogenetic signal was not strong for any genetic metric.

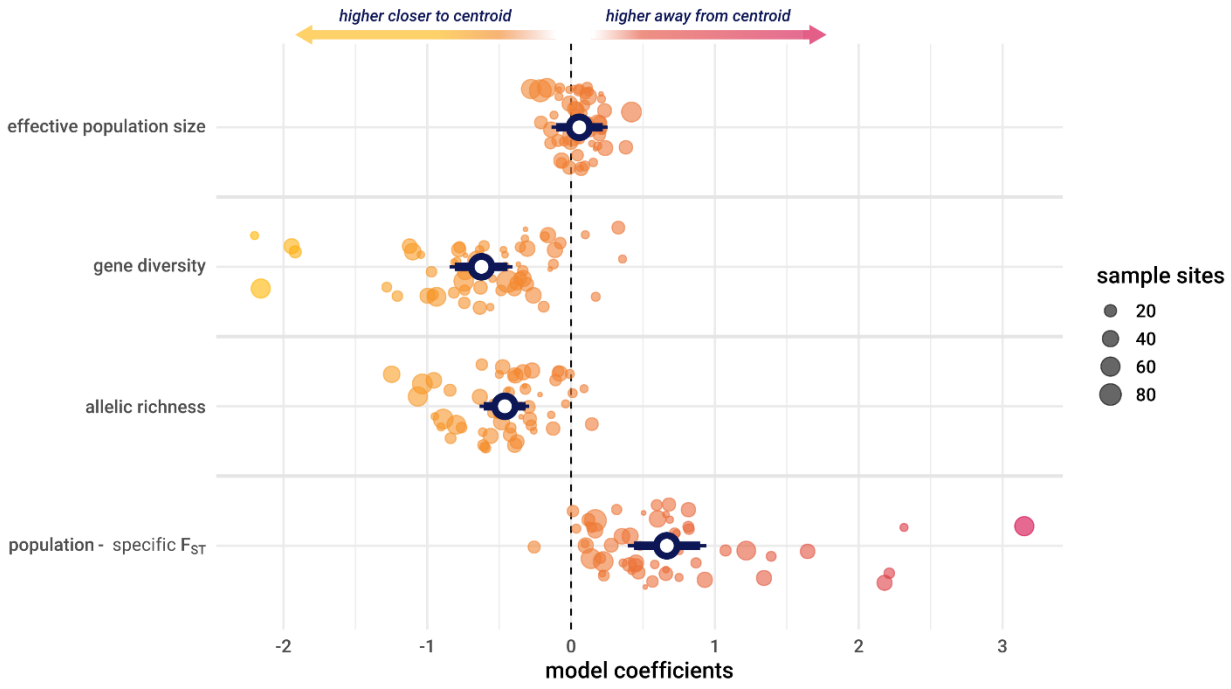

Fig S3. Effect of distance to range centroid on genetic diversity and differentiation. Model coefficients of the effect of distance to range centroid on each genetic metric (y axis) from Bayesian generalized mixed models controlling for the spatial distribution of sites and species relatedness. Open circles represent the relationship between range position and the genetic metrics across all species within 90% (thin lines) and 95% (thick lines) credible intervals. Filled circles are estimated species-specific effects of range position. The dashed vertical line indicates an effect size of 0. Negative effect sizes indicate genetic diversity is higher closer to the centroid, while positive effect sizes mean genetic differentiation increases with increasing distance from the centroid.

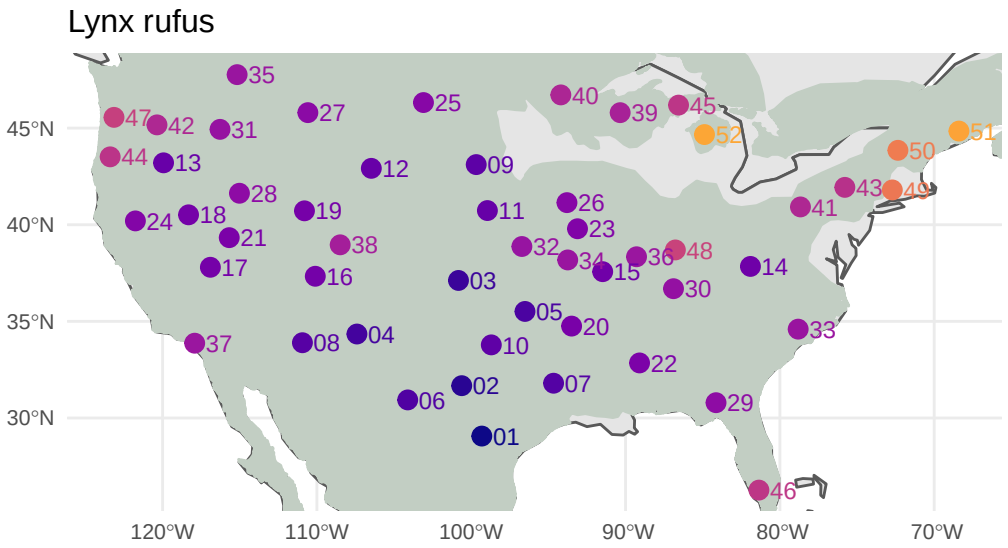
Lynx rufus
45°N
40°N
35°N
30°N
120°W
110°W
100°W
90°W
80°W
70°W

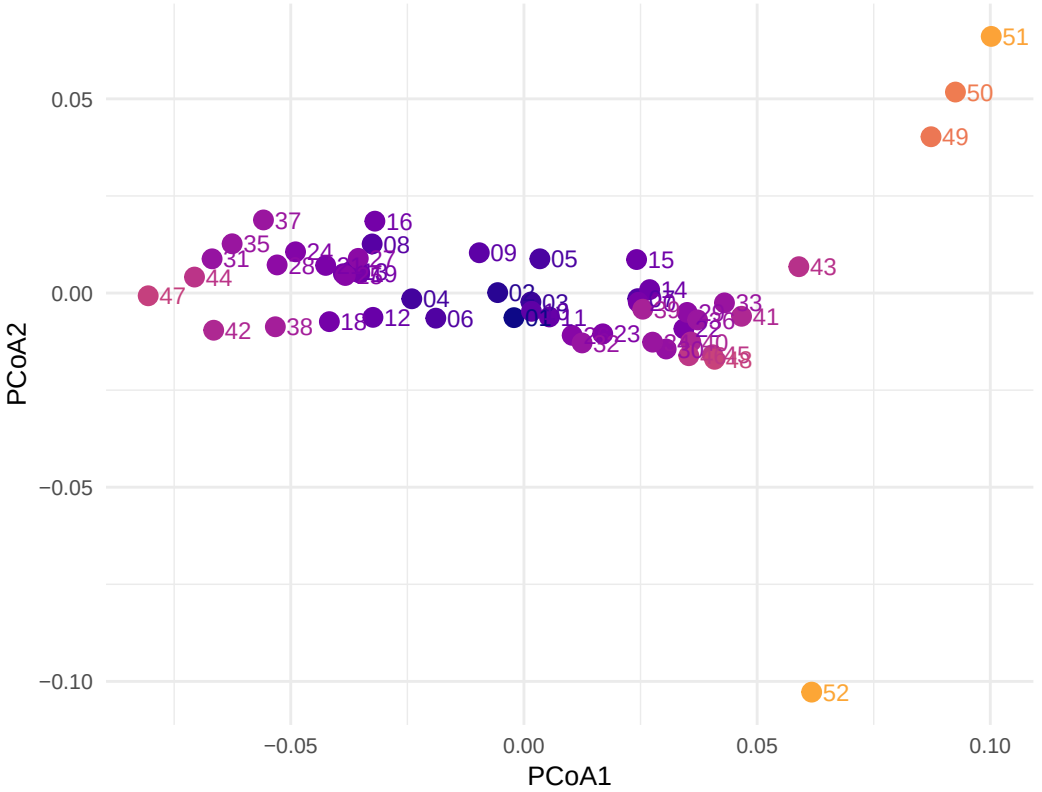
PCoA2
PCoA1
0.05
0.00
−0.05
−0.10
−0.05
0.00
0.05
0.10

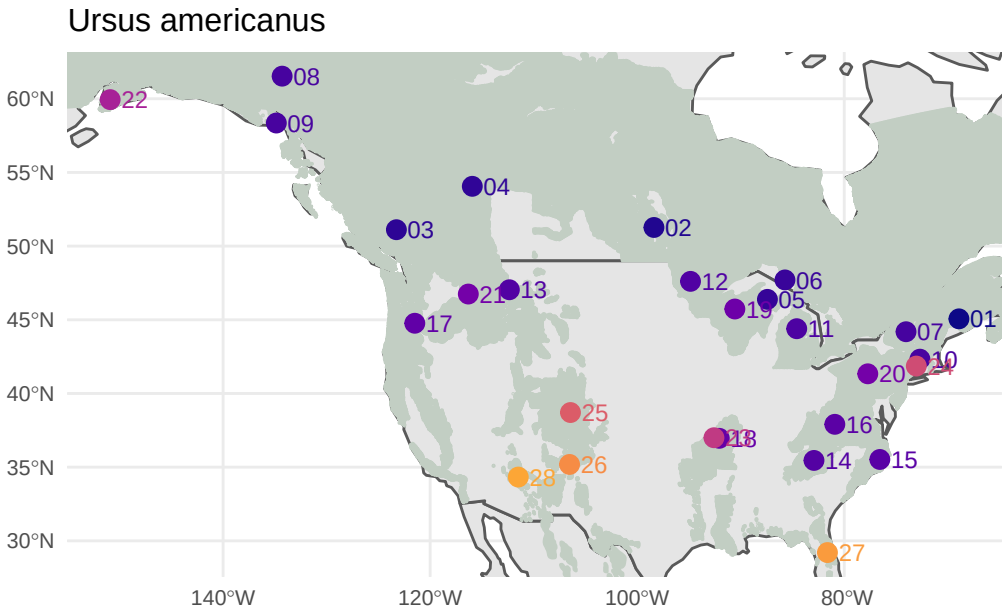
Ursus americanus
60°N
55°N
50°N
45°N
40°N
35°N
30°N
140°W
120°W
100°W
80°W

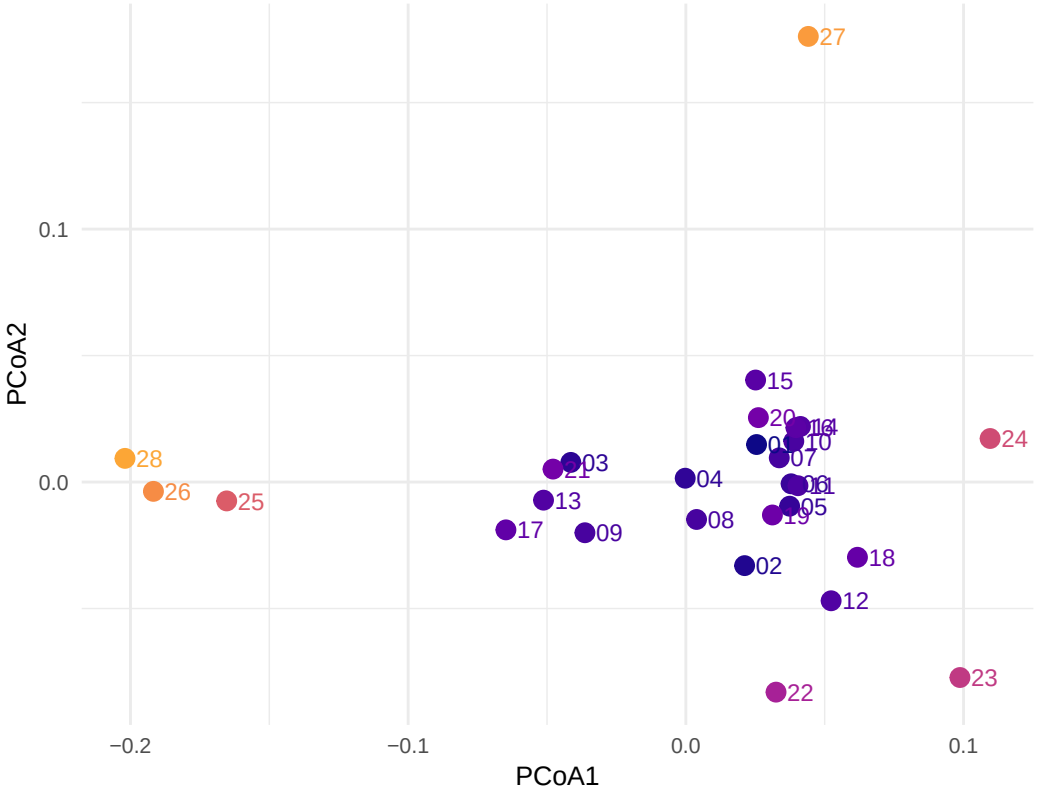
PCoA2
PCoA1
0.1
0.0
−0.2
−0.1
0.0
0.1

Vicugna vicugna

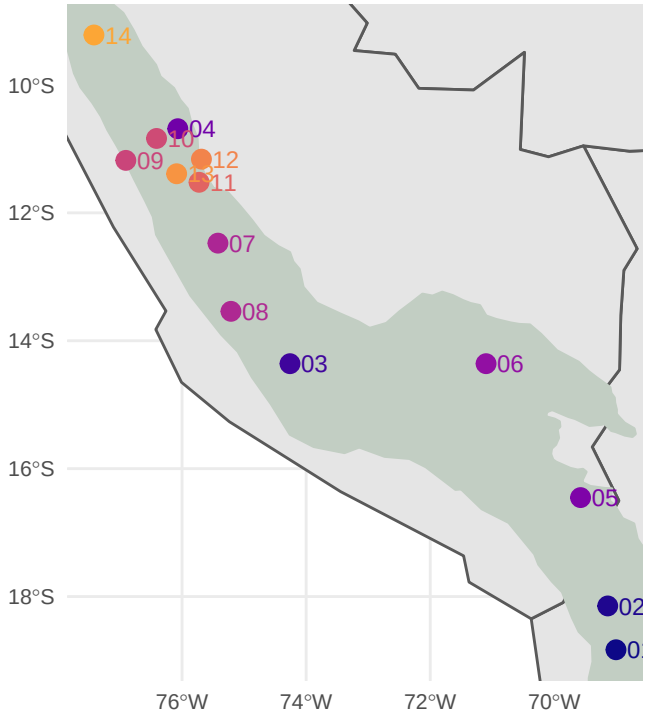

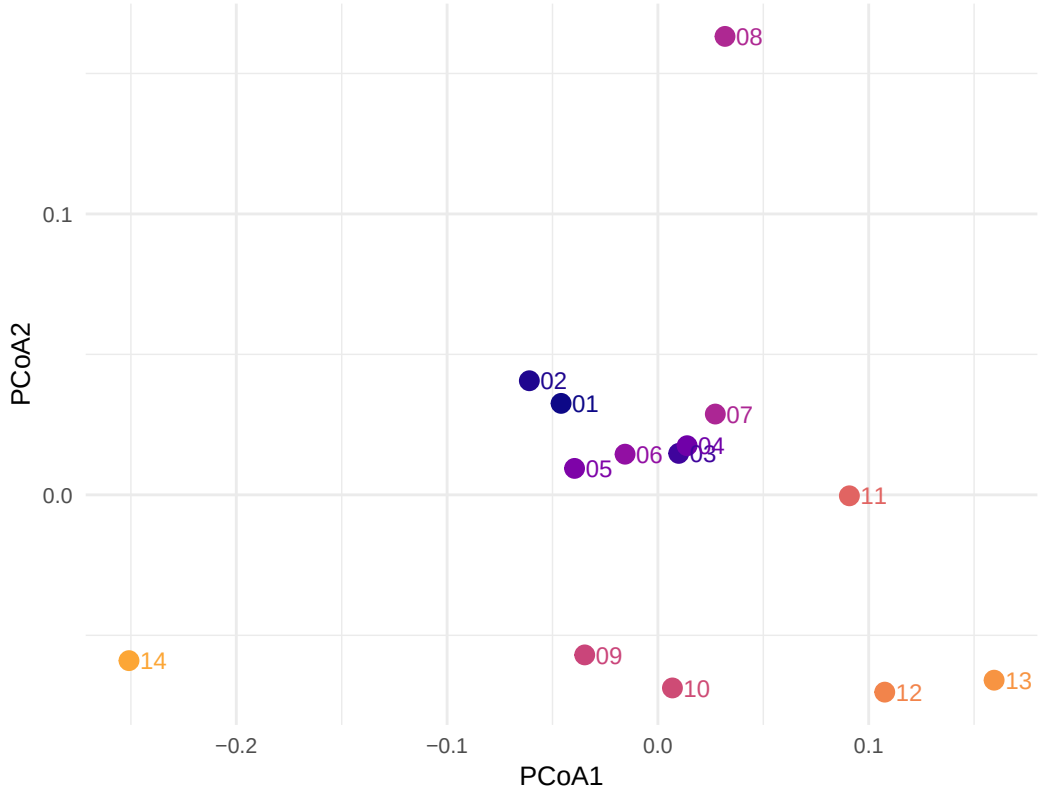

Lepus americanus

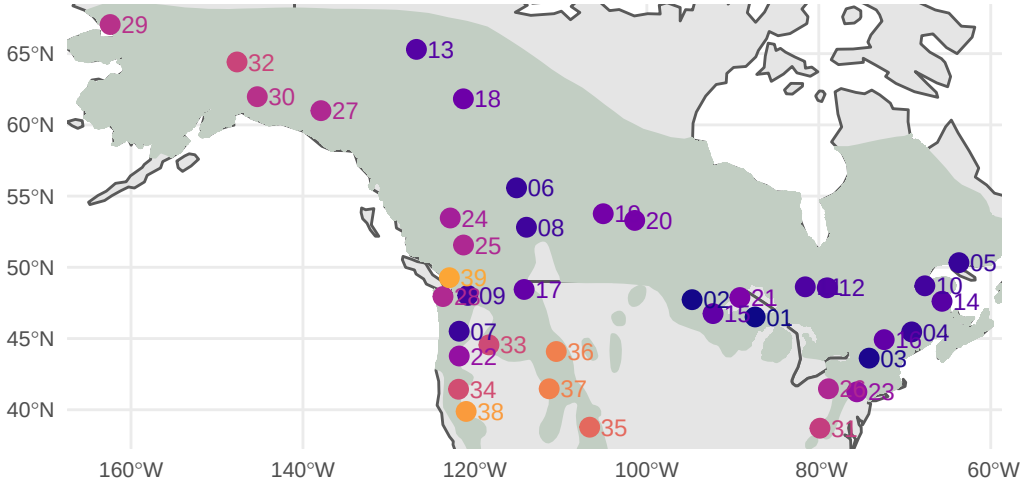

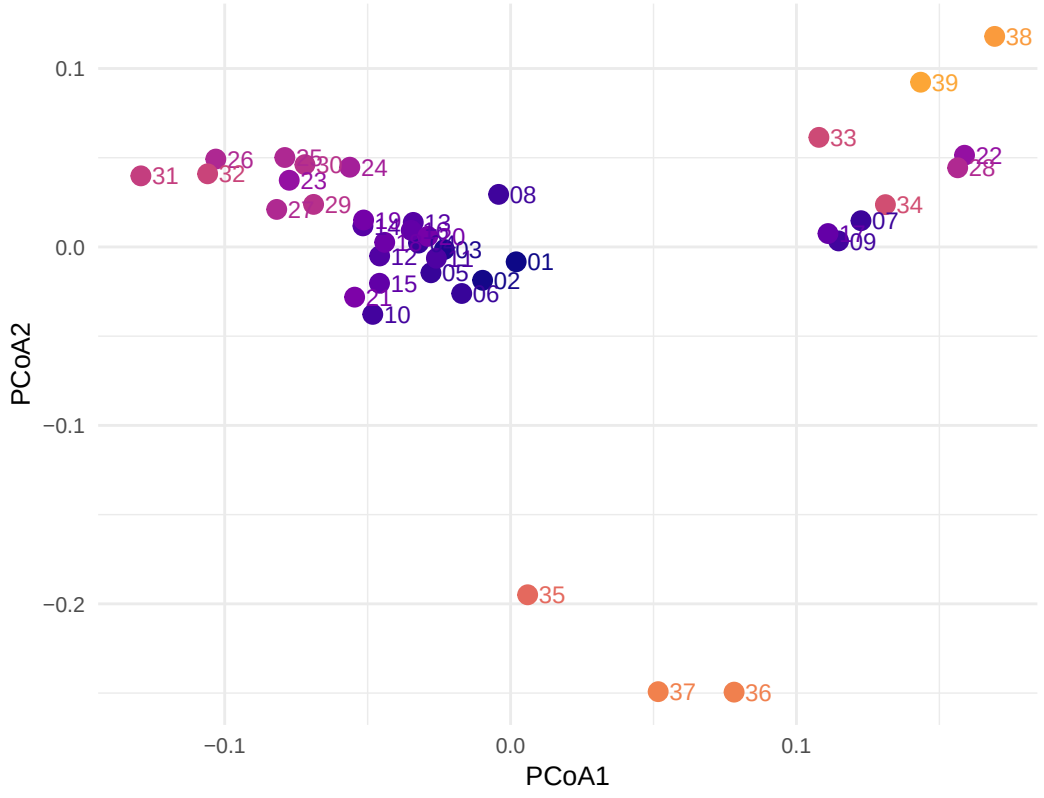

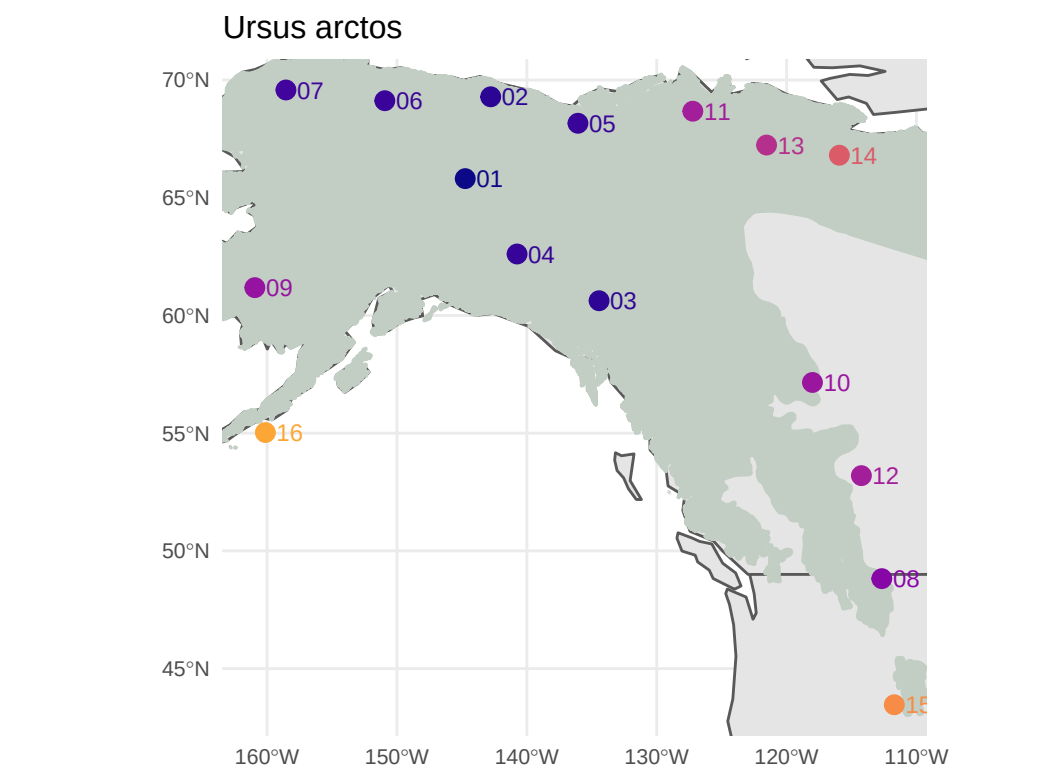
Ursus arctos
70°N
65°N
60°N
55°N
50°N
45°N
160°W
150°W
140°W
130°W
120°W
110°W
07
06
02
05
11
13
14
01
04
09
03
10
16
12
08
15

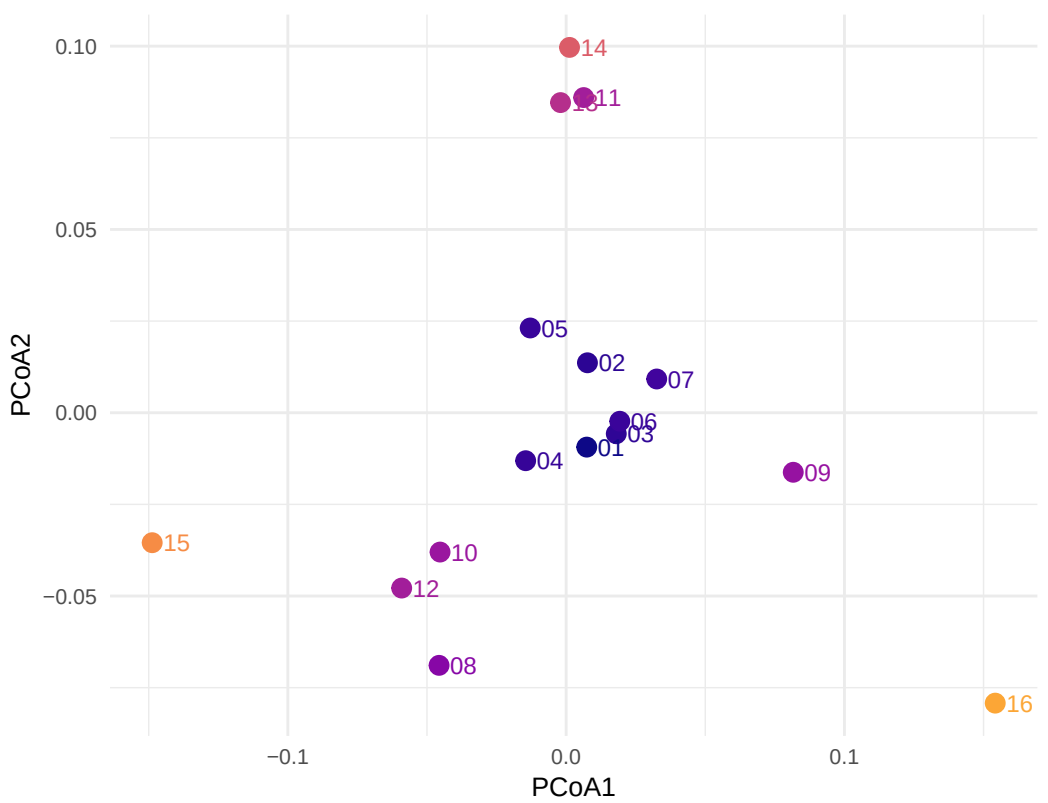
PCoA2
PCoA1
0.10
0.05
0.00
−0.05
−0.1
0.0
0.1
14
11
05
02
07
06
03
01
04
09
15
10
12
08
16

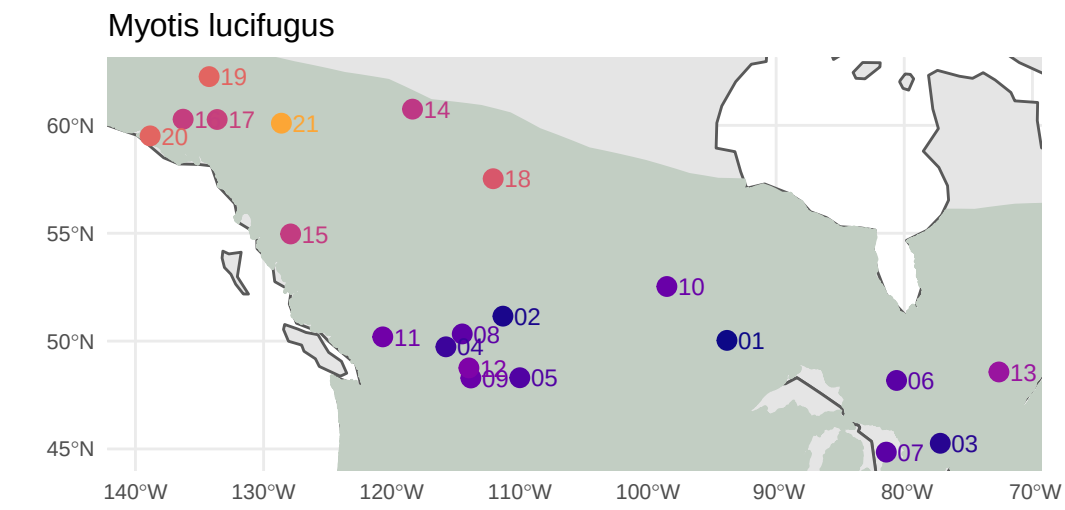
Myotis lucifugus
60°N
55°N
50°N
45°N
140°W
130°W
120°W
110°W
100°W
90°W
80°W
70°W
19
17
21
20
14
18
15
10
11
02
08
04
12
09
05
01
06
13
07
03

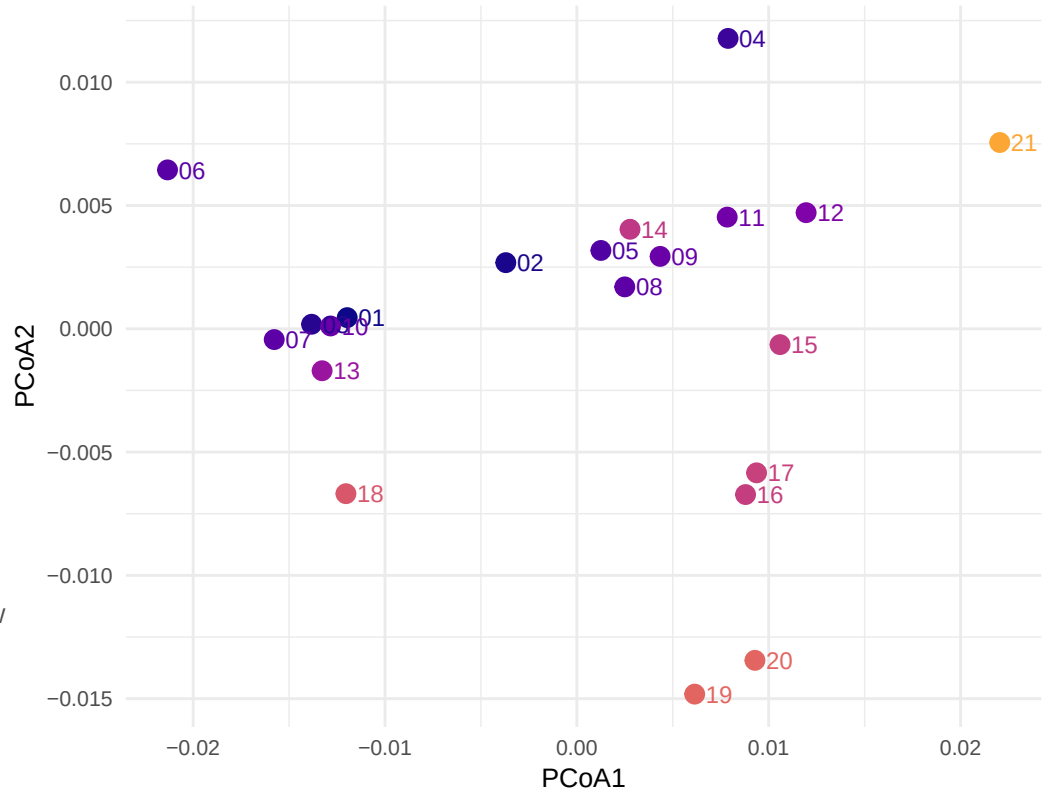
PCoA2
PCoA1
0.010
0.005
0.000
−0.005
−0.010
−0.015
−0.02
−0.01
0.00
0.01
0.02
04
21
06
11
12
14
05
09
02
08
01
07
10
15
13
17
18
16
20
19

Meles meles

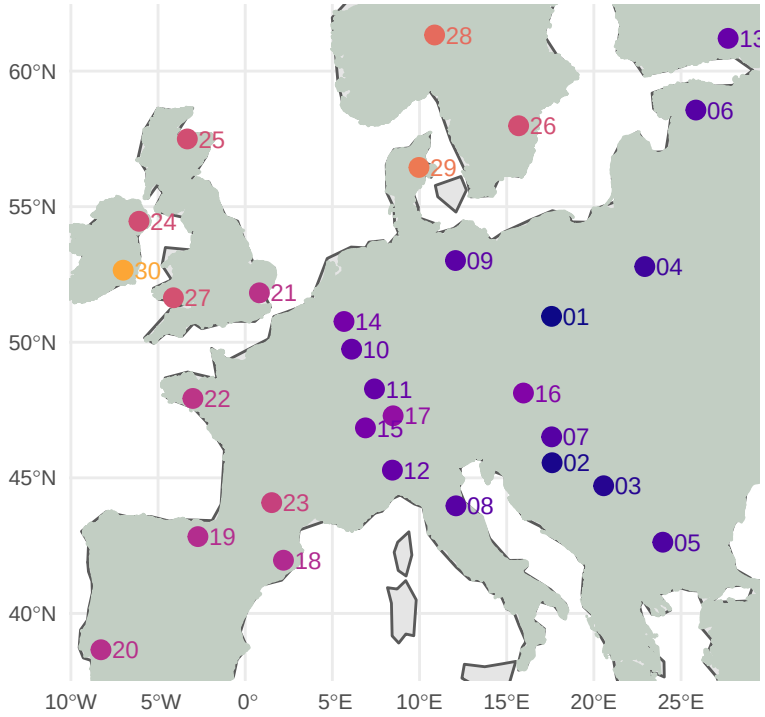

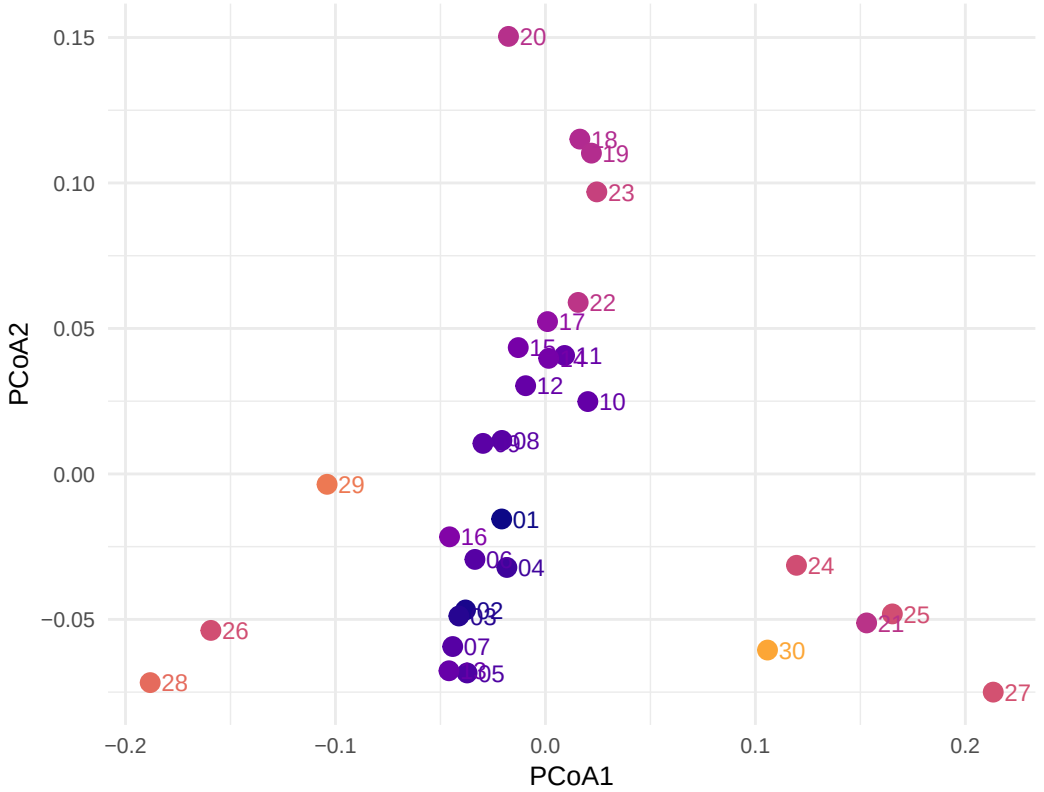

Lemmus lemmus

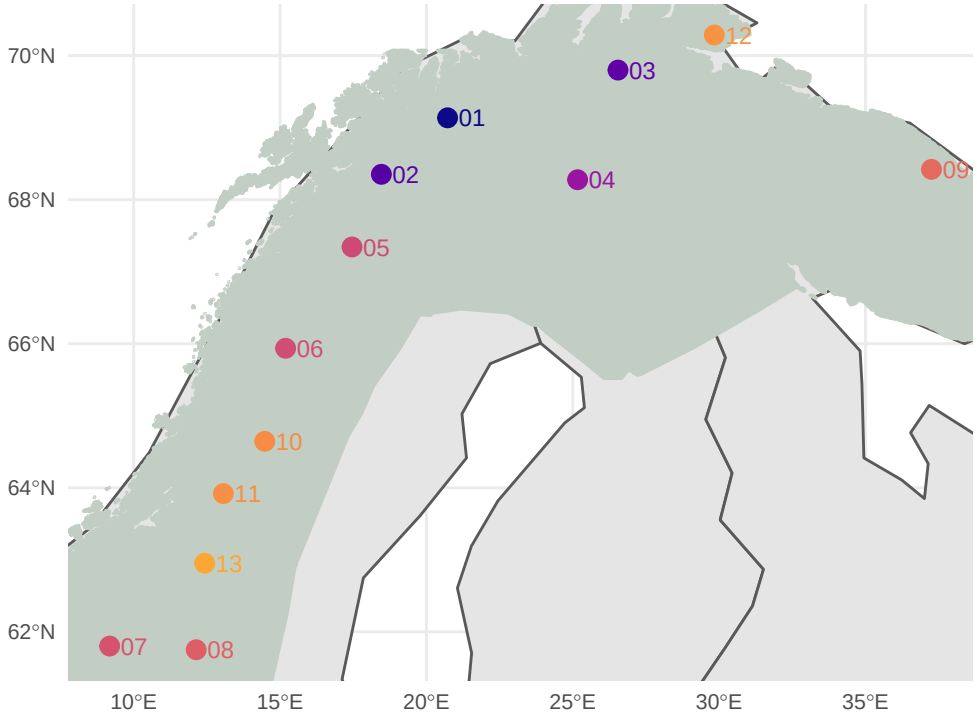

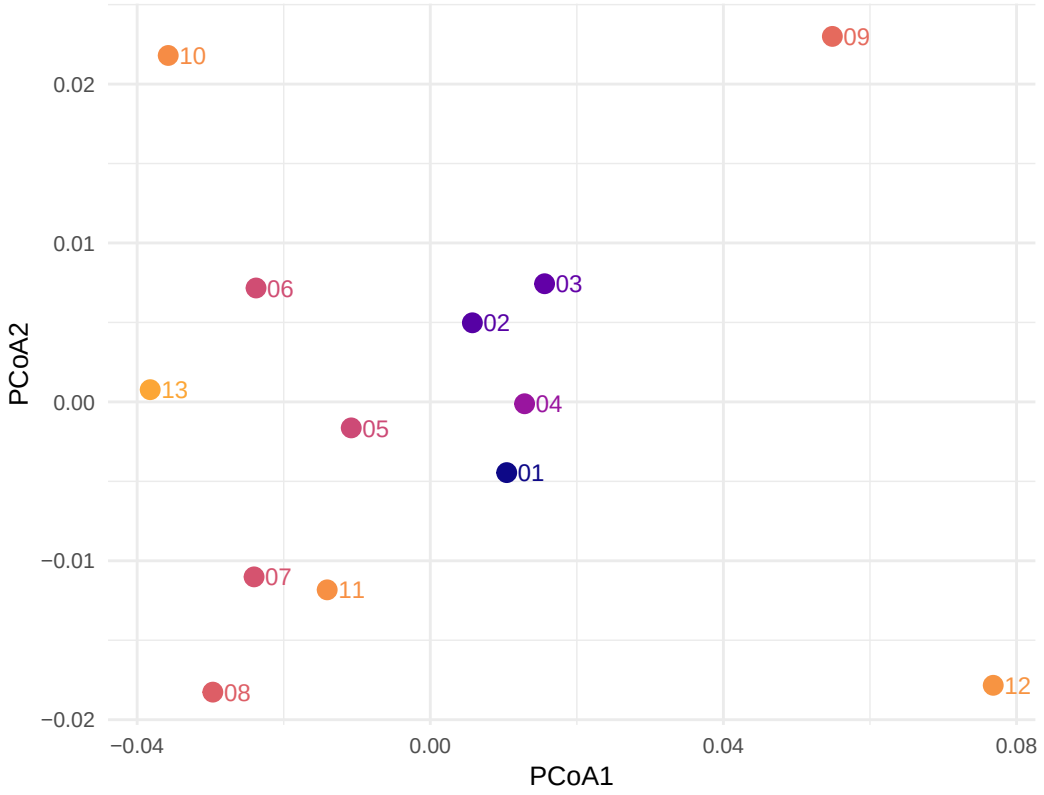

Lepus granatensis

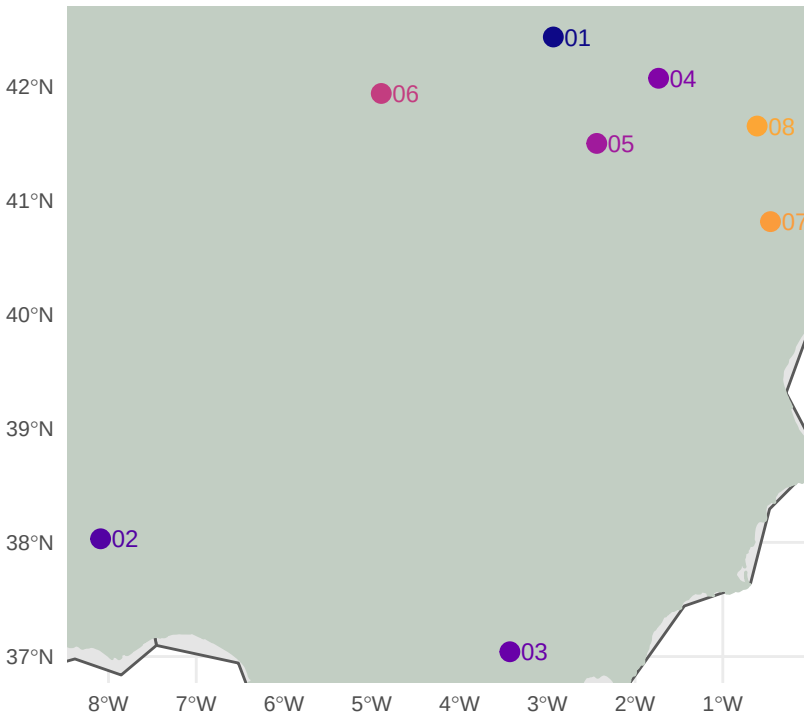

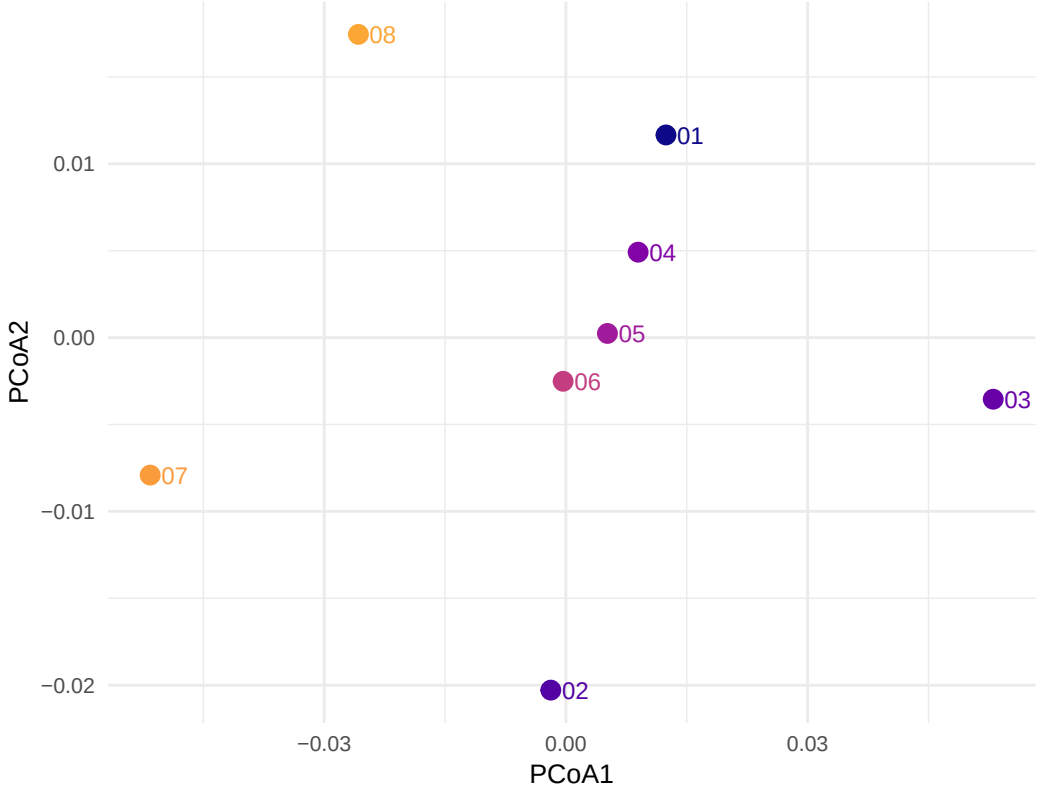

Odocoileus hemionus

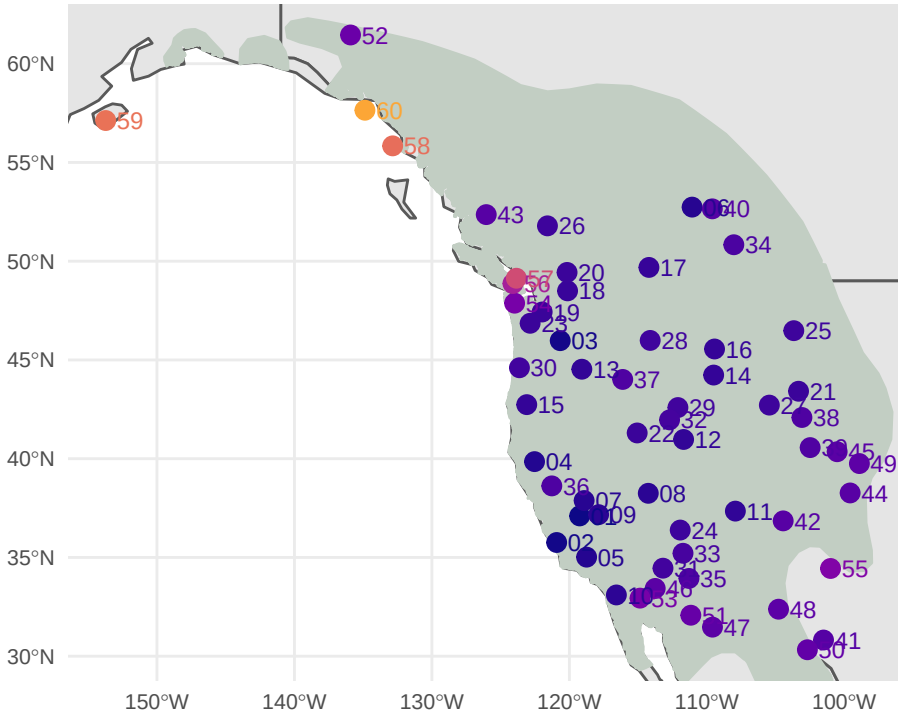

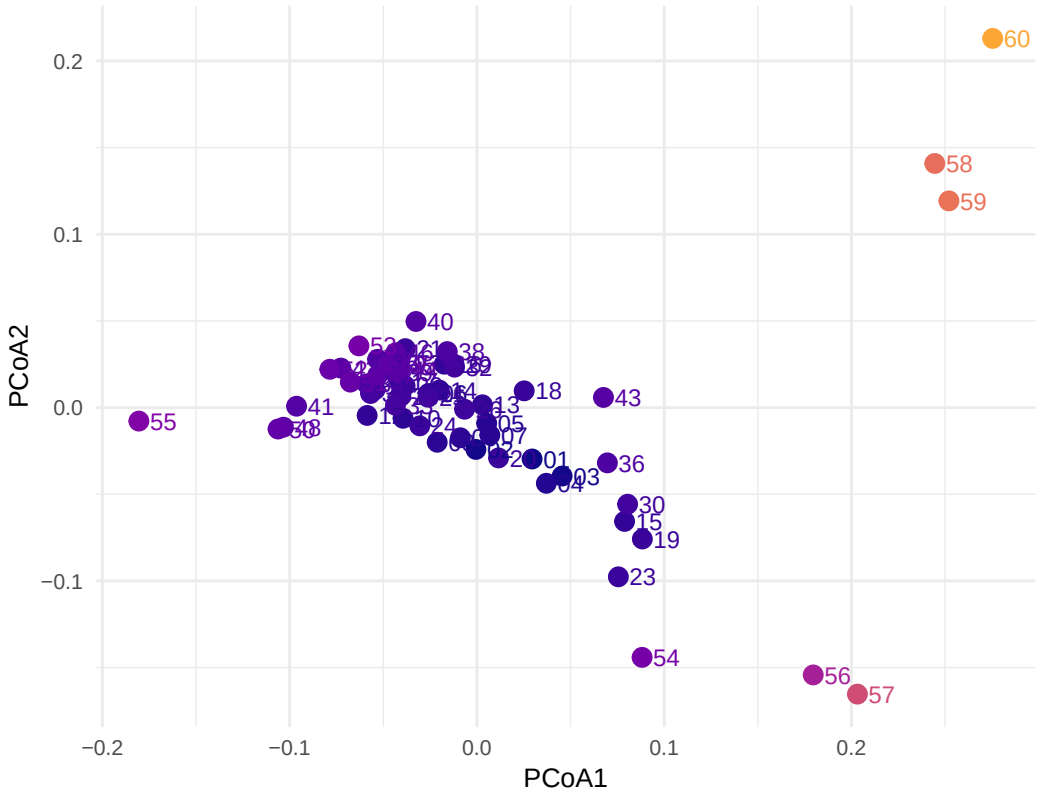

Myotis escalerai

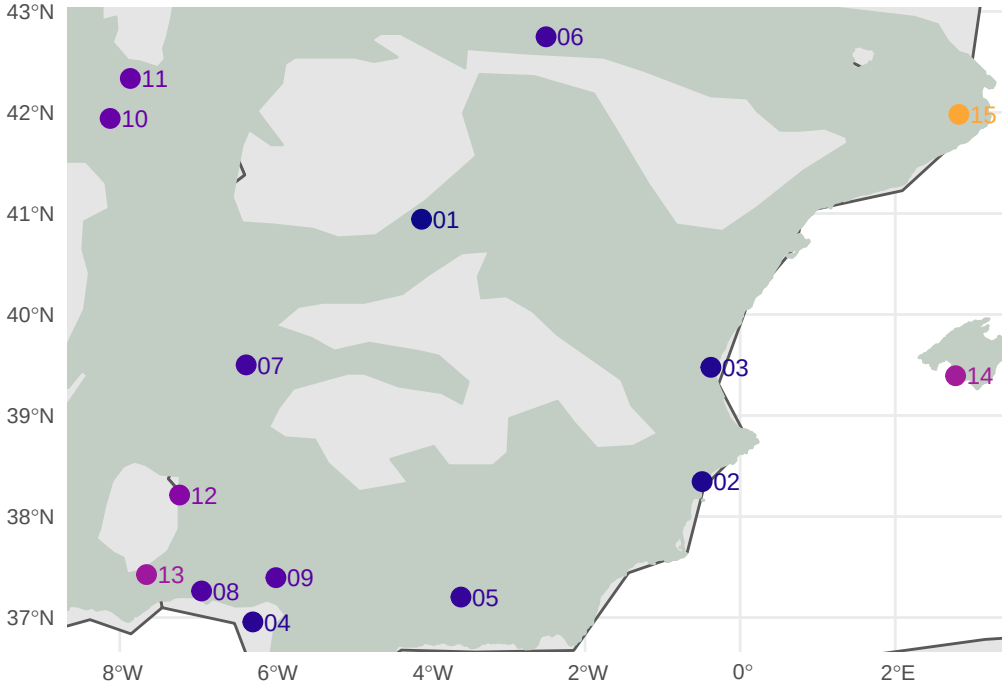

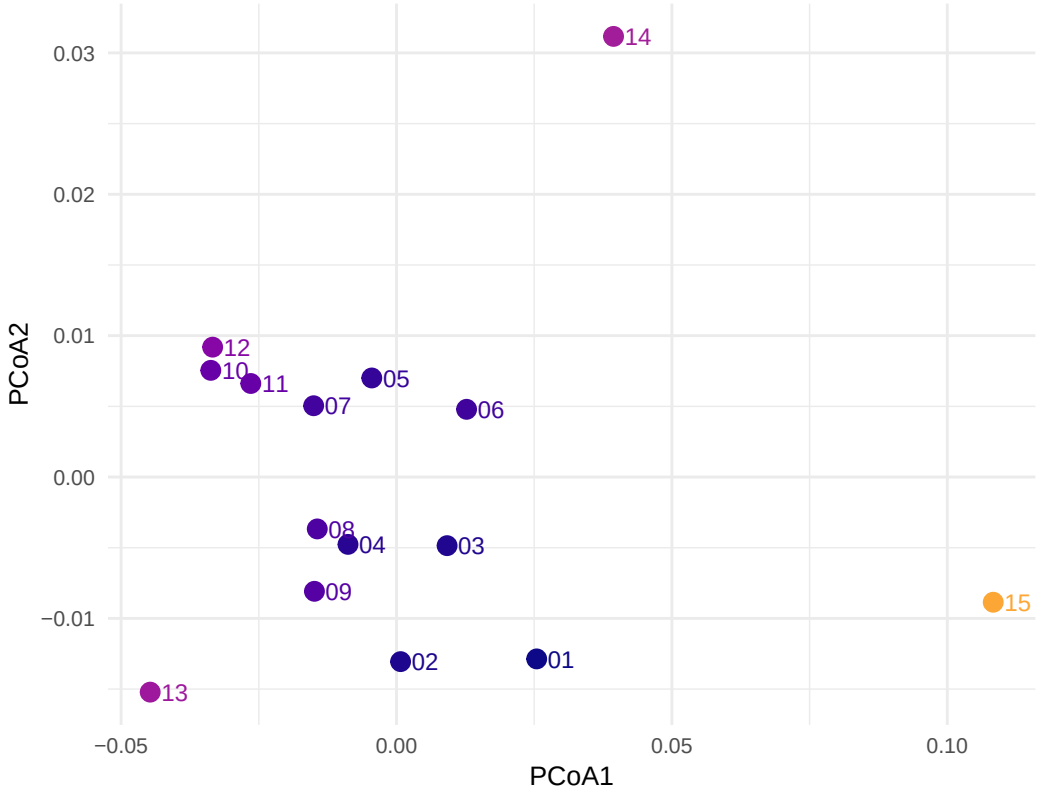

Cervus elaphus

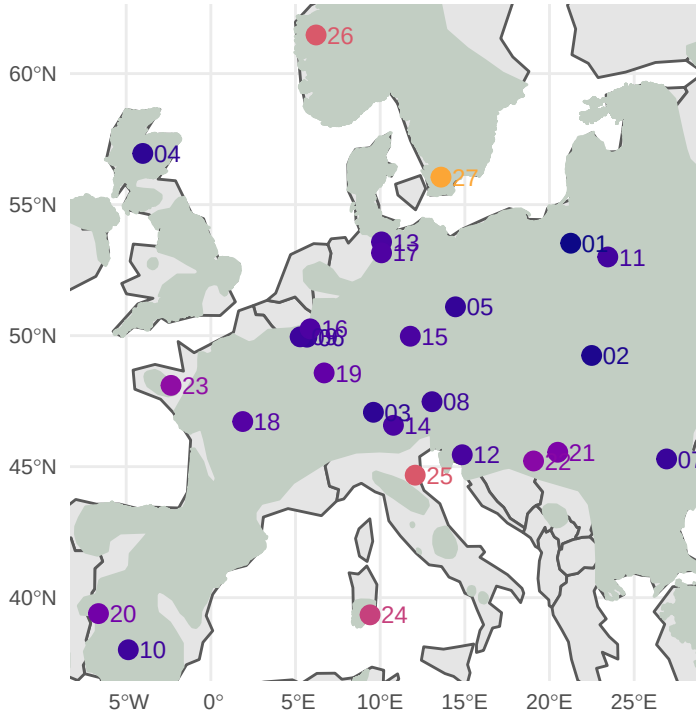

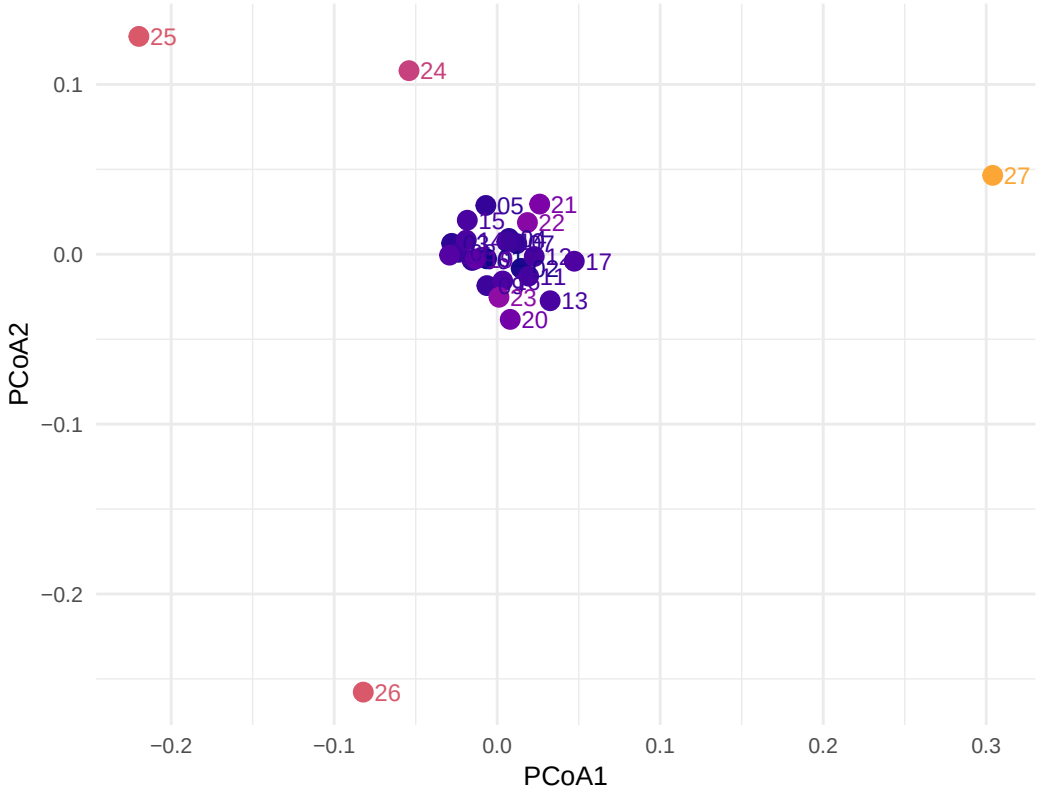

Fig. S4. Plots of pairwise and population-specific F_{ST}. For each species, the left plot shows population-specific F_{ST} values across the sampling extent. Lighter colors represent sites (numbered points) that are the furthest diverged from the common ancestor of all sites in the sample, darker colors are the least diverged and most connected sites. The right plot shows sample sites plotted along the first two PCoA axes of pairwise genetic differentiation (Nei's pairwise F_{ST}). Across both plots, colors correspond to population-specific F_{ST} and numbers are site IDs.

Table S1. Data summary. Summary of aggregated microsatellite data. For each species, the number of spatial locations and the total number of individuals in the sample across all sites (sites, individuals) is given along with means and standard deviations for gene diversity and population specific-F_{ST} (F_{ST}), and medians and ranges for allelic richness and effective population size (N_e). References are listed for source publications and datasets.

Species	Sites (individuals)	Gene diversity	Allelic richness	N_e	F_{ST}	Reference
Alces alces	22 (912)	0.65 (0.08)	4.10 (2.51-4.55)	56.40 (18.10-3617.90)	0.04 (0.05)	(*1–4*)
Apodemus flavicollis	19 (879)	0.73 (0.15)	6.02 (3.54-6.43)	75.40 (6.50-227.40)	0.04 (0.06)	(*5–8*)
Artibeus jamaicensis	24 (386)	0.71 (0.03)	4.97 (4.30-5.14)	78.30 (30.20-1000.60)	0.01 (0.03)	(*9, 10*)
Bison bison	8 (184)	0.47 (0.03)	2.63 (2.46-2.85)	63.30 (3.00-437.90)	0.13 (0.05)	(*11, 12*)
Canis latrans	41 (303)	0.77 (0.03)	5.83 (4.86-13.70)	22.20 (1.20-439.30)	0.02 (0.03)	(*13, 14*)
Capreolus capreolus	13 (371)	0.62 (0.06)	3.36 (2.88-4.58)	86.90 (11.00-324.50)	0.16 (0.08)	(*15, 16*)
Carollia castanea	24 (348)	0.69 (0.02)	4.33 (4.05-4.62)	97.60 (15.00-891.50)	0.01 (0.02)	(*9, 10*)
Cervus elaphus	27 (638)	0.63 (0.10)	4.18 (2.14-4.78)	51.10 (2.10-236.90)	0.17 (0.12)	(*17, 18*)
Ctenomys minutus	25 (323)	0.55 (0.11)	3.21 (1.83-4.21)	11.40 (0.50-39.00)	0.32 (0.13)	(*19, 20*)
Dama dama	10 (340)	0.30 (0.09)	1.92 (1.50-2.25)	36.80 (2.00-313.40)	0.49 (0.15)	(*21, 22*)
Dipodomys ingens	7 (558)	0.88 (0.04)	7.15 (6.58-7.37)	35.15 (22.90-354.30)	0.02 (0.01)	(*23, 24*)
Eptesicus serotinus	34 (694)	0.59 (0.05)	3.57 (2.96-4.24)	42.10 (5.60-1843.20)	0.06 (0.07)	(*25, 26*)
Felis silvestris	15 (620)	0.66 (0.04)	4.20 (3.18-4.86)	41.45 (2.60-497.10)	0.10 (0.05)	(*27, 28*)
Glaucomys volans	8 (278)	0.75 (0.05)	5.23 (4.67-6.61)	39.80 (24.20-111.60)	0.03 (0.04)	(*29, 30*)
Lama guanicoe	12 (223)	0.68 (0.06)	4.10 (3.08-4.59)	15.70 (1.90-81.50)	0.10 (0.07)	(*31–34*)
Lemmus lemmus	13 (276)	0.72 (0.04)	4.59 (4.22-5.20)	47.15 (22.20-163.30)	0.04 (0.04)	(*35, 36*)
Lepus americanus	39 (853)	0.66 (0.08)	4.47 (2.93-5.16)	30.35 (1.10-231.80)	0.16 (0.10)	(*37, 38*)
Lepus europaeus	6 (109)	0.49 (0.04)	3.32 (2.87-3.53)	42.00 (7.10-181.70)	0.09 (0.07)	(*39, 40*)
Lepus granatensis	8 (194)	0.36 (0.03)	2.50 (2.27-2.82)	10.50 (3.00-26.20)	0.04 (0.09)	(*39, 40*)
Loxodonta africana	7 (689)	0.73 (0.01)	4.33 (4.29-4.60)	49.60 (30.80-132.80)	0.03 (0.01)	(*41, 42*)
Lycaon pictus	5 (156)	0.67 (0.05)	3.81 (3.54-4.30)	9.10 (0.80-14.60)	0.17 (0.06)	(*43, 44*)
Lynx canadensis	33 (1258)	0.72 (0.05)	4.47 (2.65-4.68)	58.45 (11.40-3175.70)	0.03 (0.07)	(*29, 30, 45, 46*)
Lynx rufus	57 (1737)	0.74 (0.03)	4.52 (3.47-5.10)	114.35 (12.20-3544.80)	0.06 (0.04)	(*47–50*)
Martes americana	29 (653)	0.63 (0.03)	3.87 (3.32-4.12)	75.45 (4.90-1362.40)	0.02 (0.04)	(*51, 52*)
Meles meles	30 (675)	0.57 (0.07)	3.55 (2.50-5.78)	54.60 (8.20-284.20)	0.18 (0.10)	(*53, 54*)
Microtus arvalis	33 (717)	0.65 (0.21)	4.89 (1.64-6.40)	15.00 (2.00-8003.80)	0.23 (0.24)	(*55–58*)

Microtus duodecimcostatus	10 (60)	0.41 (0.09)	2.65 (2.11-4.23)	8.40 (2.10-207.30)	0.29 (0.16)	(*59*, *60*)
Microtus lusitanicus	5 (42)	0.60 (0.09)	3.41 (3.21-4.87)	2.50 (1.60-45.30)	0.13 (0.12)	(*59*, *60*)
Miniopterus schreibersii	22 (312)	0.41 (0.02)	2.75 (2.52-3.02)	15.90 (3.40-231.80)	0.06 (0.05)	(*61*, *62*)
Myodes glareolus	14 (492)	0.78 (0.05)	5.21 (4.50-6.40)	38.00 (14.90-105.30)	0.05 (0.03)	(*7*, *8*, *63*, *64*)
Myotis escalerai	15 (442)	0.81 (0.04)	5.57 (4.26-6.07)	21.90 (3.80-470.40)	0.04 (0.04)	(*65*, *66*)
Myotis lucifugus	65 (3099)	0.82 (0.04)	5.86 (4.81-9.24)	117.10 (16.00-53777.40)	0.01 (0.02)	(*67–72*)
Myotis septentrionalis	15 (896)	0.87 (0.01)	6.63 (6.35-6.75)	96.70 (11.60-3569.60)	0.00 (0.01)	(*71*, *72*)
Nyctalus leisleri	14 (183)	0.72 (0.04)	4.60 (4.10-5.33)	107.85 (2.90-136861.70)	0.03 (0.03)	(*73*, *74*)
Odocoileus hemionus	60 (1714)	0.61 (0.10)	3.70 (1.65-4.22)	88.20 (1.10-1348.90)	0.12 (0.14)	(*75*, *76*)
Odocoileus virginianus	64 (2069)	0.81 (0.01)	5.51 (5.12-5.87)	192.50 (23.90-7931.30)	0.01 (0.01)	(*77*, *78*)
Ovis canadensis	14 (579)	0.61 (0.05)	3.35 (2.54-3.64)	27.20 (18.90-530.70)	0.12 (0.08)	(*79*, *80*)
Panthera tigris	7 (165)	0.65 (0.08)	4.10 (3.24-10.20)	2.65 (0.90-16.20)	0.15 (0.09)	(*81*, *82*)
Papio anubis	6 (93)	0.73 (0.03)	4.81 (4.68-6.97)	24.95 (18.40-76.10)	0.06 (0.02)	(*83*, *84*)
Papio cynocephalus	5 (354)	0.73 (0.05)	4.61 (4.01-5.62)	63.50 (10.40-6595.80)	0.07 (0.05)	(*83*, *84*)
Parantechinus apicalis	6 (196)	0.63 (0.08)	3.77 (2.96-3.91)	34.15 (2.00-61.20)	0.05 (0.10)	(*85*, *86*)
Pekania pennanti	34 (722)	0.62 (0.03)	3.59 (2.98-4.01)	38.75 (8.30-1372.80)	0.07 (0.05)	(*87*, *88*)
Peromyscus leucopus	36 (775)	0.82 (0.03)	5.82 (4.67-10.10)	40.85 (9.80-259.60)	0.05 (0.04)	(*89–94*)
Peromyscus maniculatus	9 (105)	0.77 (0.01)	5.54 (5.30-5.68)	14.30 (2.20-41.30)	0.08 (0.02)	(*95*, *96*)
Pseudocheirus occidentalis	7 (145)	0.58 (0.03)	3.16 (2.93-3.30)	14.60 (8.80-33.80)	0.04 (0.05)	(*97*, *98*)
Puma concolor	8 (354)	0.45 (0.07)	2.59 (1.97-2.90)	23.85 (1.90-84.30)	0.22 (0.13)	(*99*, *100*)
Rangifer tarandus	82 (2637)	0.77 (0.07)	5.22 (2.29-6.54)	122.05 (6.30-12930.20)	0.06 (0.08)	(*101–110*)
Rhinolophus ferrumequinum	27 (950)	0.73 (0.04)	4.62 (3.47-4.79)	137.40 (30.80-6270.70)	0.04 (0.05)	(*111*, *112*)
Rousettus aegyptiacus	34 (490)	0.61 (0.05)	3.75 (3.03-5.26)	70.65 (1.30-754.30)	0.13 (0.06)	(*113*, *114*)
Sorex antinorii	17 (213)	0.78 (0.03)	5.54 (4.66-5.94)	67.35 (11.40-2395.80)	0.06 (0.03)	(*115*, *116*)
Sus scrofa	17 (541)	0.60 (0.04)	3.60 (2.72-6.70)	27.20 (1.80-76.80)	0.11 (0.07)	(*117*, *118*)
Tamiasciurus douglasii	14 (186)	0.65 (0.03)	4.11 (3.69-4.43)	48.00 (8.80-193.50)	0.03 (0.04)	(*119*, *120*)
Tamiasciurus hudsonicus	12 (188)	0.66 (0.08)	4.51 (4.17-5.70)	67.75 (20.80-190.30)	0.07 (0.09)	(*119*, *120*)
Taxidea taxus	8 (236)	0.71 (0.12)	4.39 (2.52-5.10)	30.70 (11.20-268.20)	0.10 (0.15)	(*121*, *122*)
Ursus americanus	35 (773)	0.70 (0.11)	4.68 (1.95-7.15)	49.60 (1.00-534.20)	0.15 (0.13)	(*123–126*)
Ursus arctos	16 (831)	0.68 (0.08)	4.02 (2.93-4.65)	29.70 (11.30-84.50)	0.11 (0.10)	(*127*, *128*)
Ursus maritimus	25 (2550)	0.69 (0.05)	4.10 (3.68-4.52)	110.65 (11.80-1328.80)	0.04 (0.03)	(*127–130*)
Vicugna vicugna	14 (374)	0.48 (0.08)	3.08 (2.07-4.15)	29.20 (2.70-443.90)	0.17 (0.13)	(*31*, *32*)

Vulpes vulpes	5 (257)	0.71 (0.04)	4.42 (3.60-4.46)	222.80 (22.80-572.30)	0.03 (0.05)	(*131, 132*)

References

1. B. Jesmer, Data from: A test of the niche variation hypothesis in a ruminant herbivore, version 3, Dryad (2020); https://doi.org/10.5061/DRYAD.BCC2FQZ9Q.
2. B. R. Jesmer, M. J. Kauffman, M. A. Murphy, J. R. Goheen, A test of the Niche Variation Hypothesis in a ruminant herbivore. *Journal of Animal Ecology* **89**, 2825–2839 (2020).
3. M. Niedziałkowska, K. J. Hundertmark, B. Jędrzejewska, V. E. Sidorovich, H. Zalewska, R. Veeroja, E. J. Solberg, S. Laaksonen, H. Sand, V. A. Solovyev, A. Sagaydak, J. Tiainen, R. Juškaitis, G. Done, V. A. Borodulin, E. A. Tulandin, K. Niedziałkowski, Data from: The contemporary genetic pattern of European moose is shaped by postglacial recolonization, bottlenecks, and the geographical barrier of the Baltic Sea, version 1, Dryad (2015); https://doi.org/10.5061/DRYAD.0TC6Q.
4. M. Niedziałkowska, K. J. Hundertmark, B. Jędrzejewska, V. E. Sidorovich, H. Zalewska, R. Veeroja, E. J. Solberg, S. Laaksonen, H. Sand, V. A. Solovyev, A. Sagaydak, J. Tiainen, R. Juškaitis, G. Done, V. A. Borodulin, E. A. Tulandin, K. Niedziałkowski, The contemporary genetic pattern of European moose is shaped by postglacial recolonization, bottlenecks, and the geographical barrier of the Baltic Sea. *Biol. J. Linn. Soc.* **117**, 879–894 (2016).
5. S. D. Czarnomska, M. Niedziałkowska, T. Borowik, B. Jędrzejewska, Regional and local patterns of genetic variation and structure in yellow-necked mice - the roles of geographic distance, population abundance, and winter severity. *Ecology and Evolution* **8**, 8171–8186 (2018).
6. S. D. Czarnomska, M. Niedziałkowska, T. Borowik, B. Jędrzejewska, Data from: Regional and local patterns of genetic variation and structure in yellow-necked mice − the roles of geographic distance, population abundance and winter severity, version 1, Dryad (2019); https://doi.org/10.5061/DRYAD.F8Q8QF5.
7. B. Tschirren, M. Andersson, K. Scherman, H. Westerdahl, L. Råberg, Data from: Contrasting patterns of diversity and population differentiation at the innate immunity gene Toll-like receptor 2 (TLR2) in two sympatric rodent species, version 1, Dryad (2011); https://doi.org/10.5061/DRYAD.744V6T51.
8. B. Tschirren, M. Andersson, K. Scherman, H. Westerdahl, L. Råberg, Contrasting patterns of diversity and population differentiation at the innate immunity gene toll-like receptor 2 (TLR2) in two sympatric rodent species. *Evolution* **66**, 720–731 (2012).
9. K. A. Cleary, L. P. Waits, B. Finegan, Comparative landscape genetics of two frugivorous bats in a biological corridor undergoing agricultural intensification. *Molecular Ecology* **26**, 4603–4617 (2017).
10. K. A. Cleary, L. P. Waits, B. Finegan, Data from: Comparative landscape genetics of two frugivorous bats in a biological corridor undergoing agricultural intensification, version 1, Dryad (2017); https://doi.org/10.5061/DRYAD.NV92Q.
11. M. A. Cronin, M. D. Macneil, N. Vu, V. Leesburg, H. D. Blackburn, J. N. Derr, Genetic variation and differentiation of bison (Bison bison) subspecies and cattle (Bos taurus) breeds and subspecies. *Journal of Heredity* **104**, 500–509 (2013).
12. M. A. Cronin, M. D. Macneil, N. Vu, V. Leesburg, H. D. Blackburn, J. N. Derr, Data from: Genetic variation and differentiation of extant bison (Bison bison) subspecies and cattle (Bos taurus) breeds and subspecies, *Journal of Heredity* (2013). https://doi.org/10.5061/dryad.7k66b.

13. E. Heppenheimer, D. S. Cosio, K. E. Brzeski, D. Caudill, K. van Why, M. J. Chamberlain, J. W. Hinton, B. VonHoldt, Demographic history influences spatial patterns of genetic diversityin recently expanded coyote (Canis latrans) populations. *Heredity*, 1–13 (2017).
14. E. Heppenheimer, C. DS, B. KE, D. Caudill, V. W. K, C. MJ, H. JW, B. vonHoldt, Data from: Demographic history influences spatial patterns of genetic diversity in recently expanded coyote (Canis latrans) populations, *Heredity* (2017). https://doi.org/10.5061/dryad.2t965.
15. K. H. Baker, A. R. Hoelzel, Data from: Evolution of population genetic structure of the British roe deer by natural and anthropogenic processes (Capreolus capreolus), version 1, Dryad (2013); https://doi.org/10.5061/DRYAD.V90P5.
16. K. H. Baker, A. Rus Hoelzel, Evolution of population genetic structure of the British roe deer by natural and anthropogenic processes (*Capreolus capreolus*). *Ecol Evol* **3**, 89–102 (2013).
17. F. E. Zachos, A. C. Frantz, R. Kuehn, S. Bertouille, M. Colyn, M. Niedzialkowska, J. Pérez-González, A. Skog, N. Šprem, M.-C. Flamand, Data from: Genetic structure and effective population sizes in European red deer (Cervus elaphus) at a continental scale: insights from microsatellite DNA, version 1, Dryad (2016); https://doi.org/10.5061/DRYAD.1V6P1.
18. F. E. Zachos, A. C. Frantz, R. Kuehn, S. Bertouille, M. Colyn, M. Niedziałkowska, J. Pérez-González, A. Skog, N. Sprěm, M.-C. Flamand, Genetic Structure and Effective Population Sizes in European Red Deer (*Cervus elaphus*) at a Continental Scale: Insights from Microsatellite DNA. *JHERED* **107**, 318–326 (2016).
19. C. M. Lopes, S. S. F. Ximenes, A. Gava, T. R. O. De Freitas, The role of chromosomal rearrangements and geographical barriers in the divergence of lineages in a South American subterranean rodent (Rodentia: Ctenomyidae: Ctenomys minutus). *Heredity* **111**, 293–305 (2013).
20. C. M. Lopes, S. S. F. Ximenes, A. Gava, T. R. O. De Freitas, Data from: The role of chromosomal rearrangements and geographical barriers in the divergence of lineages in a South American subterranean rodent (Rodentia: Ctenomyidae: Ctenomys minutus), version 1, Dryad (2013); https://doi.org/10.5061/DRYAD.D12J8.
21. K. H. Baker, H. W. I. Gray, V. Ramovs, D. Mertzanidou, Ç. Akın Pekşen, C. C. Bilgin, N. Sykes, A. R. Hoelzel, Strong population structure in a species manipulated by humans since the Neolithic: the European fallow deer (Dama dama dama). *Heredity* **119**, 16–26 (2017).
22. K. H. Baker, H. W. I. Gray, V. Ramovs, D. Mertzanidou, C. Akin Peksen, C. C. Bilgin, N. Sykes, A. R. Hoelzel, Data from: Strong population structure in a species manipulated by humans since the Neolithic: the European fallow deer (Dama dama dama), version 1, Dryad (2017); https://doi.org/10.5061/DRYAD.D2G8V.
23. M. J. Statham, W. T. Bean, N. Alexander, M. F. Westphal, B. N. Sacks, Historical Population Size Change and Differentiation of Relict Populations of the Endangered Giant Kangaroo Rat. *Journal of Heredity* **110**, 548–558 (2019).
24. M. J. Statham, W. T. Bean, N. Alexander, M. F. Westphal, B. N. Sacks, Dryad Data -- Historical population size change and differentiation of relict populations of the endangered giant kangaroo rat (2019). https://doi.org/10.5061/dryad.5jh21k3.

25. C. Moussy, H. Atterby, A. G. F. Griffiths, T. R. Allnut, F. Mathews, G. C. Smith, J. N. Aegerter, S. Bearhop, D. J. Hosken, Data from: Population genetic structure of serotine bats (Eptesicus serotinus) across Europe and implications for the potential spread of bat rabies (European bat lyssavirus EBLV-1), version 1, Dryad (2015); https://doi.org/10.5061/DRYAD.665NP.
26. C. Moussy, H. Atterby, A. G. F. Griffiths, T. R. Allnutt, F. Mathews, G. C. Smith, J. N. Aegerter, S. Bearhop, D. J. Hosken, Population genetic structure of serotine bats (Eptesicus serotinus) across Europe and implications for the potential spread of bat rabies (European bat lyssavirus EBLV-1). *Heredity* **115**, 83–92 (2015).
27. F. Mattucci, R. Oliveira, L. A. Lyons, P. C. Alves, E. Randi, European wildcat populations are subdivided into five main biogeographic groups: consequences of Pleistocene climate changes or recent anthropogenic fragmentation? *Ecology and Evolution* **6**, 3–22 (2016).
28. F. Mattucci, R. Oliveira, L. A. Lyons, P. C. Alves, E. Randi, Data from: European wildcat populations are subdivided into five main biogeographic groups: consequences of Pleistocene climate changes or recent anthropogenic fragmentation?, version 1, Dryad (2016); https://doi.org/10.5061/DRYAD.KB13M.
29. R. R. Marrotte, J. Bowman, M. G. C. Brown, C. Cordes, K. Y. Morris, M. B. Prentice, P. J. Wilson, Multi-species genetic connectivity in a terrestrial habitat network. *Movement Ecology* **5**, 1–11 (2017).
30. R. R. Marrotte, J. Bowman, M. G. C. Brown, C. Cordes, K. Y. Morris, M. B. Prentice, P. J. Wilson, Data from: Multi-species genetic connectivity in a terrestrial habitat network, *Movement Ecology* (2017). https://doi.org/10.5061/dryad.qn4kq.
31. C. S. Casey, P. Orozco-terWengel, K. Yaya, M. Kadwell, M. Fernández, J. C. Marín, R. Rosadio, L. Maturrano, D. Hoces, Y. Hu, J. C. Wheeler, M. W. Bruford, Comparing genetic diversity and demographic history in co-distributed wild South American camelids. *Heredity* **121**, 387–400 (2018).
32. C. S. Casey, P. Orozco-TerWengel, K. Yaya, M. Kadwell, M. Fernández, J. C. Marin, R. Rosadio, L. Maturrano, D. Hoces, Y. Hu, J. C. Wheeler, M. W. Bruford, Data from: Comparing genetic diversity and demographic history in co-distributed wild South American camelids, version 1, Dryad (2018); https://doi.org/10.5061/DRYAD.G8D77FT.
33. B. A. González, P. Orozco-terWengel, R. Von Borries, W. E. Johnson, W. L. Franklin, J. C. Marín, Maintenance of Genetic Diversity in an Introduced Island Population of Guanacos after Seven Decades and Two Severe Demographic Bottlenecks: Implications for Camelid Conservation. *PLoS ONE* **9**, e91714 (2014).
34. B. A. González, P. Orozco-TerWengel, R. Von Borries, W. E. Johnson, W. L. Franklin, J. C. Marín, Data from: Maintenance of genetic diversity in an introduced island population of Guanacos after seven decades and two severe demographic bottlenecks: implications for camelid conservation, version 1, Dryad (2014); https://doi.org/10.5061/DRYAD.06G5V.
35. V. K. Lagerholm, K. Norén, D. Ehrich, R. A. Ims, S. T. Killengren, N. I. Abramson, J. Niemimaa, A. Angerbjörn, H. Henttonen, L. Dalén, Data from: Run to the hills: gene flow among mountain areas leads to low genetic differentiation in the Norwegian lemming, version 1, Dryad (2016); https://doi.org/10.5061/DRYAD.KR966.
36. V. K. Lagerholm, K. Norén, D. Ehrich, R. A. Ims, S. T. Killengreen, N. I. Abramson, J. Niemimaa, A. Angerbjörn, H. Henttonen, L. Dalén, Run to the hills: gene flow among

mountain areas leads to low genetic differentiation in the Norwegian lemming. *Biological Journal of the Linnean Society* **121**, 1–14 (2017).
37. E. Cheng, K. E. Hodges, J. Melo-Ferreira, P. C. Alves, L. S. Mills, Conservation implications of the evolutionary history and genetic diversity hotspots of the snowshoe hare. *Molecular Ecology* **23**, 2929–2942 (2014).
38. E. Cheng, K. E. Hodges, J. Melo-Ferreira, P. C. Alves, L. S. Mills, Data from: Conservation implications of the evolutionary history and genetic diversity hotspots of the snowshoe hare, *Molecular Ecology* (2014). https://doi.org/10.5061/dryad.dh63p.
39. J. Melo-Ferreira, L. Farelo, H. Freitas, F. Suchentrunk, P. Boursot, P. C. Alves, Data from: Home loving boreal hare mitochondria survived several invasions in Iberia: the relative roles of recurrent hybridisation and allele surfing, version 1, Dryad (2013); https://doi.org/10.5061/DRYAD.QJ864.
40. J. Melo-Ferreira, L. Farelo, H. Freitas, F. Suchentrunk, P. Boursot, P. C. Alves, Home-loving boreal hare mitochondria survived several invasions in Iberia: the relative roles of recurrent hybridisation and allele surfing. *Heredity* **112**, 265–273 (2014).
41. G. Lohay, C. Weathers, A. Estes, B. McGrath, D. Cavener, Genetic connectivity and population structure of African savanna elephants (Loxodonta africana) in Tanzania, version 2, Dryad (2020); https://doi.org/10.5061/DRYAD.ZS7H44J4M.
42. G. G. Lohay, T. C. Weathers, A. B. Estes, B. C. McGrath, D. R. Cavener, Genetic connectivity and population structure of African savanna elephants (*Loxodonta africana*) in Tanzania. *Ecology and Evolution* **10**, 11069–11089 (2020).
43. C. D. Marsden, R. Woodroffe, M. G. L. Mills, J. W. McNutt, S. Creel, R. Groom, M. Emmanuel, S. Cleaveland, P. Kat, G. S. A. Rasmussen, J. Ginsberg, R. Lines, J.-M. André, C. Begg, R. K. Wayne, B. K. Mable, Data from: Spatial and temporal patterns of neutral and adaptive genetic variation in the endangered African wild dog (Lycaon pictus), version 2, Dryad (2011); https://doi.org/10.5061/DRYAD.86P82F43.
44. C. D. Marsden, R. Woodroffe, M. G. L. Mills, J. W. McNUTT, S. Creel, R. Groom, M. Emmanuel, S. Cleaveland, P. Kat, G. S. A. Rasmussen, J. Ginsberg, R. Lines, J. André, C. Begg, R. K. Wayne, B. K. Mable, Spatial and temporal patterns of neutral and adaptive genetic variation in the endangered African wild dog (*Lycaon pictus*). *Molecular Ecology* **21**, 1379–1393 (2012).
45. M. B. Prentice, J. Bowman, K. Khidas, E. L. Koen, J. R. Row, D. L. Murray, P. J. Wilson, Selection and drift influence genetic differentiation of insular Canada lynx (*Lynx canadensis*) on Newfoundland and Cape Breton Island. *Ecology and Evolution* **7**, 3281–3294 (2017).
46. M. B. Prentice, J. Bowman, K. Khidas, E. L. Koen, J. R. Row, D. L. Murray, P. J. Wilson, Data from: Selection and drift influence genetic differentiation of insular Canada lynx (Lynx canadensis) on Newfoundland and Cape Breton Island, *Ecology and Evolution* (2017). https://doi.org/10.5061/dryad.8ff46.
47. J. E. Janecka, M. E. Tewes, I. A. Davis, A. M. Haines, A. Caso, T. L. Blankenship, R. L. Honeycutt, Genetic differences in the response to landscape fragmentation by a habitat generalist, the bobcat, and a habitat specialist, the ocelot. *Conservation Genetics* **17**, 1093–1108 (2016).
48. J. E. Janecka, M. E. Tewes, I. A. Davis, A. M. Haines, A. Caso, T. L. Blankenship, R. L. Honeycutt, Data from: Genetic differences in the response to landscape fragmentation by

a habitat generalist, the bobcat, and a habitat specialist, the ocelot, *Conservation Genetics* (2016). https://doi.org/10.5061/dryad.5b2k6.
49. D. M. Reding, A. M. Bronikowski, W. E. Johnson, W. R. Clark, Pleistocene and ecological effects on continental-scale genetic differentiation in the bobcat (Lynx rufus). *Molecular Ecology* **21**, 3078–3093 (2012).
50. D. M. Reding, A. M. Bronikowski, W. E. Johnson, W. R. Clark, Data from: Pleistocene and ecological effects on continental-scale genetic differentiation in the bobcat (Lynx rufus), *Molecular Ecology* (2012). https://doi.org/10.5061/dryad.d3t16pd2.
51. E. L. Koen, J. Bowman, P. J. Wilson, Data from: Node-based measures of connectivity in genetic networks, *Molecular Ecology Resources* (2015). https://doi.org/10.5061/dryad.4tg23.
52. E. L. Koen, J. Bowman, P. J. Wilson, Node-based measures of connectivity in genetic networks. *Molecular Ecology Resources* **16**, 69–79 (2016).
53. A. C. Frantz, A. D. McDevitt, L. C. Pope, J. Kochan, J. Davison, C. F. Clements, M. Elmeros, G. Molina-Vacas, A. Ruiz-Gonzalez, A. Balestrieri, K. Van Den Berge, P. Breyne, E. Do Linh San, E. O. Ågren, F. Suchentrunk, L. Schley, R. Kowalczyk, B. I. Kostka, D. Ćirović, N. Šprem, M. Colyn, M. Ghirardi, V. Racheva, C. Braun, R. Oliveira, J. Lanszki, A. Stubbe, M. Stubbe, N. Stier, T. Burke, Revisiting the phylogeography and demography of European badgers (Meles meles) based on broad sampling, multiple markers and simulations. *Heredity* **113**, 443–453 (2014).
54. A. C. Frantz, A. D. McDevitt, L. C. Pope, J. Kochan, J. Davison, C. F. Clements, M. Elmeros, G. Molina-Vacas, A. Ruiz-Gonzalez, A. Balestrieri, K. Van Den Berge, P. Breyne, E. Do Linh San, E. O. Ågren, F. Suchentrunk, L. Schley, R. Kowalczyk, B. I. Kostka, D. Ćirović, N. Šprem, M. Colyn, M. Ghirardi, V. Racheva, C. Braun, R. Oliveira, J. Lanszki, A. Stubbe, M. Stubbe, N. Stier, T. Burke, Data from: Re-visiting the phylogeography and demography of European badgers (Meles meles) based on broad sampling, multiple markers and simulations, version 1, Dryad (2014); https://doi.org/10.5061/DRYAD.5NM5G.
55. B. Gauffre, K. Berthier, P. Inchausti, Y. Chaval, V. Bretagnolle, J. Cosson, Short-term variations in gene flow related to cyclic density fluctuations in the common vole. *Molecular Ecology* **23**, 3214–3225 (2014).
56. B. Gauffre, K. Berthier, P. Inchausti, Y. Chaval, J.-F. Cosson, V. Bretagnolle, Data from: Short-term variations in gene flow related to cyclic density fluctuations in the common vole, version 1, Dryad (2014); https://doi.org/10.5061/DRYAD.JF7SN.
57. N. Martínková, R. Barnett, T. Cucchi, R. Struchen, M. Pascal, M. Pascal, M. C. Fischer, T. Higham, S. Brace, S. Y. W. Ho, J.-P. Quéré, P. O'Higgins, L. Excoffier, G. Heckel, A. R. Hoelzel, K. M. Dobney, J. B. Searle, Data from: Divergent evolutionary processes associated with colonization of offshore islands, version 1, Dryad (2013); https://doi.org/10.5061/DRYAD.9RF5M.
58. N. Martínková, R. Barnett, T. Cucchi, R. Struchen, M. Pascal, M. Pascal, M. C. Fischer, T. Higham, S. Brace, S. Y. W. Ho, J. Quéré, P. O'Higgins, L. Excoffier, G. Heckel, A. Rus Hoelzel, K. M. Dobney, J. B. Searle, Divergent evolutionary processes associated with colonization of offshore islands. *Molecular Ecology* **22**, 5205–5220 (2013).
59. C. Bastos-Silveira, S. M. Santos, R. Monarca, M. D. L. Mathias, G. Heckel, Data from: Deep mitochondrial introgression and hybridization among ecologically divergent vole species, version 1, Dryad (2012); https://doi.org/10.5061/DRYAD.Q3NG0.

60. C. Bastos-Silveira, S. M. Santos, R. Monarca, M. D. L. Mathias, G. Heckel, Deep mitochondrial introgression and hybridization among ecologically divergent vole species. *Molecular Ecology* **21**, 5309–5323 (2012).
61. F. Witsenburg, L. Clément, L. Dutoit, A. López-Baucells, J. Palmeirim, D. Scaravelli, M. Ševčík, N. Salamin, J. Goudet, P. Christe, I. Pavlinić, Data from: How a haemosporidian parasite of bats gets around: the genetic structure of a parasite, vector and host compared, version 1, Dryad (2015); https://doi.org/10.5061/DRYAD.2M1P0.
62. F. Witsenburg, L. Clément, A. López-Baucells, J. Palmeirim, I. Pavlinić, D. Scaravelli, M. Ševčík, L. Dutoit, N. Salamin, J. Goudet, P. Christe, How a haemosporidian parasite of bats gets around: the genetic structure of a parasite, vector and host compared. *Molecular Ecology* **24**, 926–940 (2015).
63. V. Weber De Melo, H. Sheik Ali, J. Freise, D. Kühnert, S. Essbauer, M. Mertens, K. M. Wanka, S. Drewes, R. G. Ulrich, G. Heckel, H. Sheikh Ali, Data from: Spatiotemporal dynamics of Puumala hantavirus associated with its rodent host, Myodes glareolus, version 1, Dryad (2015); https://doi.org/10.5061/DRYAD.P1K7K.
64. V. Weber De Melo, H. Sheikh Ali, J. Freise, D. Kühnert, S. Essbauer, M. Mertens, K. M. Wanka, S. Drewes, R. G. Ulrich, G. Heckel, Spatiotemporal dynamics of Puumala hantavirus associated with its rodent host, *Myodes glareolus*. *Evolutionary Applications* **8**, 545–559 (2015).
65. O. Razgour, I. Salicini, C. Ibáñez, E. Randi, J. Juste, Unravelling the evolutionary history and future prospects of endemic species restricted to former glacial refugia. *Molecular Ecology* **24**, 5267–5283 (2015).
66. O. Razgour, I. Salicini, C. Ibáñez, E. Randi, J. Juste, Data from: Unravelling the evolutionary history and future prospects of endemic species restricted to former glacial refugia, version 1, Dryad (2015); https://doi.org/10.5061/DRYAD.V1V47.
67. L. E. Burns, T. R. Frasier, H. G. Broders, Genetic connectivity among swarming sites in the wide ranging and recently declining little brown bat (Myotis lucifugus). *Ecology and Evolution* **4**, 4130–4149 (2014).
68. L. E. Burns, T. R. Frasier, H. G. Broders, Data from: Genetic connectivity among swarming sites in the wide ranging and recently declining little brown bat (Myotis lucifugus), *Ecology and Evolution* (2014). https://doi.org/10.5061/dryad.hs37s.
69. C. M. Davy, M. E. Donaldson, Y. Rico, C. L. Lausen, K. Dogantzis, K. Ritchie, C. K. R. Willis, D. W. Burles, T. S. Jung, S. McBurney, A. Park, D. F. McAlpine, K. J. Vanderwolf, C. J. Kyle, Prelude to a panzootic: gene flow and immunogenetic variation in northern little brown myotis vulnerable to bat white-nose syndrome. *FACETS* **2**, 690–714 (2017).
70. C. M. Davy, M. E. Donaldson, Y. Rico, C. L. Lausen, K. Dogantzis, K. Ritchie, C. K. R. Willis, D. W. Burles, T. S. Jung, S. McBurney, A. Park, D. F. McAlpine, K. J. Vanderwolf, C. J. Kyle, Data from: Prelude to a panzootic: gene flow and immunogenetic variation in northern little brown myotis vulnerable to bat white-nose syndrome, *FACETS* (2017). https://doi.org/10.5061/dryad.h7n25.
71. L. N. L. Johnson, B. A. McLeod, L. E. Burns, K. Arseneault, T. R. Frasier, H. G. Broders, Population Genetic Structure Within and among Seasonal Site Types in the Little Brown Bat (Myotis lucifugus) and the Northern Long-Eared Bat (M. septentrionalis). *PLOS ONE* **10**, 1–18 (2015).

72. L. N. L. Johnson, B. A. McLeod, L. E. Burns, K. Arseneault, T. R. Frasier, H. G. Broders, Data from: Population genetic structure within and among seasonal site types in the little brown bat (Myotis lucifugus) and the northern long-eared bat (M. septentrionalis), *PLOS ONE* (2015). https://doi.org/10.5061/dryad.47nm0.
73. E. S. M. Boston, W. Ian Montgomery, R. Hynes, P. A. Prodöhl, New insights on postglacial colonization in western Europe: the phylogeography of the Leisler's bat (*Nyctalus leisleri*). *Proc. R. Soc. B.* **282**, 20142605 (2015).
74. E. S. M. Boston, W. I. Montgomery, R. Hynes, P. A. Prodöhl, P. A. Prodohl, Data from: New insights on postglacial colonisation in Western Europe: the phylogeography of the Leisler's bat (Nyctalus leisleri), version 1, Dryad (2015); https://doi.org/10.5061/DRYAD.6G6R6.
75. E. K. Latch, D. M. Reding, J. R. Heffelfinger, C. H. Alcalá-Galván, O. E. Rhodes, Range-wide analysis of genetic structure in a widespread, highly mobile species (Odocoileus hemionus) reveals the importance of historical biogeography. *Molecular Ecology* **23**, 3171–3190 (2014).
76. E. K. Latch, D. M. Reding, J. R. Heffelfinger, C. H. Alcalá-Galván, O. E. Rhodes, Data from: Range-wide analysis of genetic structure in a widespread, highly mobile species (Odocoileus hemionus) reveals the importance of historical biogeography, *Molecular Ecology* (2014). https://doi.org/10.5061/dryad.ns2jn.
77. S. J. Robinson, M. D. Samuel, D. L. Lopez, P. Shelton, The walk is never random: Subtle landscape effects shape gene flow in a continuous white-tailed deer population in the Midwestern United States. *Molecular Ecology* **21**, 4190–4205 (2012).
78. S. J. Robinson, M. D. Samuel, D. L. Lopez, P. Shelton, Data from: The walk is never random: subtle landscape effects shape gene flow in a continuous white-tailed deer population in the Midwestern United States, *Molecular Ecology* (2012). https://doi.org/10.5061/dryad.p7639.
79. C. W. Epps, R. S. Crowhurst, B. S. Nickerson, Assessing changes in functional connectivity in a desert bighorn sheep metapopulation after two generations. *Molecular Ecology* **27**, 2334–2346 (2018).
80. C. W. Epps, R. S. Crowhurst, B. S. Nickerson, Data from: Assessing changes in functional connectivity in a desert bighorn sheep metapopulation after two generations, *Molecular Ecology* (2018). https://doi.org/10.5061/dryad.mp71t50.
81. B. Yumnam, Y. V. Jhala, Q. Qureshi, J. E. Maldonado, R. Gopal, S. Saini, Y. Srinivas, R. C. Fleischer, Prioritizing Tiger Conservation through Landscape Genetics and Habitat Linkages. *PLoS ONE* **9**, e111207 (2014).
82. B. Yumnam, Y. V. Jhala, Q. Qureshi, J. E. Maldonado, R. Gopal, S. Saini, Y. Srinivas, R. C. Fleischer, Data from: Prioritizing tiger conservation through landscape genetics and habitat linkages, version 1, Dryad (2015); https://doi.org/10.5061/DRYAD.C7V41.
83. M. J. E. Charpentier, M. C. Fontaine, J. P. Renoult, T. Jenkins, E. Cherel, L. Benoit, N. Barthès, S. C. Alberts, J. Tung, Data from: Genetic structure in a dynamic baboon hybrid zone corroborates behavioral observations in a hybrid population, version 1, Dryad (2011); https://doi.org/10.5061/DRYAD.SK013.
84. M. J. E. Charpentier, M. C. Fontaine, E. Cherel, J. P. Renoult, T. Jenkins, L. Benoit, N. Barthès, S. C. Alberts, J. Tung, Genetic structure in a dynamic baboon hybrid zone corroborates behavioural observations in a hybrid population. *Molecular Ecology* **21**, 715–731 (2012).

85. R. Thavornkanlapachai, W. J. Kennington, K. Ottewell, J. A. Friend, H. R. Mills, Data from: Dispersal, philopatry and population genetic structure of the mainland dibbler, Parantechinus apicalis, version 1, Dryad (2019); https://doi.org/10.5061/DRYAD.F1BN36C.
86. R. Thavornkanlapachai, W. J. Kennington, K. Ottewell, J. A. Friend, H. R. Mills, Dispersal, philopatry and population genetic structure of the mainland dibbler, Parantechinus apicalis. *Conserv Genet* **20**, 1087–1099 (2019).
87. P. Bertrand, J. Bowman, R. Dyer, M. Manseau, W. PJ, Data from: Sex-specific graphs: Relating group-specific topology to demographic and landscape data, *Molecular Ecology* (2017). https://doi.org/10.5061/dryad.167d5.
88. P. Bertrand, J. Bowman, R. Dyer, M. Manseau, W. PJ, Sex-specific graphs: Relating group-specific topology to demographic and landscape data. *Molecular Ecology* **26**, 3898–3912 (2017).
89. J. Munshi-South, K. Kharchenko, Rapid, pervasive genetic differentiation of urban white-footed mouse (Peromyscus leucopus) populations in New York City. *Molecular Ecology* **19**, 4242–4254 (2010).
90. J. Munshi-South, K. Kharchenko, Data from: Rapid, pervasive genetic differentiation of urban white-footed mouse (Peromyscus leucopus) populations in New York City, *Molecular Ecology* (2010). https://doi.org/10.5061/dryad.1893.
91. A. Rogic, N. Tessier, P. Legendre, F.-J. Lapointe, V. Millien, Genetic structure of the white-footed mouse in the context of the emergence of Lyme disease in southern Québec. *Ecology and Evolution* **3**, 2075–2088 (2013).
92. A. Rogic, N. Tessier, P. Legendre, F.-J. Lapointe, V. Millien, Data from: Genetic structure of the white-footed mouse in the context of the emergence of Lyme disease in southern Québec, *Ecology and Evolution* (2013). https://doi.org/10.5061/dryad.43vg5.
93. Z. S. Taylor, S. M. G. Hoffman, Landscape models for nuclear genetic diversity and genetic structure in white-footed mice (Peromyscus leucopus). *Heredity* **112**, 588–595 (2014).
94. Z. S. Taylor, S. M. G. Hoffman, Data from: Landscape models for nuclear genetic diversity and genetic structure in white-footed mice (Peromyscus leucopus), *Heredity* (2014). https://doi.org/10.5061/dryad.j272c.
95. Z. S. Taylor, S. M. G. Hoffman, Data from: Microsatellite genetic structure and cytonuclear discordance in naturally fragmented populations of deer mice (Peromyscus maniculatus), *Journal of Heredity* (2011). https://doi.org/10.5061/dryad.gs048.
96. Z. S. Taylor, S. M. G. Hoffman, Microsatellite genetic structure and cytonuclear discordance in naturally fragmented populations of deer mice (Peromyscus maniculatus). *Journal of Heredity* **103**, 71–79 (2012).
97. K. Yokochi, W. J. Kennington, R. Bencini, An Endangered Arboreal Specialist, the Western Ringtail Possum (Pseudocheirus occidentalis), Shows a Greater Genetic Divergence across a Narrow Artificial Waterway than a Major Road. *PLoS ONE* **11**, e0146167 (2016).
98. K. Yokochi, W. J. Kennington, R. Bencini, Data from: An endangered arboreal specialist, the western ringtail possum (Pseudocheirus occidentalis), shows a greater genetic divergence across a narrow artificial waterway than a major road, version 1, Dryad (2016); https://doi.org/10.5061/DRYAD.14Q5G.

99. H. B. Ernest, T. W. Vickers, S. A. Morrison, M. R. Buchalski, W. M. Boyce, Fractured genetic connectivity threatens a Southern California puma (Puma concolor) population. *PLoS ONE* **9** (2014).
100. H. B. Ernest, T. W. Vickers, S. A. Morrison, M. R. Buchalski, W. M. Boyce, Data from: Fractured genetic connectivity threatens a southern California puma (Puma concolor) population, *PLoS ONE* (2014). https://doi.org/10.5061/dryad.dp0qj.
101. K. E. Colson, K. H. Mager, K. J. Hundertmark, Reindeer introgression and the population genetics of caribou in southwestern Alaska. *Journal of Heredity* **105**, 585–596 (2014).
102. K. E. Colson, K. H. Mager, K. J. Hundertmark, Data from: Reindeer introgression and the population genetics of caribou in Southwestern Alaska, *Journal of Heredity* (2014). https://doi.org/10.5061/dryad.9qh56.
103. K. H. Mager, K. E. Colson, P. Groves, K. J. Hundertmark, Population structure over a broad spatial scale driven by nonanthropogenic factors in a wide-ranging migratory mammal, Alaskan caribou. *Molecular Ecology* **23**, 6045–6057 (2014).
104. K. H. Mager, K. E. Colson, P. Groves, K. J. Hundertmark, Data from: Population structure over a broad spatial scale driven by non-anthropogenic factors in a wide-ranging migratory mammal, Alaskan caribou, *Molecular Ecology* (2014). https://doi.org/10.5061/dryad.3hp5v.
105. R. Serrouya, D. Paetkau, M. BN, S. Boutin, J. DA, M. Campbell, Data from: Population size and major valleys explain microsatellite variation better than taxonomic units for caribou in western Canada, *Molecular Ecology* (2012). https://doi.org/10.5061/dryad.250c3s47.
106. R. Serrouya, D. Paetkau, B. N. McLellan, S. Boutin, M. Campbell, D. A. Jenkins, Population size and major valleys explain microsatellite variation better than taxonomic units for caribou in western Canada. *Molecular Ecology* **21**, 2588–2601 (2012).
107. B. V. Weckworth, M. Musiani, A. D. McDevitt, M. Hebblewhite, S. Mariani, Reconstruction of caribou evolutionary history in Western North America and its implications for conservation. *Molecular Ecology* **21**, 3610–3624 (2012).
108. B. V. Weckworth, M. Musiani, A. D. McDevitt, M. Hebblewhite, S. Mariani, Data from: Reconstruction of caribou evolutionary history in Western North America and its implications for conservation, *Molecular Ecology* (2012). https://doi.org/10.5061/dryad.gn22271h.
109. G. Yannic, L. Pellissier, M. Le Corre, C. Dussault, L. Bernatchez, S. D. Côté, Temporally dynamic habitat suitability predicts genetic relatedness among caribou. *Proceedings. Biological sciences* **281** (2014).
110. G. Yannic, L. Pellissier, M. Le Corre, C. Dussault, L. Bernatchez, S. D. Côté, Data from: Temporally dynamic habitat suitability predicts genetic relatedness among caribou, *Proceedings of the Royal Society B* (2014). https://doi.org/10.5061/dryad.qn1cj.
111. O. Tournayre, J. Pons, M. Leuchtmann, R. Leblois, S. Piry, O. Filippi-Codaccioni, A. Loiseau, J. Duhayer, I. Garin, F. Mathews, S. Puechmaille, N. Charbonnel, D. Pontier, Integrating population genetics to define conservation units from the core to the edge of *Rhinolophus ferrumequinum* western range. *Ecology and Evolution* **9**, 12272–12290 (2019).
112. O. Tournayre, J.-B. Pons, M. Leuchtmann, R. Leblois, S. Piry, A. Loiseau, O. Filippi-Codaccioni, J. Duhayer, I. Garin, F. Mathews, S. Puechmaille, N. Charbonnel, D. Pontier, Data from: Integrating population genetics to define conservation units from the core to

the edge of Rhinolophus ferrumequinum western range, version 3, Dryad (2020); https://doi.org/10.5061/DRYAD.R44T5DK.
113. P. Hulva, T. Maresova, C. Dundarova, R. Bilgin, P. Benda, T. Bartonicka, I. Horacek, Data from: Environmental margin and island evolution in Middle Eastern populations of the Egyptian fruit bat, version 1, Dryad (2012); https://doi.org/10.5061/DRYAD.K68K8.
114. P. Hulva, T. Marešová, H. Dundarova, R. Bilgin, P. Benda, T. Bartonička, I. Horáček, Environmental margin and island evolution in M iddle E astern populations of the E gyptian fruit bat. *Molecular Ecology* **21**, 6104–6116 (2012).
115. G. Yannic, P. Basset, L. Büchi, J. Hausser, T. Broquet, Data from: Scale-specific sex-biased dispersal in the Valais shrew unveiled by genetic variation on the Y chromosome, autosomes, and mitochondrial DNA, version 1, Dryad (2011); https://doi.org/10.5061/DRYAD.8K3423TS.
116. G. Yannic, P. Basset, L. Büchi, J. Hausser, T. Broquet, Scale-specific sex-biased dispersal in the Valais shrew unveiled by genetic variation on the Y chromosome, autosomes, and mitochondrial DNA. *Evolution* **66**, 1737–1750 (2012).
117. P. Alexandri, H.-J. Megens, R. P. M. A. Crooijmans, M. A. M. Groenen, D. J. Goedbloed, J. M. Herrero-Medrano, L. A. Rund, L. B. Schook, E. Chatzinikos, C. Triantaphyllidis, A. Triantafyllidis, L. B. Schook, A. Triantafyllidis, Data from: Distinguishing migration events of different timing for wild boar in the Balkans, version 1, Dryad (2017); https://doi.org/10.5061/DRYAD.T722H.
118. P. Alexandri, H. Megens, R. P. M. A. Crooijmans, M. A. M. Groenen, D. J. Goedbloed, J. M. Herrero-Medrano, L. A. Rund, L. B. Schook, E. Chatzinikos, C. Triantaphyllidis, A. Triantafyllidis, Distinguishing migration events of different timing for wild boar in the Balkans. *Journal of Biogeography* **44**, 259–270 (2017).
119. A. S. Chavez, C. J. Saltzberg, G. J. Kenagy, Genetic and phenotypic variation across a hybrid zone between ecologically divergent tree squirrels (Tamiasciurus). *Molecular Ecology* **20**, 3350–3366 (2011).
120. A. S. Chavez, C. J. Saltzberg, G. J. Kenagy, Data from: Genetic and phenotypic variation across a hybrid zone between ecologically divergent tree squirrels (Tamiasciurus), *Molecular Ecology* (2011). https://doi.org/10.5061/dryad.195qg.
121. Y. Rico, D. M. Ethier, C. M. Davy, J. Sayers, R. D. Weir, B. J. Swanson, J. J. Nocera, C. J. Kyle, Spatial patterns of immunogenetic and neutral variation underscore the conservation value of small, isolated American badger populations. *Evolutionary Applications* **9**, 1271–1284 (2016).
122. Y. Rico, D. M. Ethier, C. M. Davy, J. Sayers, R. D. Weir, B. J. Swanson, J. J. Nocera, C. J. Kyle, Data from: Spatial patterns of immunogenetic and neutral variation underscore the conservation value of small, isolated American badger populations, *Evolutionary Applications* (2016). https://doi.org/10.5061/dryad.qb87r.
123. J. P. Draper, L. P. Waits, J. R. Adams, C. L. Seals, T. D. Steury, Genetic health and population monitoring of two small black bear (Ursus americanus) populations in Alabama, with a regional perspective of genetic diversity and exchange. *PLOS ONE* **12** (2017).
124. J. P. Draper, L. P. Waits, J. R. Adams, C. L. Seals, T. D. Steury, Data from: Genetic and population monitoring of two small black bear (Ursus americanus) populations in Alabama, within a regional context., *PLOS ONE* (2017). https://doi.org/10.5061/dryad.bj7r3.

125. E. E. Puckett, P. D. Etter, E. A. Johnson, L. S. Eggert, Phylogeographic analyses of American black bears (Ursus americanus) suggest four glacial refugia and complex patterns of postglacial admixture. *Molecular Biology and Evolution* **32**, 2338–2350 (2015).
126. E. E. Puckett, P. D. Etter, E. A. Johnson, L. S. Eggert, Data from: Phylogeographic analyses of American black bears (Ursus americanus) suggest four glacial refugia and complex patterns of post-glacial admixture, *Molecular Biology and Evolution* (2015). https://doi.org/10.5061/dryad.dc02b.
127. M. A. Cronin, M. D. MacNeil, Genetic relationships of extant brown bears (Ursus arctos) and polar bears (Ursus maritimus). *Journal of Heredity* **103**, 873–881 (2012).
128. M. A. Cronin, M. D. MacNeil, Data from: Genetic relationships of extant brown bears (Ursus arctos) and polar bears (Ursus maritimus), *Journal of Heredity* (2012). https://doi.org/10.5061/dryad.q30rt.
129. E. Peacock, S. SA, O. ME, A. Boltunov, R. EV, N. Ovsyanikov, J. Aars, A. SN, S. GK, H. AG, E. Zeyl, L. Bachmann, D. Ehrich, S. KT, A. SC, S. Belikov, B. EW, D. AE, I. Stirling, T. MK, Ø. Wiig, D. Paetkau, T. SL, Data from: Implications of the circumpolar genetic structure of polar bears for their conservation in a rapidly warming Arctic, *PLOS ONE* (2015). https://doi.org/10.5061/dryad.v2j1r.
130. E. Peacock, S. A. Sonsthagen, M. E. Obbard, A. Boltunov, E. V. Regehr, N. Ovsyanikov, J. Aars, S. N. Atkinson, G. K. Sage, A. G. Hope, E. Zeyl, L. Bachmann, D. Ehrich, K. T. Scribner, S. C. Amstrup, S. Belikov, E. W. Born, A. E. Derocher, I. Stirling, M. K. Taylor, Ø. Wiig, D. Paetkau, S. L. Talbot, Implications of the circumpolar genetic structure of polar bears for their conservation in a rapidly warming Arctic. *PLoS ONE* **10**, 1–30 (2015).
131. E. W. Goldsmith, B. Renshaw, C. J. Clement, A. Elizabeth, K. J. Hundertmark, K. Hueffer, Data from: Population structure of two rabies hosts relative to the known distribution of rabies virus variants in Alaska, *Molecular Ecology* (2015). https://doi.org/10.5061/dryad.dc1q8.2.
132. E. W. Goldsmith, B. Renshaw, C. J. Clement, E. A. Himschoot, K. J. Hundertmark, K. Hueffer, Population structure of two rabies hosts relative to the known distribution of rabies virus variants in Alaska. *Molecular Ecology* **25**, 675–688 (2016).

Table S2. Model summaries (no phylogenetic correction). Summaries of Bayesian hierarchical models relating genetic metrics to distance to range edge for convex hull models presented in the main text. The effect size of distance to edge is given with 95% credible intervals. Models controlled for spatial and phylogenetic correlation. $\sigma_{intercept}$ is the standard deviation of species-specific intercepts, and summarizes variation in mean genetic diversity, effective population size, or F_{ST} across species. σ_{slope} is the standard deviation of species-specific estimates of the effect of distance, and shows variation in species responses to range position. Marginal log-likelihood and DIC (Deviance Information Criterion) are two model fit metrics.

Variable	Distance	$\sigma_{intercept}$	σ_{slope}	marginal log likelihood	DIC
gene diversity	0.17 (0.06 – 0.28)	0.91 (0.73 – 1.11)	0.45 (0.32 – 0.62)	-1211.99	986.66
allelic richness	0.17 (0.06 – 0.27)	0.82 (0.66 – 1.01)	0.33 (0.23 – 0.46)	-1329.71	1176.10
effective population size	0.08 (-0.04 – 0.19)	0.50 (0.40 – 0.62)	0.33 (0.28 – 0.38)	-721.26	2287.78
population-specific F_{ST}	-0.14 (-0.27 – -0.01)	0.77 (0.61 – 0.95)	0.45 (0.31 – 0.63)	-1409.59	1723.47

Table S3. Spatial connectivity network selection. To best account for spatial autocorrelation in our models, we compared a series of models with no spatial structure, and with k-nearest neighbors connectivity networks constructed with 1 – 8 neighbors for each location. We selected connectivity networks based on models with the lowest WAIC and DIC (bold rows). Overall, models were not sensitive to the connectivity network used across those tested here.

	Convex hull		Centroid	
	DIC	WAIC	DIC	WAIC
Gene diversity				
non-spatial model	1701.37	1716.31	1867.96	1879.72
k = 1	1414.54	1456.44	1659.22	1689.71
k = 2	1311.22	1314.49	1338.98	1333.62
k = 3	1155.22	1174.38	1119.00	1120.35
k = 4	1154.82	1156.01	1117.29	1084.35
k = 5	1234.97	1233.88	793.11	717.13
k = 6	**389.14**	**429.29**	869.57	828.55
k = 7	1139.00	1155.40	758.93	675.42
k = 8	966.37	935.43	**469.04**	**415.19**
Allelic richness				
non-spatial model	2079.59	2437.90	2219.01	2382.03
k = 1	1617.89	2077.62	1838.16	2325.67
k = 2	1468.18	1826.15	1567.30	1873.81
k = 3	1326.49	1662.84	1374.55	1662.11
k = 4	1421.16	1769.86	1425.93	1837.96
k = 5	1371.85	1695.35	1368.40	1695.65
k = 6	1268.50	1448.49	1256.48	1351.65
k = 7	1332.44	1524.78	1215.73	1360.16
k = 8	**1105.27**	**1153.94**	**633.20**	**648.16**
Population-specific FST				
non-spatial model	2579.82	2602.60	2696.80	2715.99
k = 1	2344.08	2513.38	2303.98	2330.95
k = 2	2094.24	2130.23	2142.98	2143.16
k = 3	2100.22	2161.62	2007.22	1992.14
k = 4	2132.71	2206.29	1952.73	1934.38
k = 5	2039.41	2068.90	2062.62	2065.34
k = 6	2059.12	2112.60	1936.83	1920.44
k = 7	2030.52	2044.51	1852.21	1794.43
k = 8	**1911.27**	**1896.42**	**1811.62**	**1755.84**
Effective population size				
non-spatial model	2531.86	2536.80	2543.76	2546.97
k = 1	2283.51	2271.73	2348.28	2354.68
k = 2	2327.44	2336.86	2250.92	2260.86
k = 3	**2220.35**	**2216.42**	2346.08	2358.11
k = 4	2269.29	2268.22	2279.32	2280.66
k = 5	2299.53	2307.29	2262.47	2263.23
k = 6	2355.47	2358.03	2316.78	2326.99

k = 7	2269.52	2270.01	2291.11	2307.79
k = 8	2530.05	2535.68	**2224.57**	**2224.43**